PHYSICAL CHARACTERISTICS OF THE BLACK SEA INFERRED FROM ARGO PROFILING DATA

A THESIS SUBMITTED TO

THE INSTITUTE OF MARINE SCIENCES

MIDDLE EAST TECHNICAL UNIVERSITY

BY

ANIL AKPINAR

IN PARTIAL FULFILLMENT OF THE REQUIREMENTS

FOR

THE DEGREE OF MASTER OF SCIENCE

IN

PHYSICAL OCEANOGRAPHY

SEPTEMBER 2010

PHYSICAL CHARACTERISTICS OF THE BLACK SEA INFERRED FROM ARGO PROFILING DATA

submitted by **Anıl Akpınar** in partial fulfillment of the requirements for the degree of **Master of Science in Graduate School of Marine Sciences, Middle East Technical University** by,

Prof. Dr. Ferit Bingel
Director, **Graduate School of Marine Sciences** ……..

Prof. Dr. Emin Özsoy
Head of Department, **Physical Oceanography** ……..

Assoc. Prof. Dr. Bettina A. Fach
Supervisor, **Graduate School of Marine Sciences, METU** ……..

Prof.Dr. Temel Oğuz
Co-supervisor, **Graduate School of Marine Sciences, METU** ……..

Examining Committee Members:

Prof. Dr. Süleyman Tuğrul
Graduate School of Marine Sciences, METU ……..

Assoc. Prof. Dr. Barış Salihoğlu
Graduate School of Marine Sciences, METU ……..

Assoc. Prof. Dr. Bettina A. Fach
Graduate School of Marine Sciences, METU ……..

Prof. Dr. Temel Oğuz
Graduate School of Marine Sciences, METU ……..

Dr. Heather Cannaby
Graduate School of Marine Sciences, METU ……..

Date: September 15, 2010

I hereby declare that all information in this document has been obtained and presented in accordance with academic rules and ethical conduct. I also declare that, as required by these rules and conduct, I have fully cited and referenced all material and results that are not original to this work.

Name, Last name : Anıl Akpınar

Signature :

ABSTRACT

PHYSICAL CHARACTERISTICS OF THE BLACK SEA INFERRED FROM ARGO PROFILING DATA

AKPINAR, Anıl

M.Sc., Department of Physical Oceanography

Supervisor: Asst. Prof. Bettina A. Fach

Co-Supervisor: Prof. Dr. Temel Oğuz

September 2010, 89 pages

Seven argo floats have been deployed between 2002 and 2006. These floats were active until 2009, thus constituting a data set of seven years time series. In this study mixed layer, Cold Intermediate Layer and the surface layer properties of the Black Sea as inferred from the Argo float data have been studied. Temperature data from these floats show distinct interannual variability in the surface layer of the Black Sea, whereas the salinity data reveals spatial changes due to freshwater input.

Investigation of the shallow temperature minimum, known as the Cold Intermediate Layer (CIL) revealed periodic changes in the CIL thickness, the maximum depth of the CIL and the physical properties of the CIL at corresponding depths. The overall CIL thickness was found to be 44 m, which is consistent with the previous studies. The lower boundary of the CIL was found to reach down to 160 m in anticyclonic regions, which has never been observed before.

As criterion for the determination of the mixed layer a salinity gradient threshold was used to estimate the mixed layer during winter whereas a density gradient was used for the rest of the year. The mixed layer extends up to 70 m in winter and to 20 m in summer, with a seasonal cycle. Shallower mixed layer was found in cyclonic regions.

The water properties at 100 m and 200 m were also analyzed and showed distinct features depending on the float positions, which in comparison with satellite altimetry indicated that the features are observed when floats are entrained in cyclonic or anticyclonic eddies. This is the first time that such a comprehensive data set was available for the Black Sea and this data set allows us to see previously unknown features of the Black Sea thermohaline structure.

Keywords: ARGO, Float, Black Sea, Cold Intermediate Layer, Mixed layer, AVISO

ÖZ

KARADENİZİN FİZİKSEL ÖZELLİKLERİNİN ARGO TİPİ ŞAMANDIRA VERİLERİNDEN ÇIKARIMI

AKPINAR, Anıl

Yüksek Lisans, Fiziksel Oşinografi Bölümü

Tez yöneticisi: Yar. Doç. Dr. Bettina A. Fach

Eş tez yöneticisi: Prof. Dr. Temel Oğuz

Eylül 2010, 89 sayfa

2002 ile 2006 yılları arasında Karadeniz'e yedi adet Argo tipi şamandıra bırakılmıştır. 2009 yılına kadar aktif olan bu şamandıralar yedi yıllık bir veri serisini oluşturmaktadır. Bu çalışmada Argo veri serisi işlenmiş ve Karadeniz'in yüzey tabakası, karışmış tabakası ve soğuk orta tabakası (CIL) incelenmiştir. Bu şamandıralardan alınan sıcaklık verileri Karadeniz'in yüzeyinde dönemsel bir değişim döngüsü göstermiştir, tuzluluk verileriyse şamandıraların konumuna bağlı bir değişim göstermiştir.

Soğuk orta tabakanın (CIL) incelenmesiyle, CIL kalınlığında, CIL'in ulaştığı derinliklerde ve CIL tabakasının fiziksel özelliklerinde periyodik değişimler gözlenmiştir. Ortalama CIL kalınlığı 44 metre olarak bulunmuştur. CIL'in alt sınırının antisiklonik bölgelerde 160 metrelere kadar indiği gözlenmiştir.

Yüzeydeki karışmış tabakanın özelliklerini doğru inceleyebilmek için öncelikle karışmış tabaka derinliğinin hesaplanması için en uygun yöntem incelenmiştir. Kış ayları için tuzluluk verisinde bir katsayı eşiği en iyi sonucu verirken, diğer aylarda yoğunluk verisinde bir katsayı eşiği en iyi sonucu vermiştir. Yüzeydeki karışmış tabaka kışın 70 metrelere ulaşırken, yaz aylarında 20 metrelerde bulunmuştur ve genel olarak siklonik bölgelerde sığ seviyelerde kalmıştır. 100m ve 200 metrelerdeki su özellikleri de incelenmiş ve bariz sıcaklık ve tuzluluk farklılıkları gözlenmiştir. Bu noktalardaki şamandıra konumlarının uydudan alınan deniz seviyesi yükseklikleriyle kıyaslanması siklonik ve antisiklonik bölgelerin saptanmasını sağlamıştır. Bu veri setiyle beraber Karadeniz'de ilk defa bu kadar kapsamlı veriler elde edilmiştir. Bu veriler bize daha önce saptanmamış olan fiziksel özellikleri inceleme şansı vermiştir.

Anahtar Kelimeler: ARGO, Şamandıra, AVISO, Soğuk Orta Tabaka, Karışmış tabaka, Karadeniz

ACKNOWLEDGEMENTS

I would like to thank my supervisor Asst. Prof. Bettina A. Fach and my co-advisor Prof. Temel Oğuz for their guidance throughout the research and during the preparation and writing of this work.

My sincere thanks to Asst.Prof. Bettina A. Fach and Asst.Prof. Barış Salihoğlu for their help throughout the study.

I would like to thank Dr. Sinan Hüsrevoğlu for his help especially with programming languages during the research.

Thanks to Ersin Tutsak, Adil Sözer, Ceren Güraslan, Ekin Akoğlu, Nusret Sevinç, Özgür Gürses and Çağlar Yumruktepe for their various contributions and help in the study.

I would also like to thank to my family for supporting and encouraging me both within this study and throughout my life.

Finally I would like to thank to “SETÜSTÜ”, all the staff and members of the institute for creating such a beautiful workplace.

TABLE OF CONTENTS

LIST OF FIGURES

Figure

LIST OF TABLES

Table

CHAPTER 1
Introduction

In the world ocean, as well as the specific case of the Black Sea, physical mechanisms influence the conditions of the marine environment. The physical oceanographic characteristics, including the circulation dynamics and the physical properties of the surrounding waters are the primary factors that determine the condition of the marine environment, influencing ecosystems of the marine environment. Because of the important role in the dynamics of marine ecosystem, studying the thermohaline structure of the Black Sea is crucial. In this study the intention is to identify the thermohaline properties of the Black Sea via profiling float data.

The Black Sea (Figure 1.1) is one of the largest inland basins of the world with a surface area of ~4.2×10^5 km^2 (zonal and meridional dimensions ~1000km and ~400km) and a maximum depth of ~2200meters. The Black Sea is almost completely isolated from the world oceans; it is connected to the Sea of Azov via the Kerch Strait in the North and to the Marmara Sea (which is connected to the Aegean Sea through Dardanelles Strait) via the Bosphorus in the southeast.

Figure1. 1 The Black Sea (retrieved from http://en.wikipedia.org/wiki/Black_Sea)

The objective of this study is to understand the thermohaline structure of the Black Sea by investigating the upper layer waters' properties. Various cruises via research vessels have been conducted in the Black Sea during the ends of the 80's and the early 90's making large data sets available for studying the oceanography of the Black Sea. The thermohaline structure, hydrographic properties and the circulation of the Black Sea has been studied (Oguz et al., 1992, 1993; Murray et al., 1991,). However when cruises are conducted the data collected represents only a snapshot of the conditions in space and time. In addition, cruises are expensive and time intense and the countries surrounding the Black Sea cannot conduct cruises on a regular basis. Thus the Argo program is extremely important for the Black Sea region. The main difference between this study and the work previously conducted is that the data used in this study is a seven year long –weekly time series data from different locations all over the Black Sea. This is actually the first time such a time-series basin wide data set is available for the Black Sea region. This Argo data set enables us to investigate the different hydro-physical properties of different regions in the Black Sea. Over time the floats drifting contemporarily around the basin have given us a chance to examine some of the mesoscale eddies and to compare the cyclones with anticyclones. A previously conducted study (Korotaev et al., 2006) with the data of these floats revealed the strength and variability of the flow field at 750m and 1550m with maximum velocity of 5 cm/s. The active role of the mesoscale features were seen at 200m, 750m and 1550m. The topographic control of deep currents was observed in this study. Current speeds were also estimated. Velocity at 1550m was calculated as 5 cm/s which are 5-10% of the surface velocity.

The combination of the Argo data set and altimetry data provides a comparative study of the cyclonic-anticyclonic eddies around the basin. For all these reasons the data set used in this study is very valuable and further Argo float deployments in near future are crucial for the attempt to learn more about the spatial and temporal variability of the Black Sea

thermohaline structure. In the rest of this chapter, a brief description of the physical characteristics of the Black Sea is provided. The technical features of the Argo floats are also described briefly as a prelude to the forthcoming chapters.

1.1 Physical Oceanography of the Black Sea

1.1.1 Circulation characteristics

The Black Sea has a basin-wide cyclonic boundary current (Rim Current) driven by the curl of the wind stress field, which is also affected by the fresh water discharges from rivers (buoyancy forces), bathymetry and thermohaline fluxes (Oguz et al., 1992) In addition to the Rim Current, the Black Sea circulation system contains many mesoscale eddies (see figure 1.2), meanders and filaments spread over the basin. The Rim Current separates the cyclonically dominated inner basin from the anticyclonically dominated coastal zone (Oguz et al., 1992) .The Sinop and Kizilirmak (Oguz et al., 1992), Batumi, Bosphorus, Sukhumi, Kerch, Sevastopol, Danube, Caucasus, Constantsa, Crimea and Sakarya eddies reside on the coastal side of the Rim Current zone. In the inner basin, two cyclonic cells (Western Gyre and Eastern Gyre) are formed (Korotaev et al., 2003).

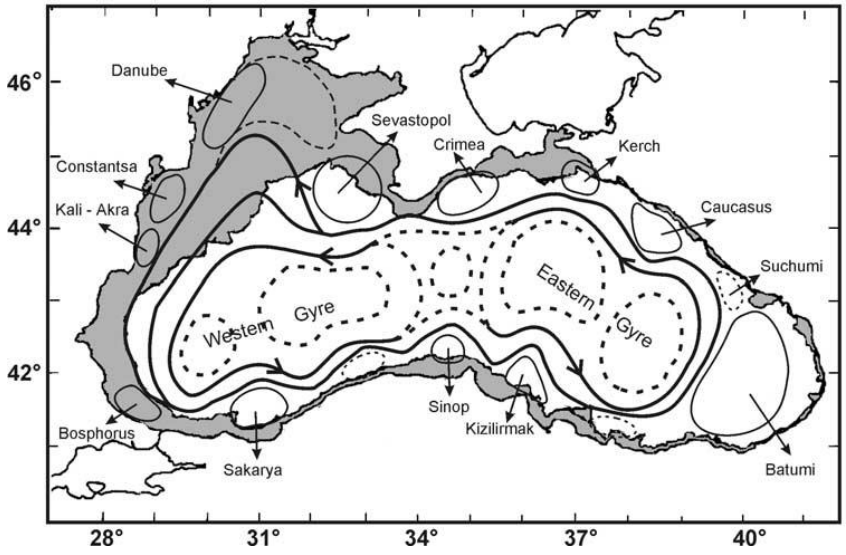

Figure 1. 2 Main features of the Black Sea circulation system (Korotaev et al., 2003)

Along the Caucasian coast, the Rim Current is limited to the continental slope, where it meanders forming an offshore jet extending towards the interior basin from the shore. This jet, separates three cyclonic eddies of the eastern basin which makes up the Eastern Basin Cyclonic Gyre (Oguz et al., 1992). The Rim Current meanders along the southern tip of Crimea spreading into two branches; the first branch flows southwestward and the second one flow into the inner shelf and supporting the southerly inner shelf current system. These two branches of the Rim Current converge again along the Turkish-Bulgarian coast (Korotaev et al., 2003).

The Black Sea is an inland basin, which means that its overall mass budget depends on the hydrological balance. The surface water characteristics of the Black Sea depend on the freshwater inflow extensively. Therefore the rivers around the Black Sea are extremely important. There are many rivers discharging into the Black Sea. The major rivers around the Black Sea are the Danube, Dnepr and Dniester which discharge into the northwestern shelf of the Black Sea which. The Danube river constitutes around half of the total river runoff. The annual mean discharge of the Danube River shows large variations of 4000-9000 m^3/s (Sur et al., 1996).

1.1.2. Stratification characteristics

The Black Sea is the world's largest basin where the deep waters and the oxygenated surface waters do not mix. The Black Sea is a strongly stratified system with 87% of its waters being anoxic. The measurable oxygen is detected in the upper ~150 meters. The density stratification together with weak vertical circulation and mixing prevents the ventilation of the sub-pycnocline waters from the surface. As a result of the continually sinking and decomposition of organic matter, a permanent anoxic zone and high concentrations of hydrogen sulfide was formed below 100-150 meters, during

approximately 7000 years (Oguz et al., 2002). The oxic and anoxic waters of the Black Sea are separated by a permanent halocline (Oguz et al., 1993).

The Black Sea surface waters have an average salinity of 18 to 18.5 ppt (parts per thousand). The low salinity of the surface waters is a result of the freshwater input, whereas the higher salinity of the deeper waters is an influence of the Mediterranean water (Ozsoy and Unluata, 1997). The temperature of the surface waters vary seasonally from 8 °C to 30°C.Temperature differences up to 2 °C have been observed in the surface layer waters (Oguz et al., 1993).

1.1.3. Cold Intermediate Layer (CIL): Below the surface waters of the Black Sea lies the Cold Intermediate Layer (CIL) which is also called the shallow temperature minimum. The CIL is defined as the layer of water with a temperature less than 8 °C (Figure 1.3).

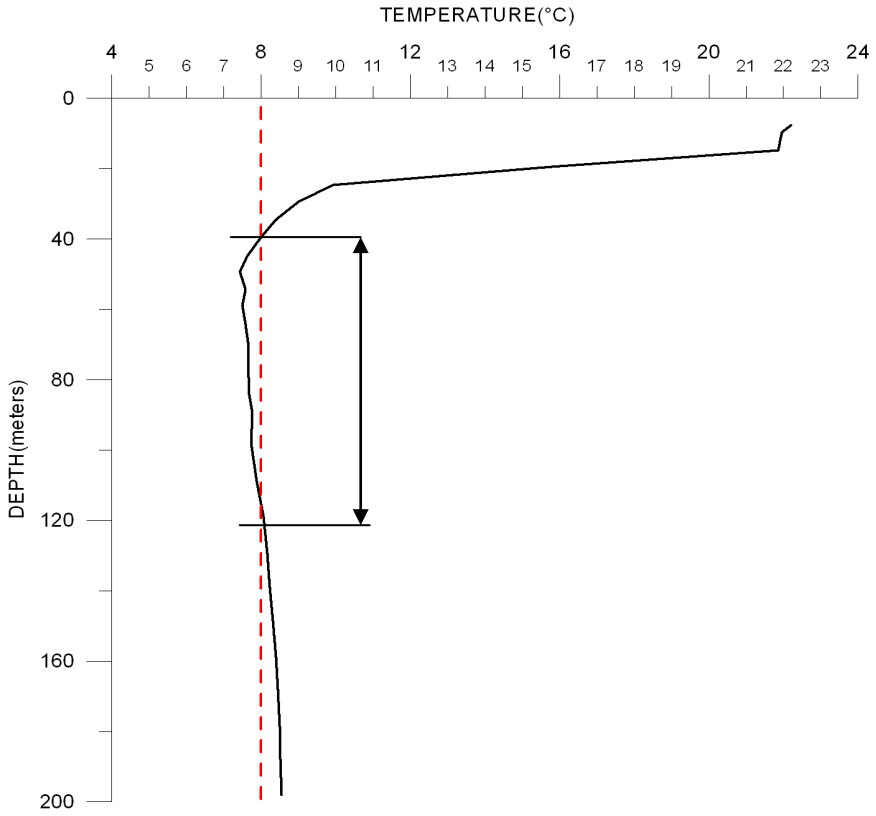

Figure 1.3: Cold Intermediate Layer is defined as the layer of water below 8°C, marked here with the arrow.

The Cold Intermediate Layer has core temperatures which is less than 8°C and may be as low as ~5°C. The CIL in anticyclonic regions is fresher and less dense but cooler than the cyclonic regions. The CIL is thinner and at shallower depths in the cyclonic regions (Oguz et al., 1993). The CIL is thought to be formed mainly on the North Western Shelf of the Black Sea (Tolmazin, 1985a) but in recent years, the centers of the cyclonic gyres were proposed to be the areas for CIL formation (Ovchinnikov and Popov, 1987; Oguz and Besiktepe, 1999).

With the stratification of the surface water via spring warming, the cold water generated by convection remains below the seasonal thermocline forming the Cold Intermediate Layer (Oguz and Besiktepe, 1999). The kinematic factor is extremely important in the formation of the CIL. The uplift of the pycnocline (halocline) forces colder and more saline water to the surface. Climatic factor (atmospheric) is also crucially important, including cold air masses intruding into the zone above the sea. The main effect of these air intrusions is that they make the hydrologic variable in the water mass reach necessary values for convective mixing (Ovchinnikov and Popov, 1987).

1.1.4. Mixed Layer: Mixed layer is known as the layer between the ocean surface and a depth ranging up to ~200 meters. The mixed layer has a constant temperature and salinity from the surface down to the thermocline. The depth of the mixed layer varies spatially and temporally. For the specific case of Black Sea the mixed layer rarely exceeds 50m during winter and it is usually less than 20m in spring and summer (Kara et al., 2009). The details of the study conducted on the mixed layer and mixed layer properties of the Black Sea are explained in the Material & Methods section.

1.1.5. Sub-pycnocline Layer: The density surface σ_t ~16.2 kg/m^3 corresponds to 150 m depth within the interior cyclonic cell. Below this pycnocline (200m), the sub-pycnocline waters show almost vertically uniform characteristics with values of temperature of ~8.9^o-9.1^{o}C, salinity of 22-22.5 ppt and density of 17-17.3 kg/m^3. (Oguz et al., 2009)

The mixing and renewal of the sub-pycnocline waters takes place via the dense Mediterranean water inflow from the Bosphorus, supported by the surface Ekman flux divergence, internal wave breaking and boundary processes. (Ozsoy et al., 2002)

1.2 ARGO FLOATS

Argo floats are freely drifting robotic probes in the ocean. They spend most of their lifetime drifting with currents at predetermined depths below the ocean surface. The drifting depths of the Argo floats are usually chosen as 2000 meters depth. The drifting depths of the floats used in this study will be mentioned later in the material and methods section (Chapter2).

The floats are 130cm long (without the ~70cm antenna) have a diameter of 16.5 cm and weigh ~26 kgs. An Argo float is illustrated in Figure 1.4. The floats have a satellite antenna on the top which communicates with the satellite and allows the data to be transmitted. Close to the antenna reside the temperature and salinity sensors. The top part of the float also includes a profiling module and microprocessors which schedule the functioning and scheduling of the float. Lower parts of the floats contain the hydraulic operating system which allows the floats to ascend and descend properly. The hydraulic operating system consists of a bladder, hydraulic fluid, a pump (piston) and the battery. With the hydraulic system, the floats have a density equal to the ambient waters and have

compressibility less than the seawater. The floats calibrate their buoyancy by changing the position of the hydraulic fluid via the pump and the bladder.

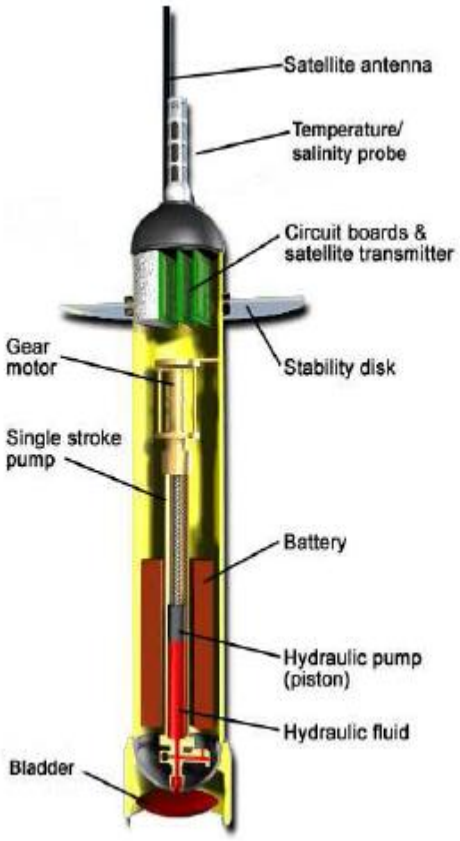

Figure1. 4 Argo Float (obtained from http://www.argo.ucsd.edu/csection.gif)

1.2.1 How Argo floats operate

The floats are deployed from ships or aircrafts. When the floats are deployed, they sink to the drifting depth. At 10 day intervals, the fluid is pumped into the bladder and the floats ascend to the surface around 6 hours. During ascend, floats measure the temperature and salinity (Gould et al., 2004). When the floats surface, the satellites fix their position and the floats transmit the data to the satellites. The floats spend 6 to 12 hours at the surface in order to have effective data transmission even in bad weather conditions. The floats have a lifetime of around 150 such cycles or around 4 years.

There are two types of float missions. First one is the simple mission operation, in which the floats descend to the parking depth, which is also the profiling depth. The second one is the park and profile type of mission, in which the float descends to the parking depth and then descends to the profiling depth which is deeper than the parking depth. Figure 1.5 shows the park and profile type of operation.

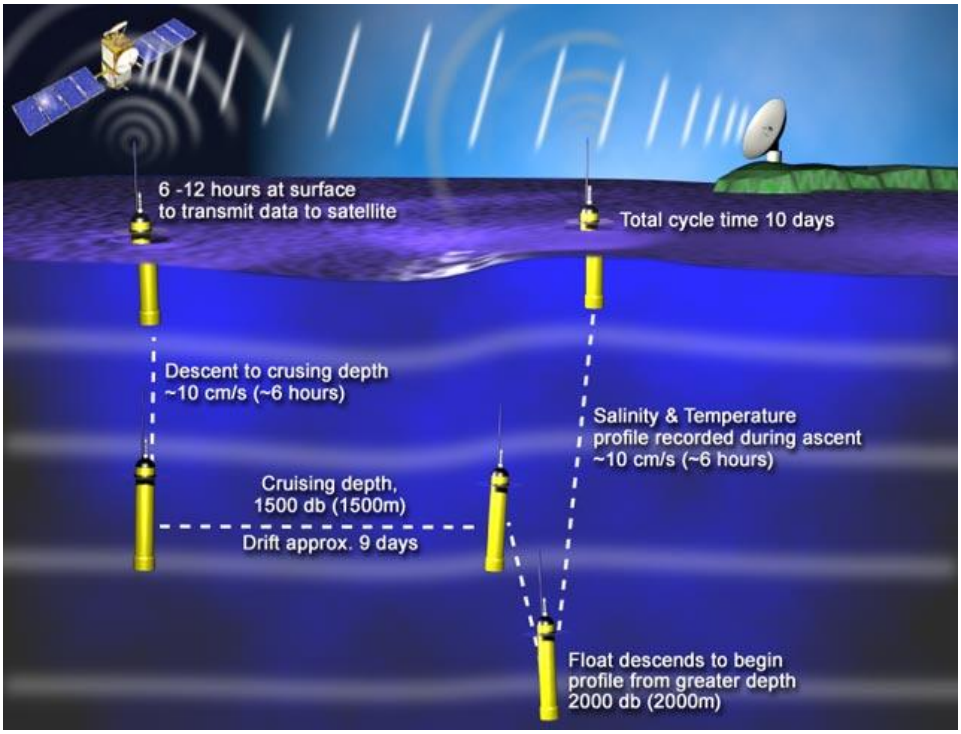

Figure1. 5 Park and profile working mechanism of the Argo float

There are three types of Argo floats. The first one is the PROVOR which is built by KANNAD in France with collaboration of IFREMER. The second one is the SOLO, which is designed and built by Scripps Institution of Oceanography. The third one is the APEX float designed by Webb Research Corporation (USA).

1.2.2 ARGO Program

Argo floats started being deployed in 2000. The aim of the Argo program was to reach three thousand profiling floats, which was accomplished in November 2007. As of today (24 March 2010), there are around 3255 Argo floats around the world.

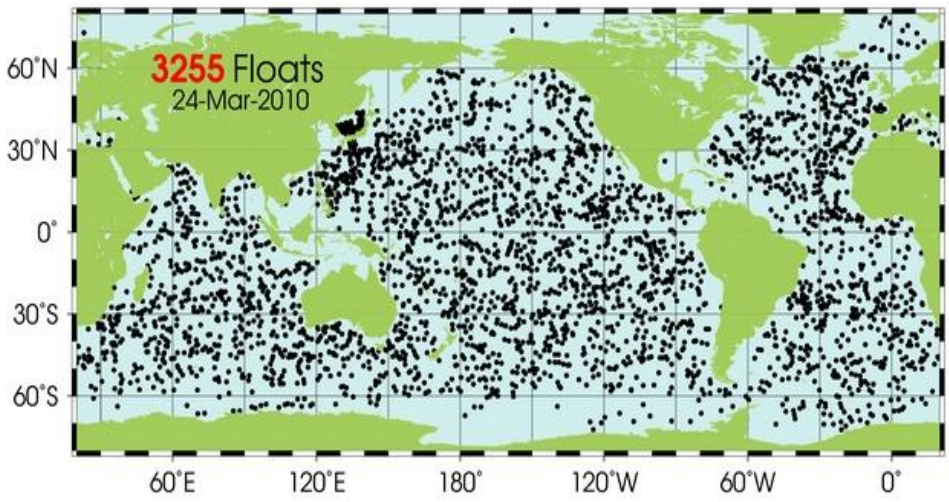

Figure1. 6 Argo floats around the world as of 24.03.2010

The Argo program is collaboration between 50 research and operational agencies. The Argo program is a part of the Integrated Ocean Observing System (IOOS). There are 26 countries participating in the Argo program with various contributions ranging from deployment help (or single float contribution) to hundreds of floats. The common goal is to build the global array and keep the Argo's open data policy. It should be noted here that all data in the Argo program are available publicly.

CHAPTER 2
Material and Methods

The data set used in this study comprised eight years (2002-2009) of time series data, obtained from Argo float measurements. In addition to the Argo float data, sea surface height anomaly data from altimetry was used as a complementary data source. The altimeter products were produced by Ssalto/*Duacs* and distributed by *Aviso*, with support from *Cnes* (http://www.aviso.oceanobs.com/duacs/).

2.1. DATA SAMPLING

The floats used in this study are all APEX (Autonomous Profiling Explorer) floats. All seven Argo floats are equipped with CTD (conductivity-temperature-depth) sensors. All of the CTD sensors are SBE 41/41CP CTD's which are manufactured by Sea-Bird Electronics Inc. The floats measure pressure, in-situ temperature, salinity, potential temperature and sigma-theta together with corresponding coordinates.

The Argo data is transmitted to the satellites when the float surfaces. In order to guarantee error free data reception in all weather conditions, the float spends 6 to 12 hours at the surface. Positions are accurate to ~100m depending on the number of satellites available and their positions. The data is transmitted to satellites via the Argos System. The data is then received by data centers and here, the data goes through quality check. The profiles of these floats are published via the GTS (Global Telecommunications System). Every profile should pass a certain data quality. The following criteria were used for rejection of profiles in the automated data quality check:

- Profiles older than 30 days were rejected
- Latitude in range -90 to 90 and longitude in range -180 to 180

- Profiles should have a general temperature range of -2.5 to 40 degrees C and a salinity in range 2 to 41.0 PSU

- Profiles that do not have a location fix were rejected. This might be a result of poor ARGOS reception.

- Profiles with observations where the pressure is less than zero or greater than 3000 dbars were neglected. This was assumed as an indication of pressure sensor problem or break down.

- Profiles with a gap between two consecutive observations that exceeded 300 dbars were rejected. Profiles with the shallowest measurement deeper than 300 dbars were also rejected. The reason to do so is to maintain the reasonable precision in the pressure to depth conversion calculation.

- Similarly profiles with the deepest observation less than 50 dbars are rejected. This is to prevent such cases where the float drifts into shallow water or becomes entangled in seaweed.

- Profiles with pressures that are not monotonous were rejected. This was done to satisfy the general quality of a well collected profile would have.

- Similarly, profiles with less than 5 measurements were rejected to maintain the general quality that a properly collected profile would have.

Despite the automated quality check done by University of Washington, there were still some misleading data in the received data set. These data (especially from float 1325) had wrong pressure values. These data were usually obtained towards the end of lifetime of the floats due to sensor drifting or malfunctioning with time. Another possibility is that the float may have been stranded. These profiles were rejected in the analysis of the data.

Salinity and temperature profiles are taken while the float ascends to the surface. For all of the seven floats, the profiling depth is 1550 dbar (meters), which means that each profile is taken from1500 m to the surface, but the parking depth is not the same for all floats. The floats, named by numbers, have the parking depths as follows; 0587, 2206 and 2619 were set to 1550 dbar (meter). 0631 was set to 750 dbar parking pressure (depth). 0634 was set to 200 dbar, 1325 was set to 500 dbar and 1550 was set to 1000 dbar (meters). The purpose of setting the parking pressures to different depth is to observe the circulation patterns of the Black Sea at different depths.

Table2. 1 General information about the floats

Float no:	Parking pressure (dbar)	Profile pressure (dbar)	Start date: (day/month/year)	End date: (dd/mm/yyyy)	Duration (~months)
0587	1550	1550	02.09.2002	21.02.2004	18
0631	750	1550	02.09.2002	21.12.2004	28
0634	200	1550	02.09.2002	16.04.2005	32
1325	500	1550	07.03.2005	18.01.2009	47
1550	1000	1550	07.03.2005	02.10.2008	43
2206	1550	1550	12.06.2006	22.02.2009	33
2619	1550	1550	12.06.2006	23.12.2009	43

Each profile includes, date, position of the transmitted data and the measured properties; pressure, potential temperature, salinity, in situ temperature and sigma theta.

The data generally has a sampling interval of 5 dbars at depths shallower than 100 meters, 10 dbars intervals between 100- 300 meters and then 25 dbars between 300- 500 meters and 50 dbars intervals at depths greater than 500 meters.

2.2. DATA ANALYSIS

2.2.1 Water Column Properties

First of all, data (with obviously wrong pressure values) were neglected. After checking the data, temperature, salinity and sigma-theta (density) profiles for each float were plotted. In order to understand the profiles in geographic space, the trajectories for the Argo floats were plotted on a bathymetry map. The profiles together with the trajectories allow us to observe the physical properties and to see the possible effects of river discharges and/or cyclones-anticyclones (eddies) in the Black Sea.

2.2.2 Surface layer properties

Next, the surface layer properties of the Black Sea were extracted from the Argo float data. Considering the vertical resolution of the Argo float data, the shallowest depth of each profile was chosen as the surface data. Profiles with the shallowest depth greater than 9 meters were neglected for this analysis, in order to obtain a proper surface layer data set. The temperature, density and salinity data were then plotted versus time (all seven years) for all of the floats.

The first three floats; 0587, 0631 and 0634 started to operate at the same time (on 02.09.2002). Similarly 1325 and 1550 were deployed at the same time (on 07.03.2005). Also the last two; 2206 and 2619 were deployed together (on 12.06.2006). To calculate average surface temperature, salinity and density the data of floats 0587-0631-0634 were averaged as well as floats 1325-1550 and 2206-2619.

2.2.3 Cold Intermediate Layer Properties

For the estimation of the CIL, Argo float data were examined and data with temperatures less than 8 °C were flagged as CIL. Each profile was individually examined and the data of all profiles were averaged to obtain mean CIL temperature, salinity and density. Similarly CIL thickness was estimated for each profile. Then from these thicknesses, average CIL thickness was estimated for each float individually. Using these calculations, CIL thicknesses vs. time for all floats were plotted. The mean temperature, salinity and density vs. time were also plotted for all floats.

2.2.4 Mixed layer properties

Mixed layer depths were also determined using the Argo float data. Data of seven floats were visually examined. Data which was lacking shallow depths or intermediate depths were removed. Data which had conspicuously bad pressure, temperature or salinity was rejected. After the data was checked, composite profiles of temperature vs. depth, salinity vs. depth and sigma-theta vs. depth for each data were plotted. Subsequently, all of these plots were visually examined in order to obtain reference mixed layer depths.

The definition of the mixed layer was important for this part of the study. Argo floats are being used all around the world, and the mixed layer is of great interest to scientists. In many studies, Argo floats have been used to observe the mixed layer depths, climatology of the mixed layer and the variability of the mixed layer (Ohno et al., 2004, 2009; Sreenivas et al., 2008; Bhaskar et al., 2007). In most of these studies, mixed layer depths were defined by certain criteria such as threshold difference or threshold gradient methods. The mixed layer is defined as the layer which has been homogenized by turbulence. This homogenized layer must be defined clearly. But the identification of the mixed layer relies on the homogeneity of temperature or density which is rather subjective that is to say there is no single or universal method for determining the mixed layer (Ohno

et al., 2009). In some previous studies in the North Pacific, the mixed layer was defined as the depth where the density increased by 0.03 kgm^{-3} from the sea surface and where the temperature increased or decreased by 0.2 °C from the surface (Oka *et al*., 2007). Since there is no previous study with Argo floats in the Black Sea and considering Black Sea is a fairly unique sea, a trial-error procedure was conducted for the determination of the mixed layer. The mixed layer for each float was estimated seperately in order to minimize the potential sensor drift or sensor malfunctioning problems.

Considering the previous studies in different parts of the world, first the threshold difference method was applied to the data. The threshold difference method finds the mixed layer depth at which density or potential temperature or salinity) is greater than that at a surface reference depth by a given threshold Ohno *et al. ,* 2009):

$$\sigma_\vartheta (MLD) = \sigma_\vartheta(reference\ depth) + \Delta\ \sigma_\vartheta(threshold) \quad (1)$$

$$S (MLD) = S (reference\ depth) + \Delta\ S (threshold) \quad (2)$$

$$T (MLD) = T (reference\ depth) + \Delta\ T (threshold) \quad (3)$$

For this method, various criterions have been used as threshold. For the density, thresholds were set to 0.7, 0.5, 0.3, 0.2 and 0.15 kg m^{-3}. These have been done in order to have a general idea about the potentially precise threshold. 0.15 was the most accurate one but even this choice still produced more than 15 % error. The same procedure was then applied to temperature with 0.3, 0.25, 0.2, 0.15 and 0.1 °C thresholds. The procedure was then applied to the salinity with 0.35, 0.30, 0.25, 0.2 and 0.15 psu. The result was the same. The threshold difference method did not seem to be working properly for our case, so another method was applied, which is known as the Threshold gradient method (Ohno *et al.,* 2009):

$$\frac{\Delta\sigma\theta}{\Delta z}/mld \geq threshold \qquad (4)$$

$$\frac{\Delta T}{\Delta z}/mld \geq threshold \qquad (5)$$

$$\frac{\Delta S}{\Delta z}/mld \geq threshold \qquad (6)$$

In this method, the smallest depth at which the gradient exceeds the threshold is found. This method was first applied to density, then temperature and salinity. The density and salinity are much more precise then temperature gradient settings. For the density, a gradient of 0.01 was set. This worked with a small error for most of the data except winter data. In winter, the density threshold gradient method becomes inaccurate. The same threshold gradient was also set for salinity but the accuracy was poor. The most accurate result was obtained by dividing the data into seasons. The data was divided into winter and non-winter groups. For the winter data a salinity gradient of 0.005 was set, and for the other seasons, a density threshold gradient of 0.01 was set. The salinity gradient was set to 0.005 for the winter seasons because salinity gradient was more precise than density; the reason for choosing such a small gradient like 0.005 instead of 0.01 is because the 0.01 salinity gradient overestimated the mixed layer. The mixed layer depth vs. time for each float was then plotted individually.

2.2.5 Properties at 100dbar and 200dbar

The Black Sea is known as a sea which means the deep waters do not mix with the upper layers. 200 meters is known to be the depth where the anoxic layer of the Black Sea starts. To understand the physical properties of this depth, data corresponding to 200m depth were extracted. The very same procedure was applied to 100m depth in order to observe the upper layer and CIL properties. The interpolated data for the 100m and 200m

levels were plotted for the three groups of floats. This way it was possible to observe different physical properties at different locations and compare them. In order to better understand these data, sea level anomalies were used for correlation.

2.2.6 Satellite data

The sea level anomalies were downloaded from AVISO (distributes satellite altimetry data from Topex/Poseidon, Jason-1, ERS-1 and ERS-2) ftp site (ftp://ftpsedr.cls.fr/pub/oceano/AVISO/SSH/duacs/regional-blacksea/dt/upd/msla/merged/h/). The weekly data set of sea level anomalies with 0.125^0x0.125^0 regular grid were interpolated and daily data set with a resolution of 0.1^0x0.0625^0. That data was then used to plot sea level anomaly maps. The sea level anomaly maps together with float positions corresponding to the same data were used to observe the cyclonic and anti-cyclonic patterns all around the Black Sea. This was an important issue in order to examine the possible effects of the cyclones and anticyclones in Black Sea on the measurements of the Argo floats.

CHAPTER 3

RESULTS

A brief presentation of the data obtained by the Argo profiling floats active in the Black Sea between 2002-2009 is given in this chapter. Figure 3.1 shows the coverage area of all seven floats released in the Black Sea. Each color represents one float.

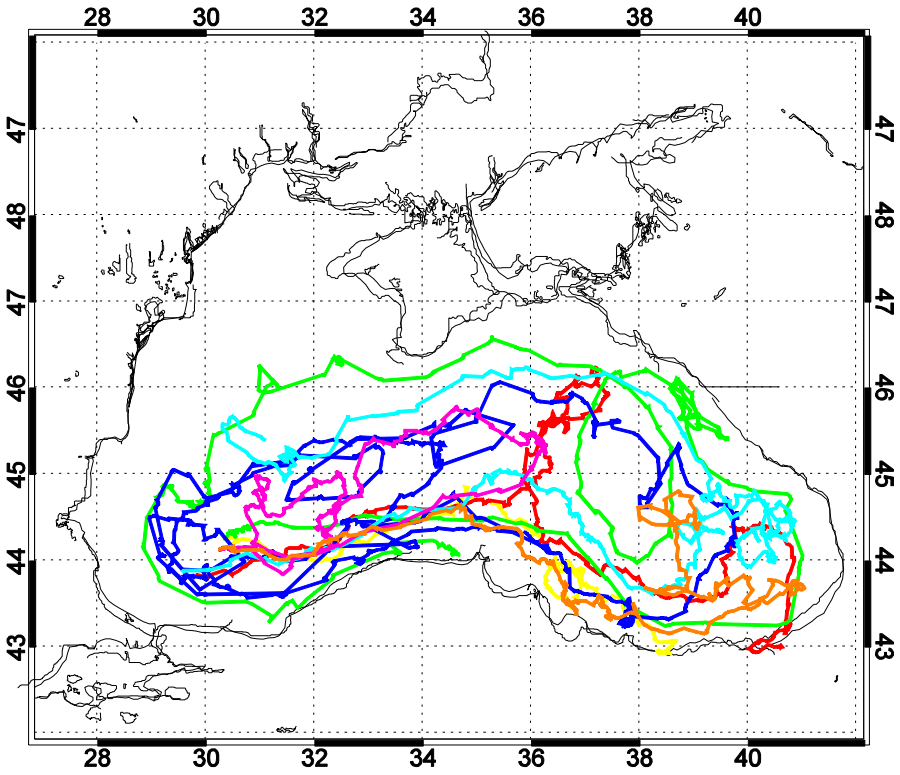

Figure 3. 1 Trajectories of the seven Argo floats active between 2002 and 2009 in the Black Sea

3.1 TRAJECTORIES

In this section the trajectories of each float in the Black Sea is examined in this section. The trajectory of float 0587 at 1550m parking depth is given in Figure 3.2 as a red line with the green dots marking the profiles taken every seven to ten days. In Figure 3.3 the same trajectory is shown together with the bathymetry of the Black Sea, where the green dots represent where the profiles are taken. In Figure 3.2, the start of the float trajectory is marked with '1', whereas '2' stands for the end of the lifetime of the float 0587.

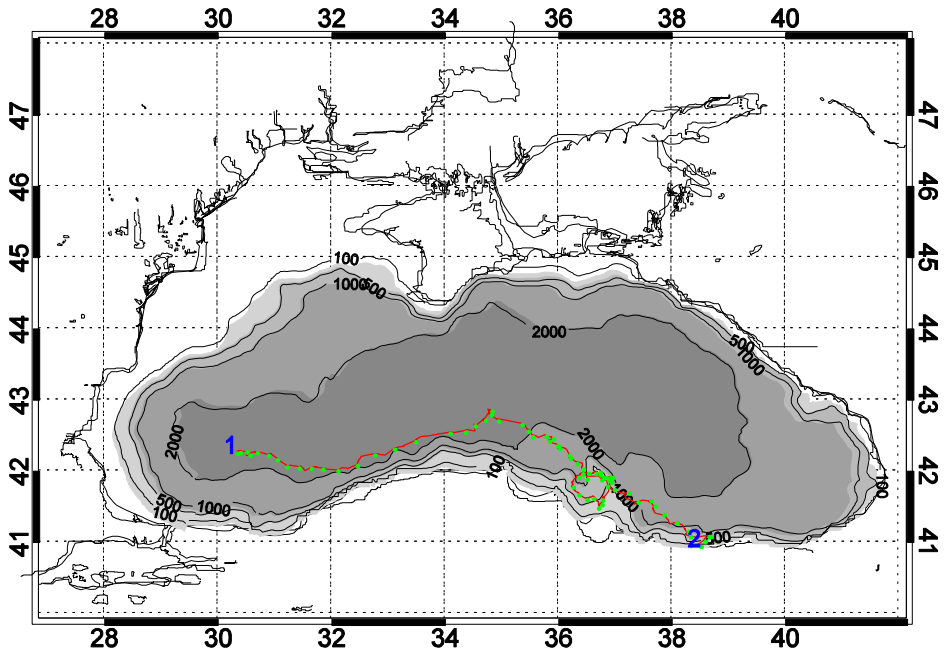

Figure 3. 2 Trajectory of the float 0587 (red line) with"1" and "2" represent start and end respectively. Green dots mark the locations of profiles taken every seven to ten days. Grey shading represents the bathymetry contours of 100m, 500m, 1000m, and 2000m.

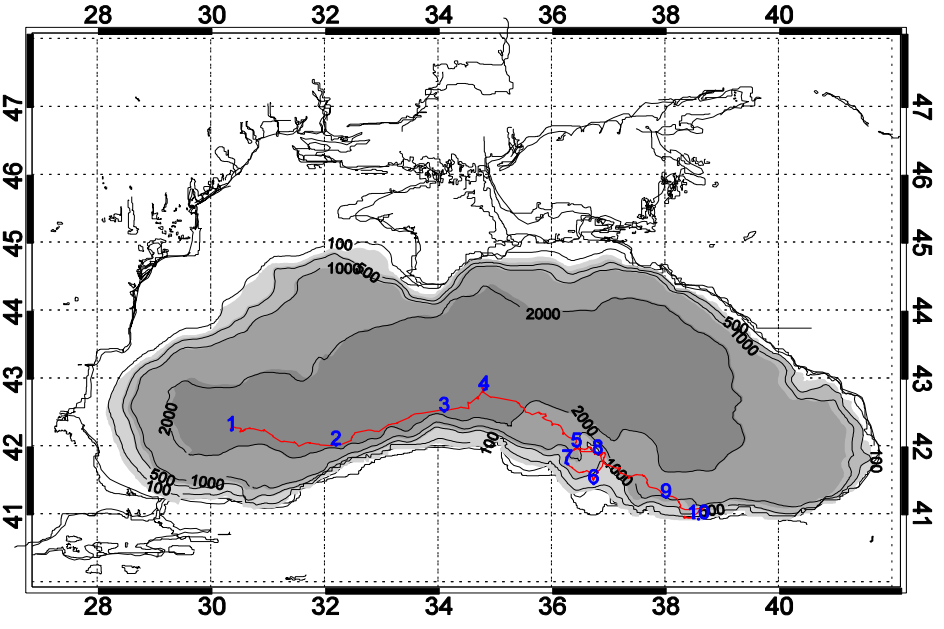

Figure 3. 3 Trajectory of the float 0587 (red line), with ten float locations marked by numbers. Details about the locations are given in Table 3.1. Grey shading represents the bathymetry contours of 100m, 500m, 1000m, and 2000m.

Table 3. 1 Float 0587 location numbers as seen in Figure 3.3

Number	Corresponding date(dd/mm/yy)	Longitude	Latitude
1	02.09.02	30.34	42.25
2	21.11.02	32.11	42.00
3	27.12.02	34.09	42.53
4	25.01.03	34.83	42.84
5	07.05.03	36.44	42.03
6	12.06.03	36.77	41.52
7	11.07.03	36.37	41.66
8	07.09.03	36.74	41.94
9	18.12.03	37.86	41.83
10	21.02.04	38.52	40.94

Float 0587, 0631 and 0634 were deployed in the western part of the Black Sea, offshore of the Bosphorus Strait. After the deployment float 0587 moved along the coast towards the east in the Rim Current, and reached the point denoted by “4” in Figure 3.3, in five months. Moving eastward, 0587 reached point “5” in ~3 months. Starting from this date (May 2003), 0587 went into an anticyclonic eddy, known as the Kizilirmak eddy, leaving this eddy in September 2003 at point “8”. It took the float another three months to reach the point shown by “9” in Figure 3.3. After the time 0587 reached the coast at depths shallower than its parking depth(1550m) where it resided on the sea floor and was able to move only once a week. The trajectory of the float 0587 illustrates a strong topographic control of deep currents (Korotaev et al., 2006).

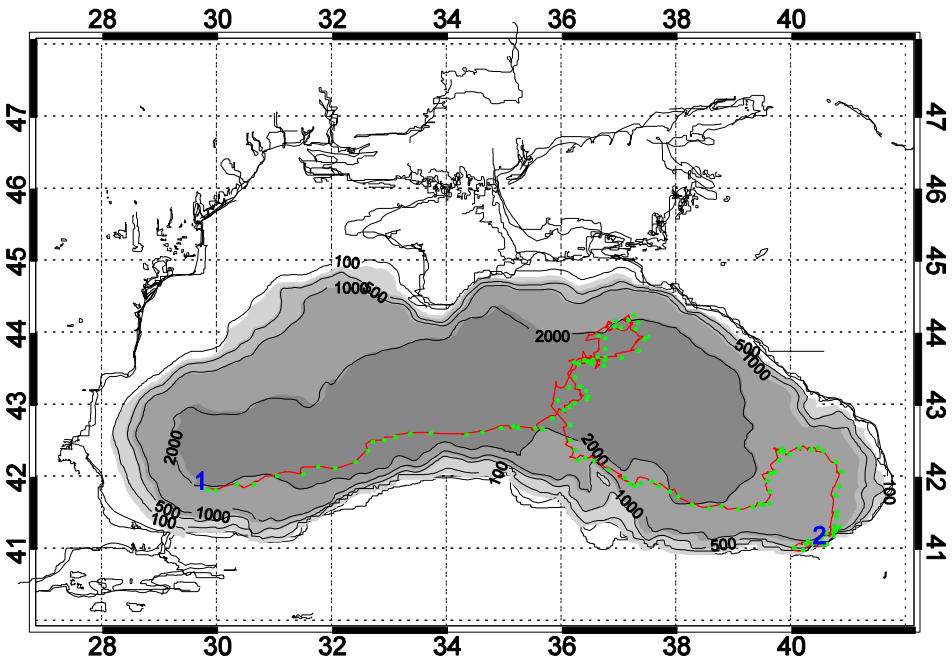

Figure 3. 4 Trajectory of the float 0631 (red line) with "1" and "2" represent start and end respectively. Green dots mark the locations of profiles taken every seven to ten days. Grey shading represents the bathymetry contours of 100m, 500m, 1000m, and 2000m.

Float 0631 (Fig. 3.4) was drifting at 750 meters and followed a very similar path as 0587 until it reached the periphery of Cape Sinop. After this point, it followed a different path, moving to the north into the basins interior. This change of route seems to be caused by the local current system consisting of the western flank of the anticyclonic eddy in the north and eastern flank of the cyclonic eddy in the south. This prevented further movement of the intermediate depth (750m) currents to the east (Korotaev et al., 2006).

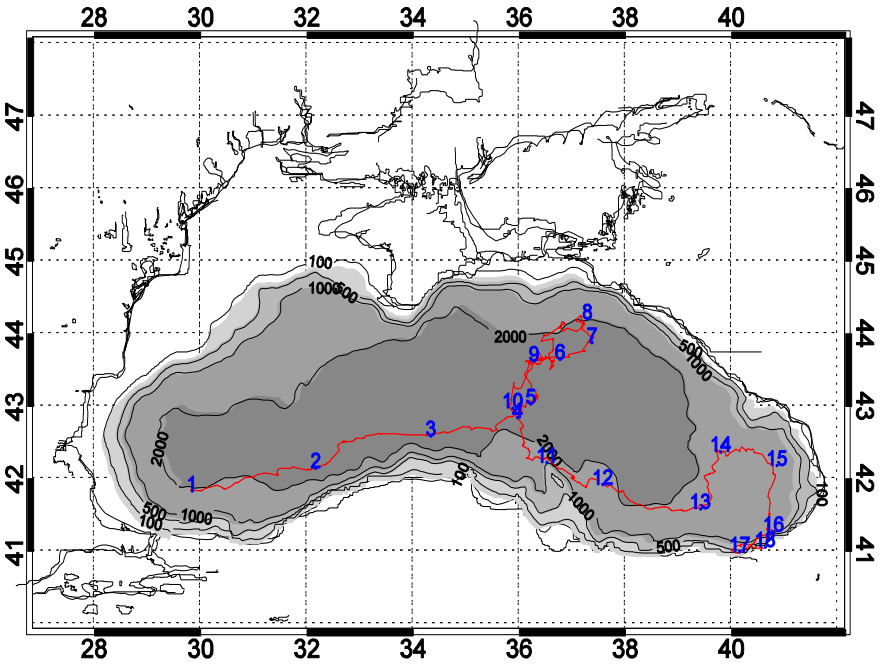

Figure 3. 5 Trajectory of the float 0631 (red line) with 17 float locations marked by numbers. Details about the locations are given in Table 3.2. Grey shading represents the bathymetry contours of 100m, 500m, 1000m, and 2000m.

Starting from February 2003 ("5" in Fig. 3.5) , the float started moving towards north into a loop, reaching up to the northern periphery of the Rim Current , shown by "8" (Fig. 3.5). 0631 then moved westward with the effect of the cyclonic Rim Current system until July. Starting from July 2003, 0631 started moving south, probably with the currents associated with the western flank of the Eastern Gyre, reaching location "10" at the end of October 2003. After this point, the float moved southeast and reached "11" in one month. Float 0631 then started to move along the main axis of the Rim Current once again, moving eastward reaching "13" on March 2004. Soon after reaching "13", the float moved north, along the eastern flank of the Rim Current until June. Starting from June 2004, float 0631 moved along the periphery of the Batumi anticyclonic eddy. Following the axis of the Batumi eddy, the float first moved towards east and then moved to the south.

Table 3. 2 Float 0631 location numbers as seen Figure 3.5

Number	Corresponding date(dd/mm/yy)	Longitude	Latitude
1	02.09.02	29.83	41.83
2	23.10.02	32.04	41.03
3	20.12.02	34.33	42.59
4	09.02.03	35.83	42.82
5	02.03.03	36.22	43.03
6	30.04.03	36.75	43.67
7	21.05.03	37.43	43.92
8	19.06.03	37.25	44.25
9	06.10.03	36.28	43.57
10	28.10.03	35.92	43.07
11	03.12.03	36.39	42.27
12	23.01.04	37.56	41.94
13	21.03.04	39.32	41.59
14	25.05.04	39.79	42.35
15	22.07.04	40.76	42.21
16	03.10.04	40.84	41.31
17	22.11.04	40.04	41.02
18	21.12.04	40.61	41.07

Float 0634 (Fig. 3.6) started moving eastward after its deployment. During the first two months, the float drifted very slowly indicating entrapment in the Western Gyre (Korotaev et al., 2006). Float 0634 kept moving eastward until it reached point “6” (Fig. 3.7) in January 2003. The float then moved south, reaching the coast in February and resided where the main axis of the Rim Current lies. The float kept drifting eastward moving close to the Batumi Gyre reaching “8” in March 2003, though it was not entrapped in the region

suggesting the absence of the Batumi Gyre at the time. Drifting along the outer edge of the Batumi Gyre, the float moved to the north reaching “9” at the end of March 2003, and then moved westward, getting close to the main axis of the Rim Current and the Eastern Gyre. Float 0634 then moved to the north again and went into an eddy, known as the Caucasian eddy. It was trapped for nearly five months in this eddy.

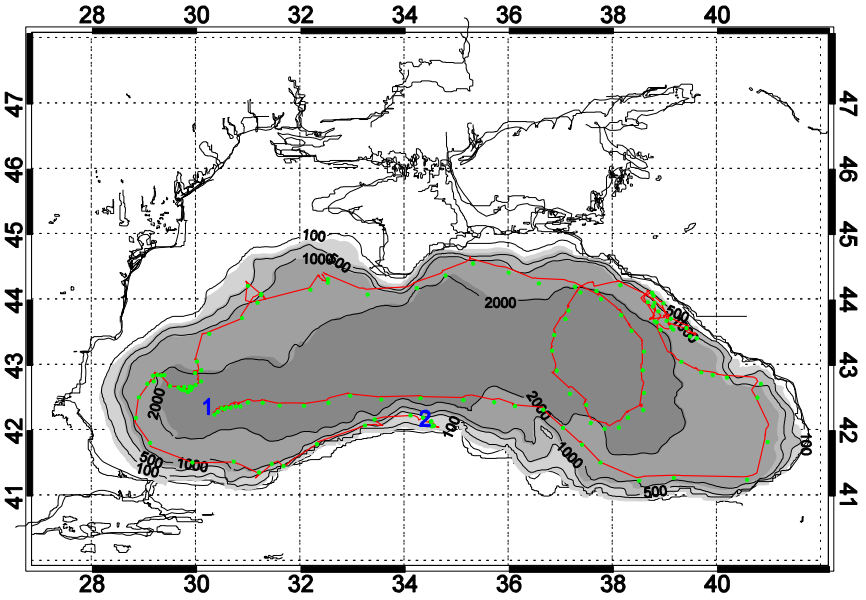

Figure 3. 6 Trajectory of the float 0634 (red line) with “1” and “2” representing start and end respectively. Green dots mark the locations of profiles taken every seven to ten days. Grey shading represents the bathymetry contours of 100m, 500m, 1000m, and 2000m.

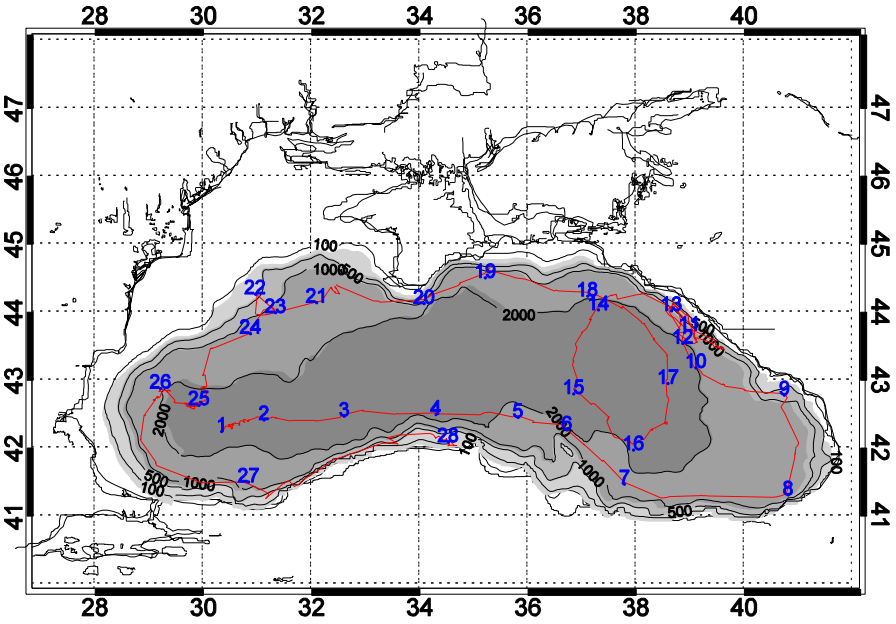

Figure 3. 7 Trajectory of the float 0634 (red line) with 28 float locations marked by numbers. Details about the locations are given in Table 3.3. Grey shading represents the bathymetry contours of 100m, 500m, 1000m, and 2000m.

0634 then left the eddy, continuing its drift westward and later south in October ("14" in Fig. 3.7), along the western edge of the Eastern Gyre. Float 0634 kept following the axis along the periphery of the Eastern Gyre and moved back to the north along the eastern flank of the Eastern Gyre. Leaving the Eastern Gyre, the float moved to the west towards the Crimean coast. Following the main axis of the Rim Current system, the float then reached the point shown with "21" in Figure 3.7, where the Rim Current bifurcates. The float followed the southern branch of the Rim Current and kept moving along the Rim Current, going into a very small eddy which corresponds to "22" and "23" in Figure 3.7. The float then kept moving south, most of the time except the movement at the region corresponding to "25" in Figure 3.7 where the float crossed the 2000 m isobath, suggesting the effect of the Western Gyre. Although the float moved towards the Western Gyre, it was not trapped in it. 0634 then followed the main axis of the Rim Current at the southern coast once again and followed the coast towards the east until it died close to Sinop.

Table 3. 3 Float 0634 location numbers as seen in Figure 3.7

Number	Corresponding date(dd/mm/yy)	Longitude	Latitude
1	02.09.02	30.33	42.24
2	31.10.02	30.97	42.43
3	29.11.02	32.52	42.43
4	20.12.02	34.29	42.50
5	04.01.03	35.71	42.43
6	18.01.03	36.65	42.32
7	09.02.03	37.75	41.51
8	03.03.03	40.56	41.25
9	25.03.03	40.83	42.72
10	15.04.03	39.30	43.05
11	23.04.03	38.90	43.54
12	22.05.03	39.14	43.55
13	22.09.03	38.78	43.96
14	13.10.03	37.36	44.12
15	19.11.03	36.90	42.92
16	18.12.03	37.83	42.03
17	23.01.04	38.56	42.92
18	28.02.04	37.26	44.20
19	21.03.04	35.30	44.56
20	05.04.04	34.22	44.19
21	03.05.04	32.18	44.16

22	18.05.04	30.98	44.22
23	25.05.04	31.24	44.08
24	09.06.04	30.87	43.72
25	27.08.04	29.89	42.62
26	08.11.04	29.24	42.85
27	05.01.05	30.70	41.53
28	17.04.05	34.51	42.06

Floats 1325 and 1550 were released on 07.03.2005 in the western part of the Black Sea, offshore of the Bosphorus strait. 1325 was released at 41.88°N, 29.50°E, just on the edge of the 2000m isobath and near the southern edge of the Western Gyre. Float 1325 was programmed to drift at 500 meters parking depth (Fig.3.8).

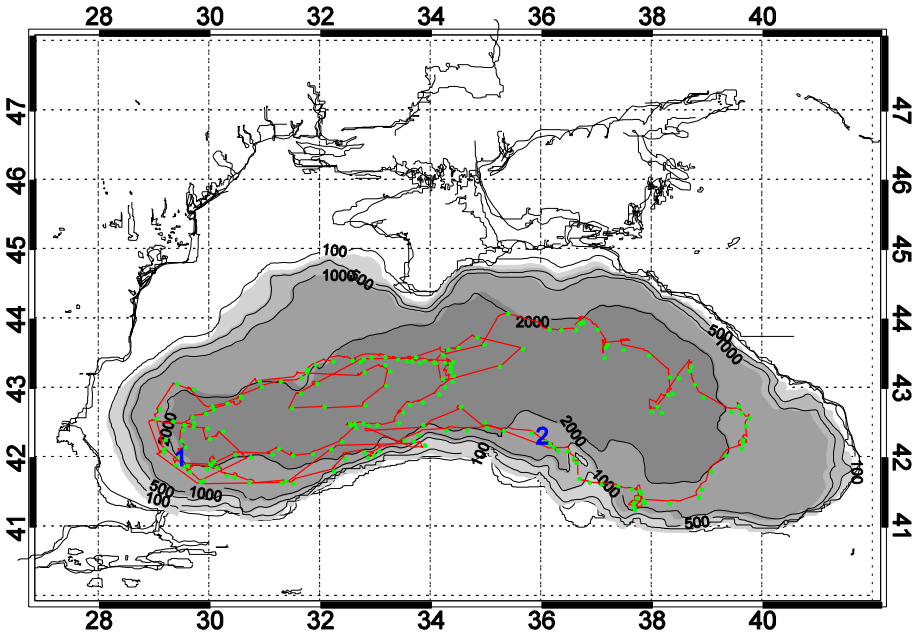

Figure 3.8 Trajectory of the float 1325 (red line) with "1" and "2" representing start and end respectively. Green dots mark the locations of profiles taken every seven to ten days. Grey shading represents the bathymetry contours of 100m, 500m, 1000m, and 2000m.

After its deployment in March 2005, float 1325 started to move eastward, following the 2000m isobath for one month, and then moving into the 2000m isobath (Fig. 3.9). Right after this intrusion, the float keeps moving northeast, suggesting entrapment in the Western Gyre. Following the eastern end of the Western Gyre, 1325 reached the northern periphery of the Western Gyre on 16.11.05 ("5" in Fig. 3.9). 1325 kept following the main axis of the Western Gyre until it reached the western boundary of the Western Gyre on 10.04.06. If "2" in Figure 3.9 is accepted as the entrapment date of the float in the Western Gyre and "8" is accepted as the exit point, then it can be said that the float was trapped in the Western Gyre for a year. After leaving the Western Gyre at point "8", 1325 started to move to the south and then followed the 2000m isobath for a few weeks and then resided on the main axis of the Rim Current, thereafter it started to move eastward reaching "11", just off Cape Sinop on 06.11.06.

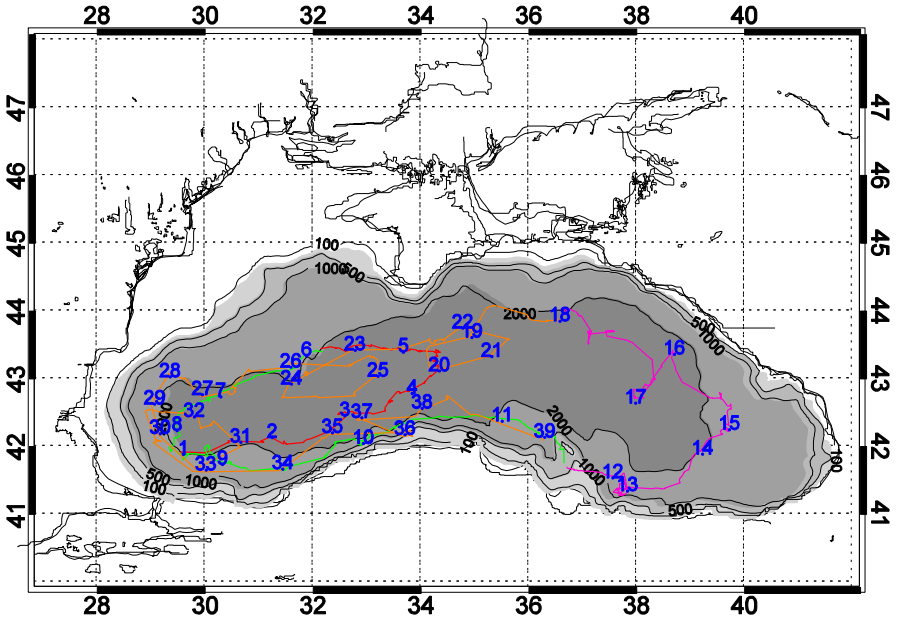

Figure 3. 9 Trajectory of the float 1325 (red line) with 39 float locations marked by numbers. Details about the locations are given in Table 3.3. Grey shading represents the bathymetry contours of 100m, 500m, 1000m, and 2000m.

Following the main axis of the Rim Current, 1325 kept moving southeast until it was trapped within an eddy at “13”. This eddy is most probably the small cyclonic eddy found from the analysis of the altimeter data (Korotaev et al., 2003), shown in Figure 1.2. Detaching from this eddy, 1325 kept moving along the axis of the Rim Current, moving northeast. After the point shown with “16” (Fig. 3.9), 1325 drifted into the Eastern Gyre, most probably via the cyclonic movement of the eastern component of the Eastern Gyre and leaving the Eastern Gyre with the cyclonic movement of the western component of the Eastern Gyre and again residing on the axis of the Rim Current. 1325 then started to move towards the Crimea eddy but then moved into an eddy on 06.02.08, which is most probably the cyclonic eddy residing between the Eastern Gyre and the Western Gyre. Leaving this eddy on 13.03.08 (“22” in Fig. 3.9), it moved westward again, followed by an entrapment in the Western Gyre right after passing “23”. Leaving the Western Gyre, the float moved westward reaching the point shown by “28” (Fig. 3.9). After this point, 1325 moved south along the 2000m isobath until it was entrapped once again by the Western Gyre, this time by the western flank of the Western Gyre. Completing the cyclonic movement of the western flank of the Western Gyre, the float once again resided on the main axis of the Rim Current and followed this axis (except small intrusions into the 2000m isobath) until it died. The trajectory of the float 1325 is an excellent example, illustrating not only the main circulation but also the quasi-permanent features of the Black Sea clearly.

Table 3. 4 Float 1325 location numbers as seen in Figure 3.9

Number	Corresponding date(dd/mm/yy)	Longitude	Latitude
1	07.03.05	29.59	41.88
2	12.04.05	31.25	42.13
3	18.05.05	32.64	42.42
4	30.07.05	33.84	42.80
5	16.11.05	33.65	43.39
6	13.01.06	31.90	43.34
7	25.02.06	30.31	42.78

8	10.04.06	29.48	42.25
9	21.06.06	30.30	41.74
10	02.09.06	32.79	42.08
11	06.11.06	35.31	42.39
12	25.01.07	37.38	41.59
13	02.03.07	37.85	41.35
14	14.05.07	39.06	41.79
15	19.06.07	39.64	42.26
16	07.09.07	38.70	43.31
17	06.10.07	37.98	42.66
18	07.01.08	36.62	43.84
19	06.02.08	34.96	43.63
20	20.02.08	34.21	43.14
21	27.02.08	35.24	43.31
22	13.03.08	34.83	43.74
23	10.04.08	32.78	43.42
24	25.04.08	31.65	42.92
25	24.05.08	33.18	43.03
26	23.06.08	31.75	43.23
27	21.07.08	30.04	42.74
28	05.08.08	29.40	43.06
29	12.08.08	29.08	42.70

30	20.08.08	29.18	42.25
31	03.09.08	30.73	42.00
32	02.10.08	29.70	42.45
33	14.11.08	29.82	41.65
34	21.11.08	31.38	41.67
35	29.11.08	32.19	42.13
36	13.12.08	33.88	42.18
37	21.12.08	32.86	42.46
38	28.12.08	33.85	42.47
39	19.01.09	36.13	42.20

Float 1550 was deployed at 41.87 ^{o}N, 29.56^{o}E to a parking depth of 1000m on the same date on 07.03.05, with float 1325. It started moving eastward along the main axis of the Rim Current and with a deflection towards offshore after Cape Sinop, it reached the point shown with “3” in Figure 3.11 at the end of July 2005. After this point, the float followed an axis parallel to the 2000m isobath, reaching the point shown with “4” on November 2005. Right after point “5” shown in Figure 3.11, the float was trapped in an eddy for 3 months. Then it moved to the east and was entrapped by another eddy on October 2006 and stayed in the same eddy until August 2007(“8” in Figure 3.11). Leaving this eddy, 1550 moved towards west and resided on the main axis of the Rim Current reaching “11” on December 2007. Float 1550 then followed the main circulation system and died in the western Black Sea, close to the northwestern flank of the Rim Current.

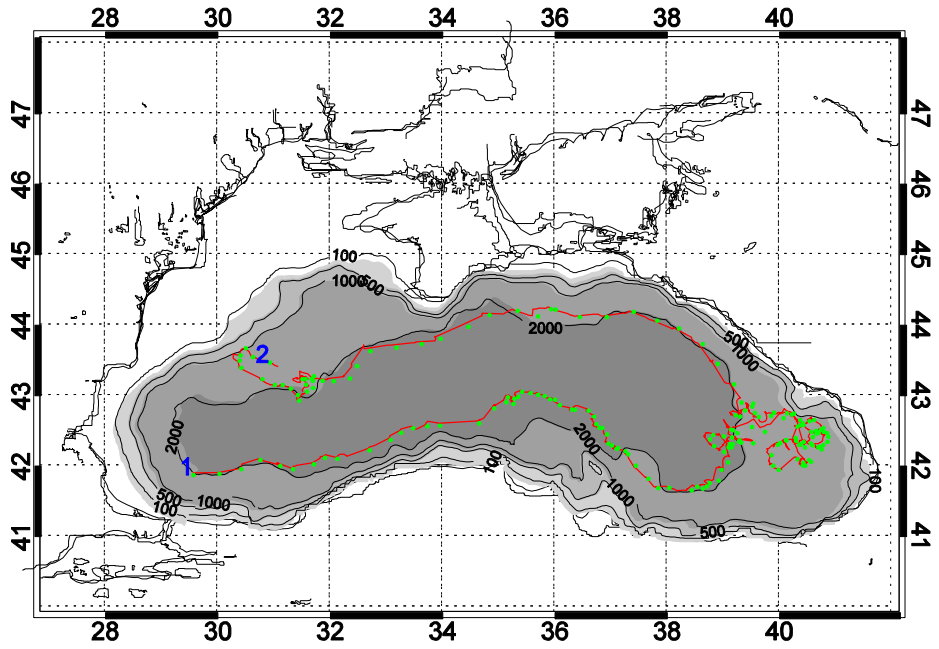

Figure 3.10 Trajectory of the float 1550 (red line) with "1" and "2" representing start and end respectively. Green dots mark the locations of profiles taken every seven to ten days. Grey shading represents the bathymetry contours of 100m, 500m, 1000m, and 2000m.

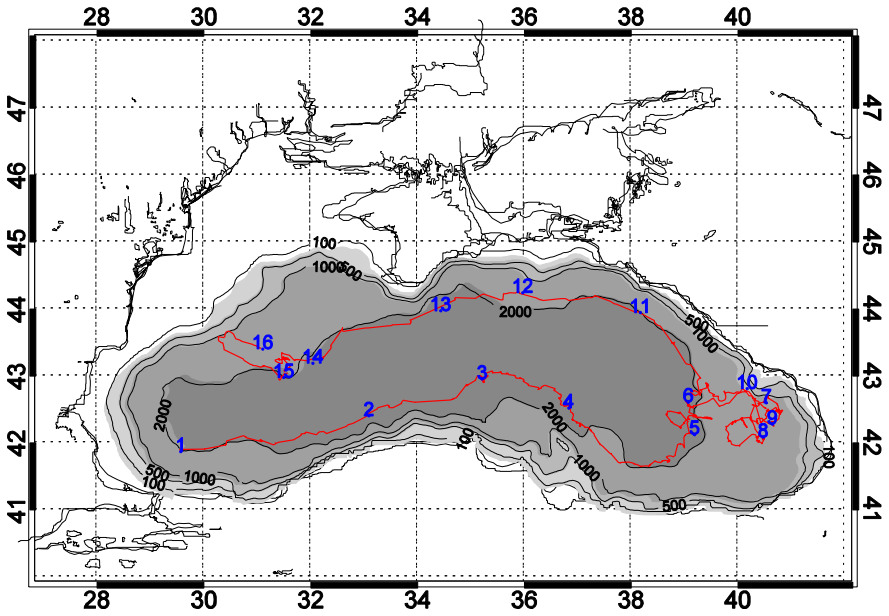

Figure 3.11 Trajectory of the float 1550 (red line) with 16 float locations marked by numbers. Details about the locations are given in Table 3.3. Grey shading represents the bathymetry contours of 100m, 500m, 1000m, and 2000m.

Table 3. 5 Float 1550 location numbers as seen in Figure 3.11

Number	Corresponding date(dd/mm/yy)	Longitude	Latitude
1	07.03.05	29.56	41.87
2	19.05.05	33.08	42.37
3	30.07.05	35.28	42.96
4	16.11.05	36.79	42.55
5	10.04.06	39.08	42.05
6	28.07.06	39.17	42.51
7	30.10.06	40.53	42.64
8	25.01.07	40.41	42.05
9	07.04.07	40.58	42.29
10	30.08.07	40.25	42.74
11	17.12.07	38.20	43.95
12	22.01.08	36.01	44.22
13	27.02.08	34.46	43.98
14	18.04.08	32.05	43.21
15	07.07.08	31.44	42.93
16	02.10.08	30.92	43.47

Float 2206 was deployed on 12.06.06 at a parking depth of 1550 meters at 42.14^{o}N, 30.36^{o}E. Float 2206 started to move eastward after it was deployed inside the 2000m isobath in the western Black Sea, very close to the Western Gyre, eventually getting entrapped in the Western Gyre. 2206 kept moving eastward, and then started to move north along the axis of the Western Gyre, reaching point “3” in Figure 3.13 on December

2006. Passing through this point, the float reached “4” which is the northern boundary of the Western Gyre on February 2007. After reaching the northern part of the Western Gyre, it started to move southeast, mainly following the northern flank of the Western Gyre. The float then moved north again, arriving “5” at the end of July 2007. Going through a very small eddy, the float started to move south again along the western boundary of the Western Gyre. After reaching the 2000m isobath at point “7” on December 2007, the float started moving eastward along the southern edge of the Western Gyre. 2206 mainly followed an axis parallel to the 2000m isobath and reached the point “8” on January 2008. Leaving this location, the float was deflected from this parallel axis and it started to move northeast. It then reached the point shown with “9” on February 2008, then moving north along the eastern edge of the Western Gyre reaching “10” on May 2008. Although the distance between “9” and “10” is relatively small, it took the float 3 months to travel this distance. This is mainly due to entrapment in the small eddy located between these points.

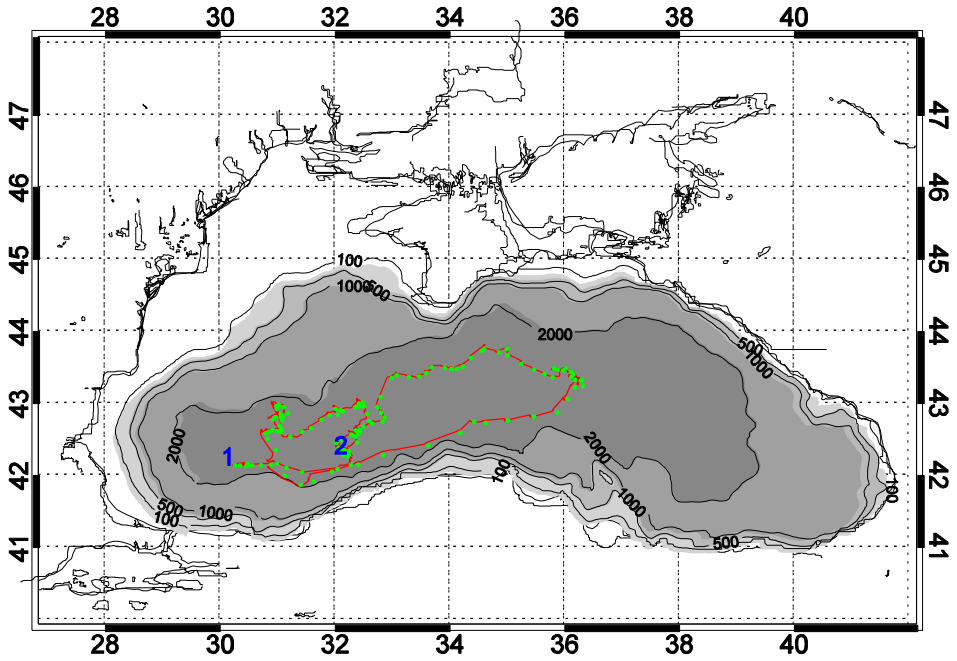

Figure 3.12 Trajectory of the float 2206 (red line) with “1” and “2” representing start and end respectively. Green dots mark the locations of profiles taken every seven to ten days. Grey shading represents the bathymetry contours of 100m, 500m, 1000m, and 2000m.

Following the cyclonic movement, the float moved to the west along the northern boundary of the Western Gyre and reached “13” on November 2008. It was then deflected south again and died inside the Western Gyre on February 2009. 2206 was the float which clearly showed the circulation path of the Western Gyre with its components.

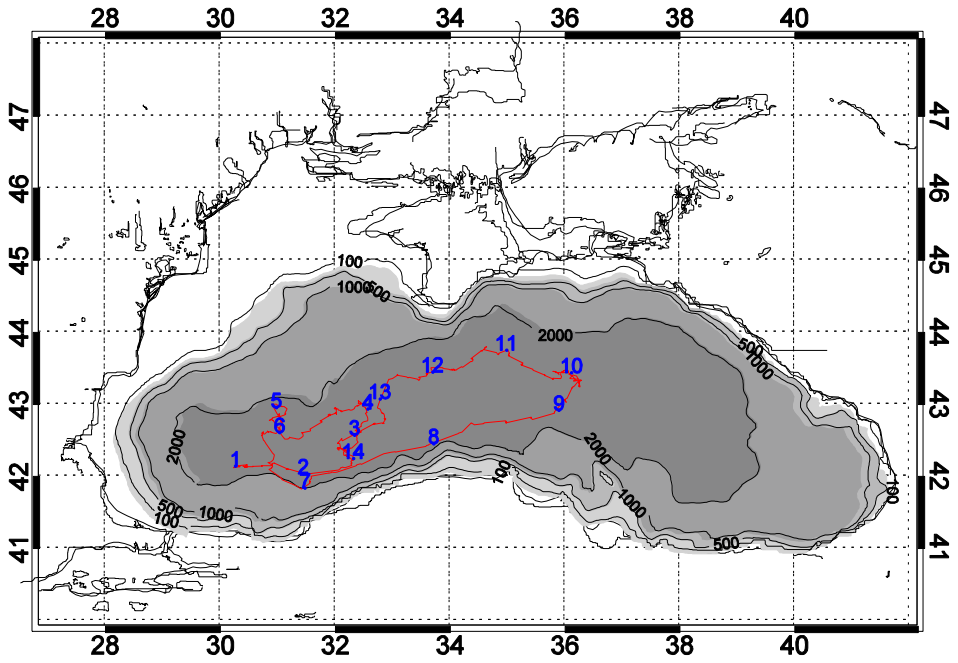

Figure 3.13 Trajectory of the float 2206 (red line) with 14 float locations marked by numbers. Details about the locations are given in Table 3.3. Grey shading represents the bathymetry contours of 100m, 500m, 1000m, and 2000m.

Table 3. 6 Float 2206 location numbers as seen in Figure 3.13

Number	Corresponding date(dd/mm/yy)	Longitude	Latitude
1	12.06.06	30.26	42.14
2	16.08.06	31.42	42.05
3	10.12.06	32.28	42.57
4	21.02.07	32.56	42.86
5	23.07.07	30.98	42.97

6	03.10.07	31.05	42.62
7	08.12.07	31.41	41.87
8	13.01.08	33.62	42.42
9	25.02.08	35.87	42.88
10	01.05.08	36.10	43.44
11	12.07.08	34.99	43.76
12	23.09.08	33.67	43.51
13	12.11.08	32.79	43.79
14	15.02.09	32.23	42.30

Float 2619 was deployed at the same date with 2206 on 12.06.06 at the same location and with the same parking depth at 1550 meters (Fig. 3.14). Similar to float 2206, 2619 also started to move eastward after deployment, though it was not entrapped in the Western Gyre as 2206. 2619 reached “2” (Fig. 3.15) in September 2006 which is approximately three months after deployment. 2619 followed an axis parallel to the 2000m isobath, which was also observed in float 2206, thus revealing the topographic control on the circulation at 1550 m depth. Following the parallel axis, 2619 reached “3” (Fig. 3.15) after another three months in December 2006. After this point, float 2619 stopped following its parallel axis and kept moving eastward following the main axis of the Rim Current, reaching “5” on June 2007 (Fig. 3.15). 2619 continued to move east until it reached the point shown by “7” (Fig. 3.15) in January 2008. After this point, it started to move in northeast direction and reached “8”on February 2008. Passing through the Batumi region, it started moving westward first and after it reached the point denoted by “10” on August 2008, it was entrapped by the Eastern Gyre and died there.

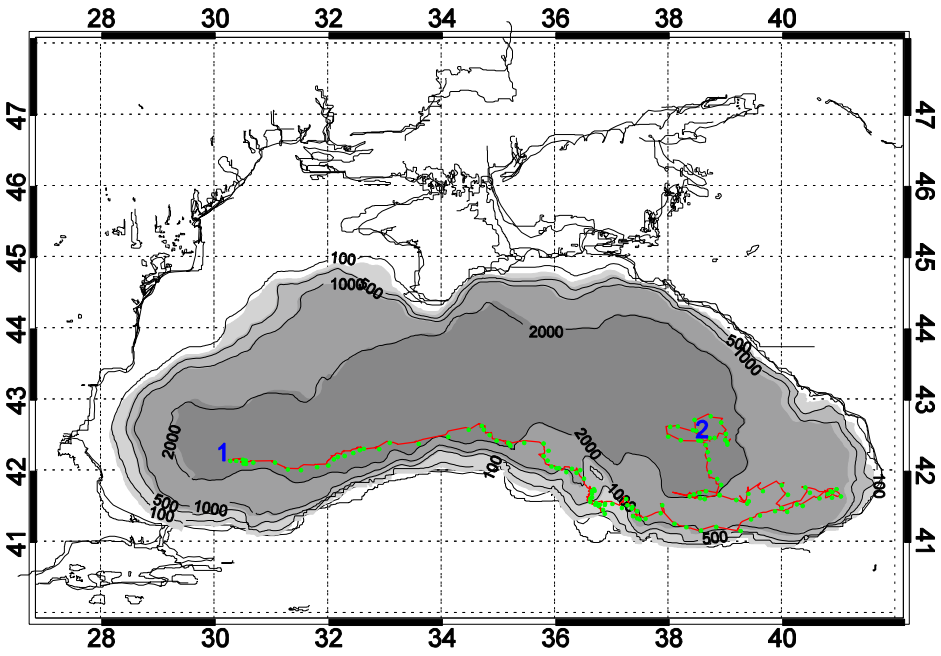

Figure 3. 14 Trajectory of the float 2619 (red line) with "1" and "2" representing start and end respectively. Green dots mark the locations of profiles taken every seven to ten days. Grey shading represents the bathymetry contours of 100m, 500m, 1000m, and 2000m.

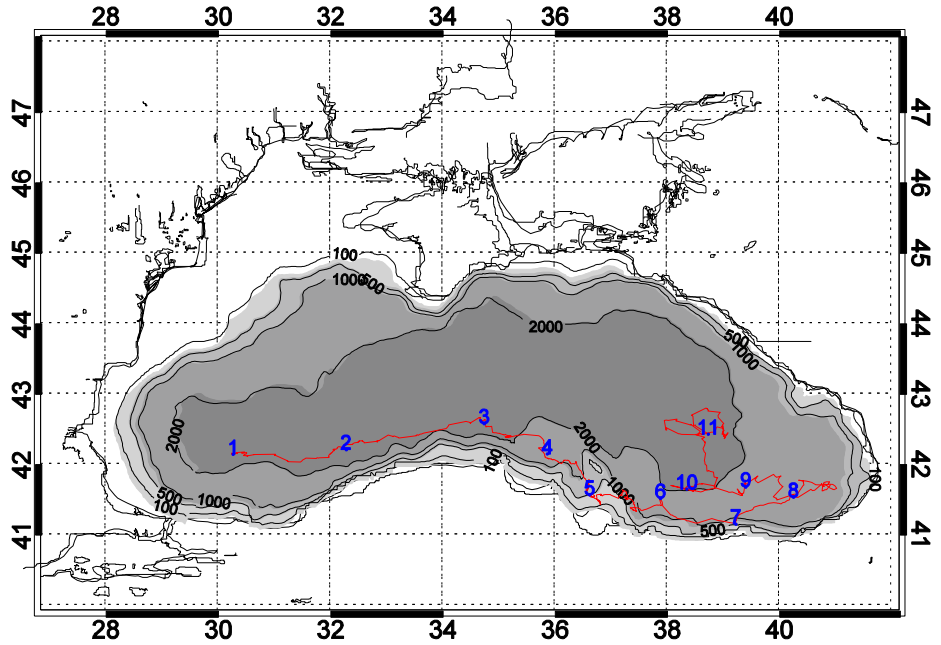

Figure 3. 15 Trajectory of the float 2619 (red line) with 11 float locations marked by numbers. Details about the locations are given in Table 3.3. Grey shading represents the bathymetry contours of 100m, 500m, 1000m, and 2000m.

Table 3. 7 Float 2619 location numbers as seen in Figure 3.15.

Number	Corresponding date(dd/mm/yy)	Longitude	Latitude
1	12.06.06	30.26	42.15
2	28.09.06	32.27	42.21
3	10.12.06	34.73	42.58
4	20.02.07	35.85	42.15
5	09.06.07	36.61	41.57
6	07.12.07	37.87	41.52
7	06.01.08	38.83	41.22
8	18.02.08	40.24	41.54
9	06.06.08	39.39	41.68
10	03.08.08	38.35	41.65
11	15.02.09	38.71	42.47

3.2 Temperature and salinity profiles

The Argo floats provide information on the physical properties of the water mass in which they are drifting. In this section composite profiles of temperature and salinity are shown for each float. Each composite-plot contains all the data profiles sent by the float at locations marked by green dots in Figures 3.2, 3.4, 3.6, 3.8, 3.10, 3.12, and 3.14. The 200 meter upper layer was plotted separately in order to see the properties of the upper layer water clearly. Figures 3.16-3.29 illustrate the composite temperature and salinity profiles for each float separately.

Float 0587 shows a wide range of surface temperature measured (Fig. 3.16) though the values are compatible with the general characteristics of the Black Sea, with warm surface waters cooling down to below 8 ^{o}C which corresponds to the CIL, and then warming up once again to ~9 ^{o}C. Salinity measurements from this float (Fig. 3.17) are also similar to the general properties of the Black Sea, starting with less saline waters at the surface (17-18 psu) and gradually becoming more saline with depth, eventually increasing up to 22 psu.

Profiles from the other floats (Fig. 3.18 – 3.29) show a similar pattern, with a wide range of temperature measurements compatible with the general characteristics of the Black Sea. In the temperature profiles of each float, the Cold Intermediate Layer can be clearly seen in most of the profiles.

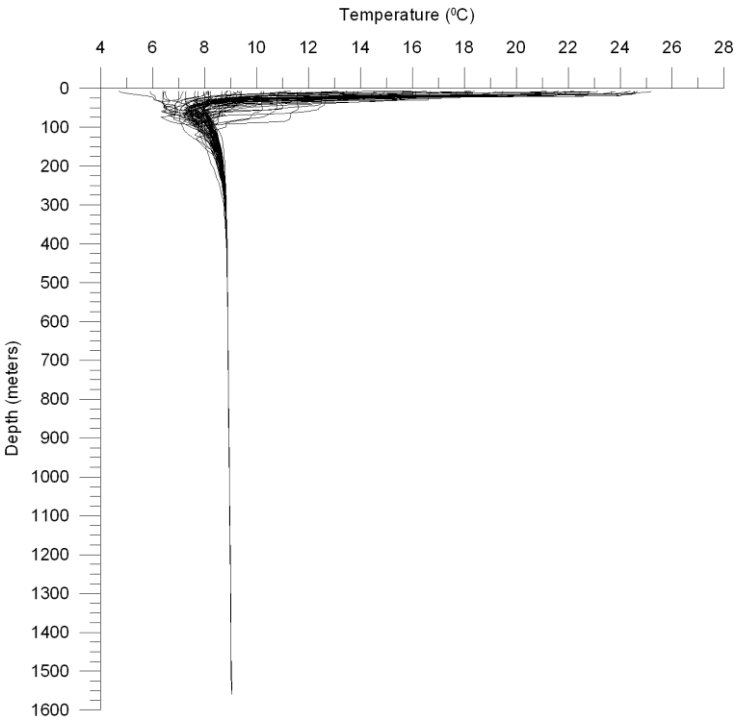

Figure 3. 16 Composite Temperature profile for float 0587

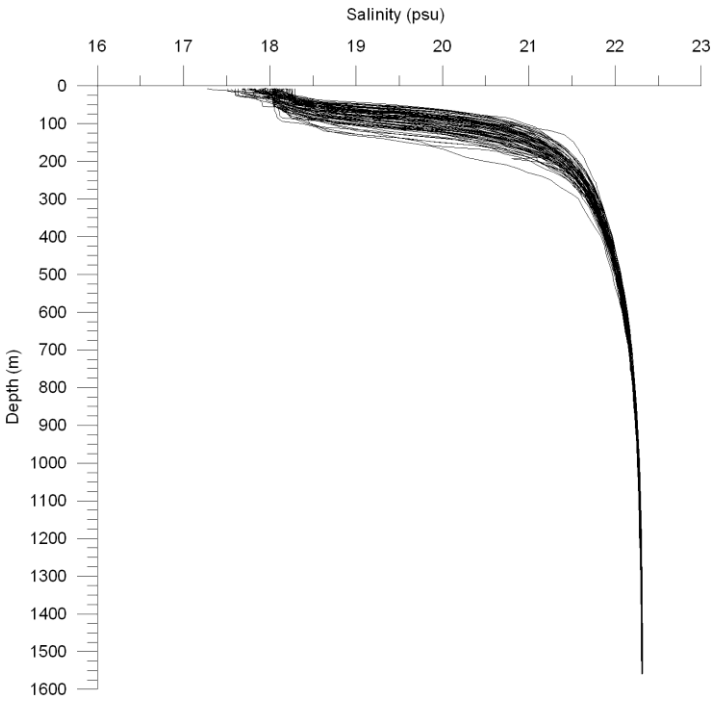

Figure 3. 17 Composite Salinity profile for float 0587

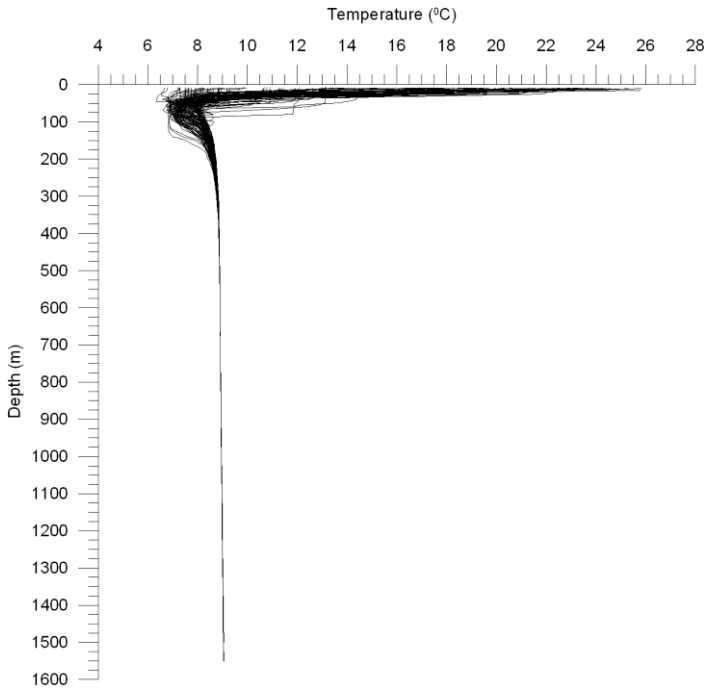

Figure 3. 18 Composite Temperature profile for float 0631

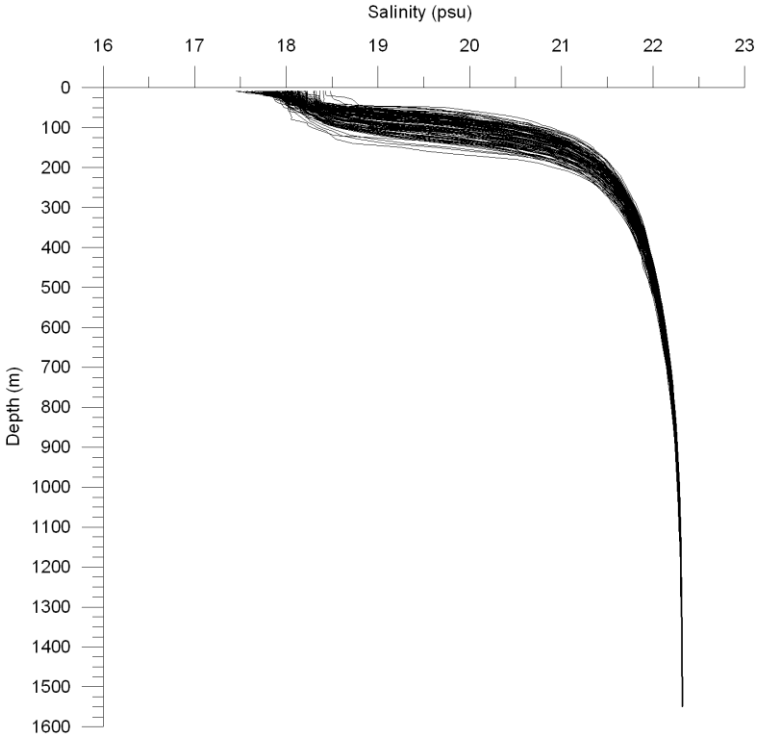

Figure 3. 19 Composite Salinity profile for float 0631

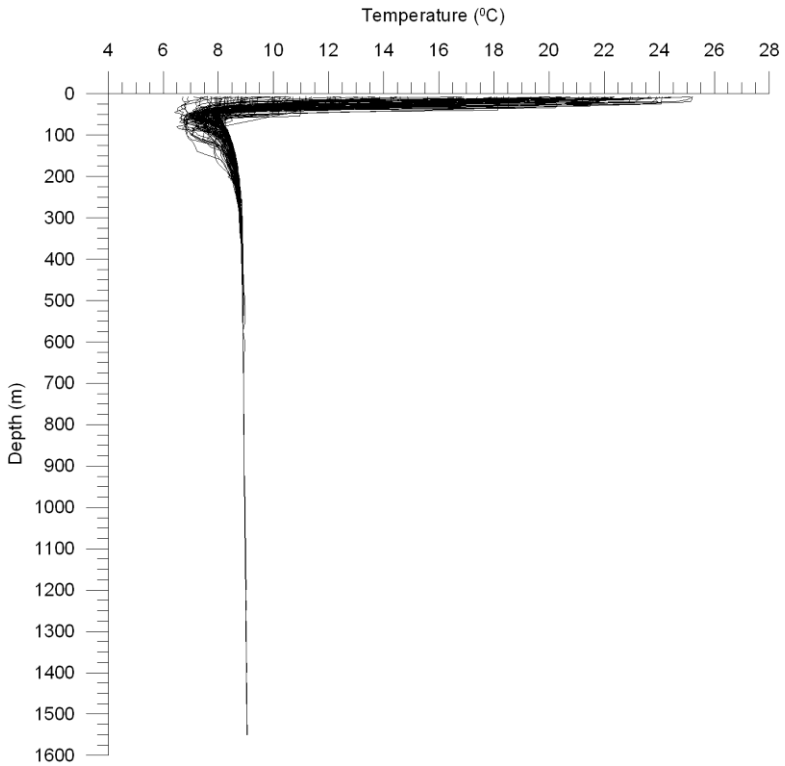

Figure 3. 20 Composite Temperature profile for float 0634

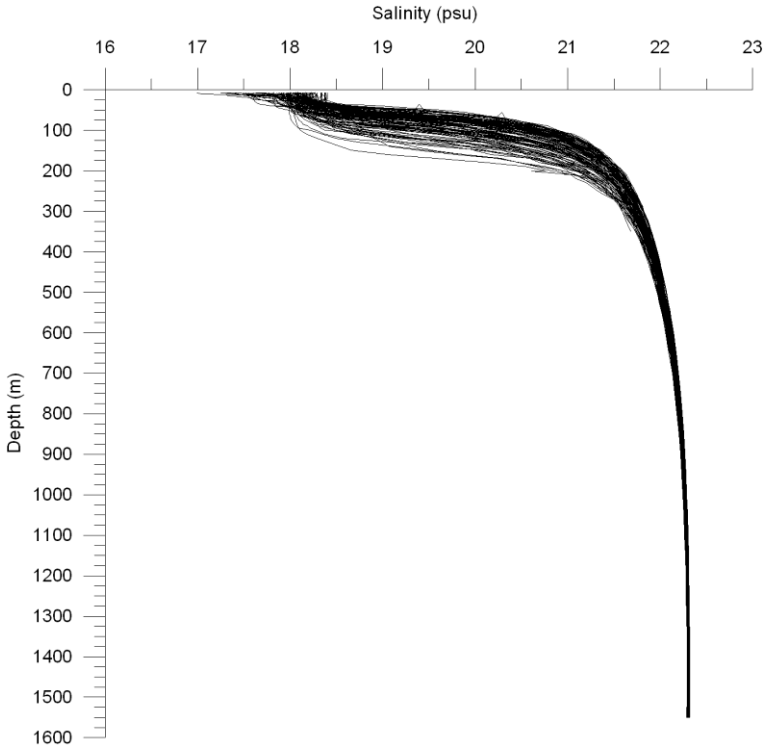

Figure 3. 21 Composite Salinity profile for float 0634

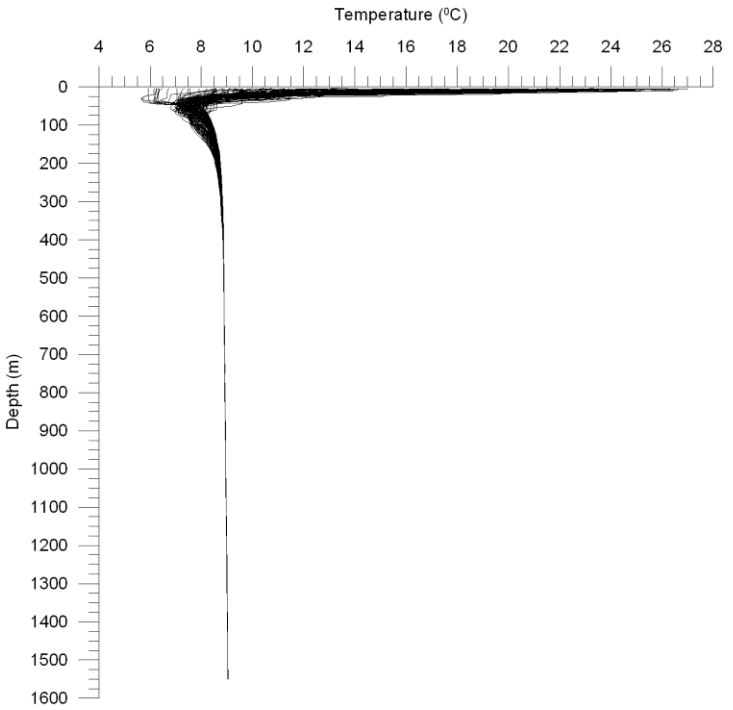

Figure 3. 22 Composite Temperature profile for float 1325

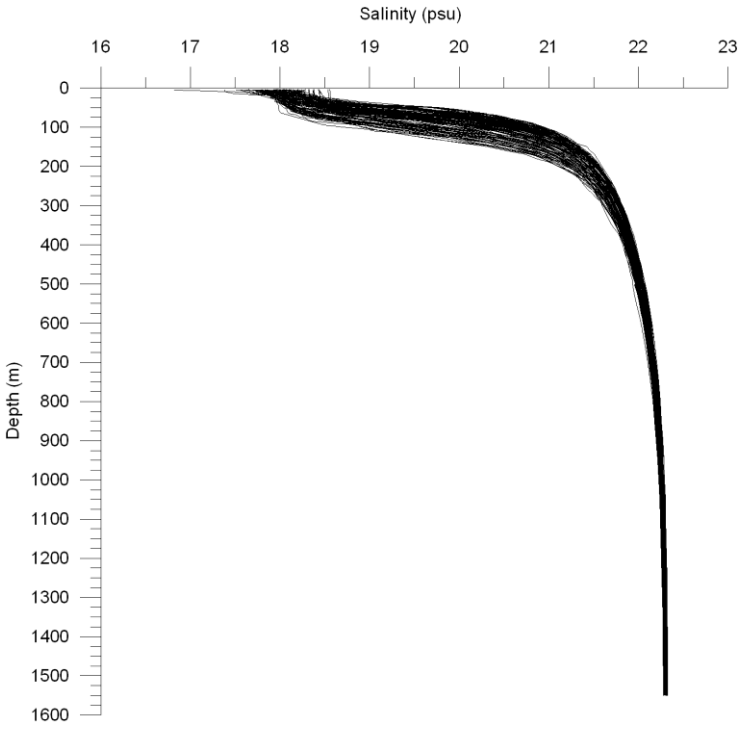

Figure 3. 23 Composite Salinity profile for float 1325

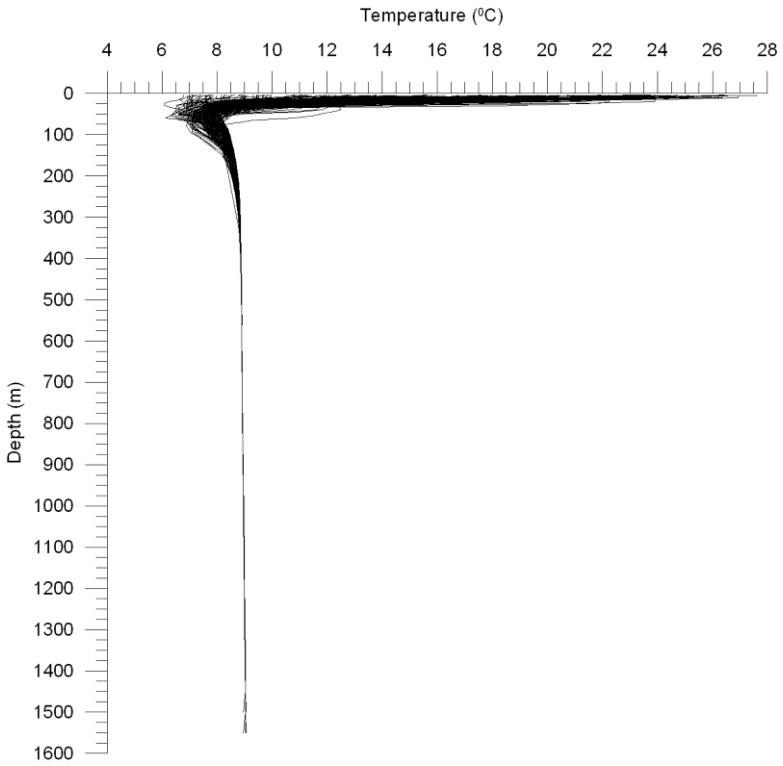

Figure 3. 24 Composite Temperature profile for float 1550

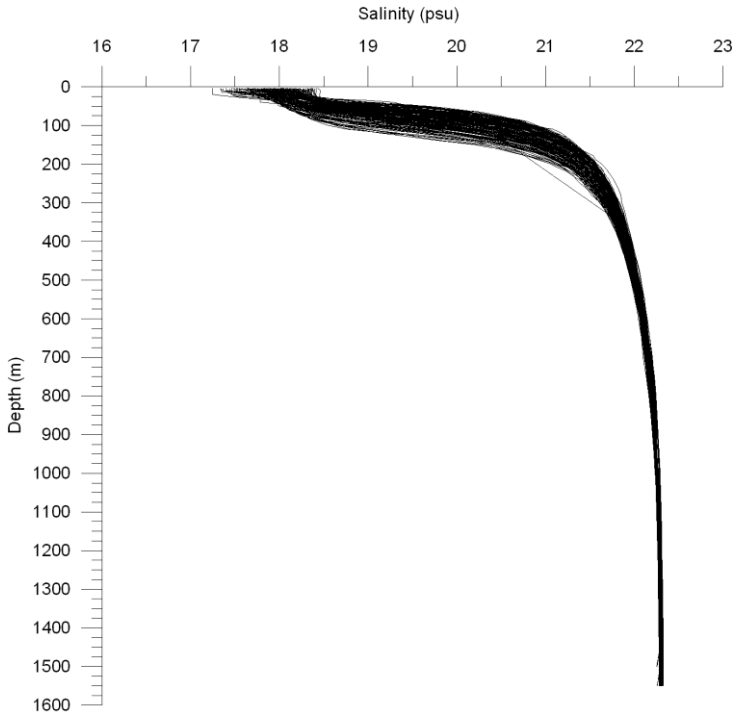

Figure 3. 25 Composite Salinity profile for float 1550

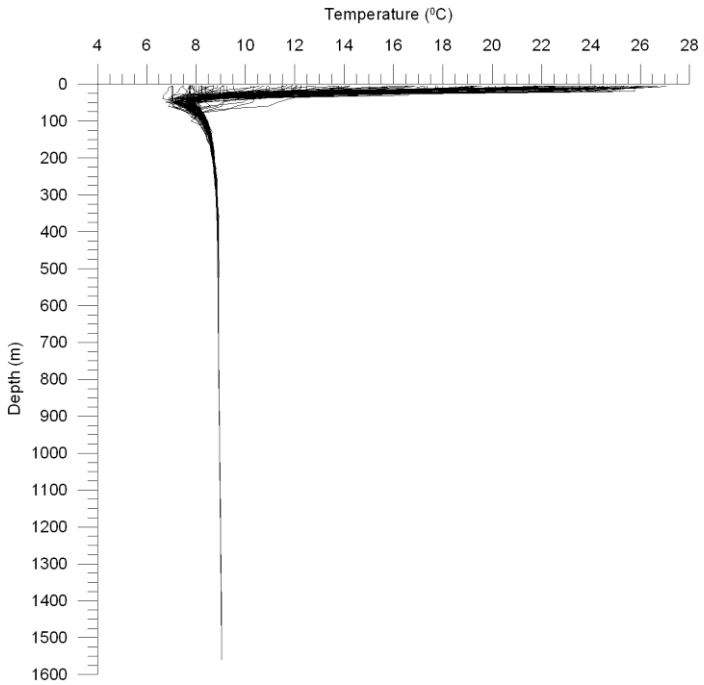

Figure 3. 26 Composite Temperature profile for float 2206

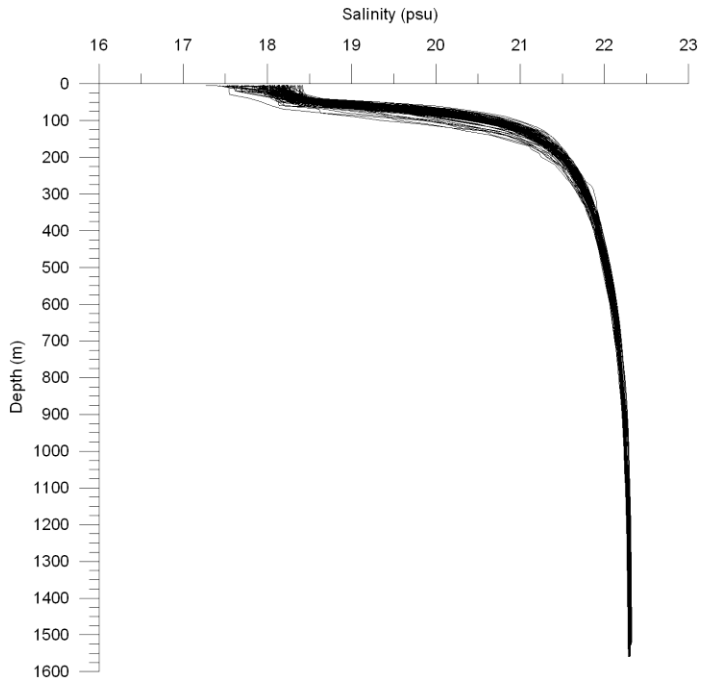

Figure 3. 27 Composite Salinity profile for float 2206

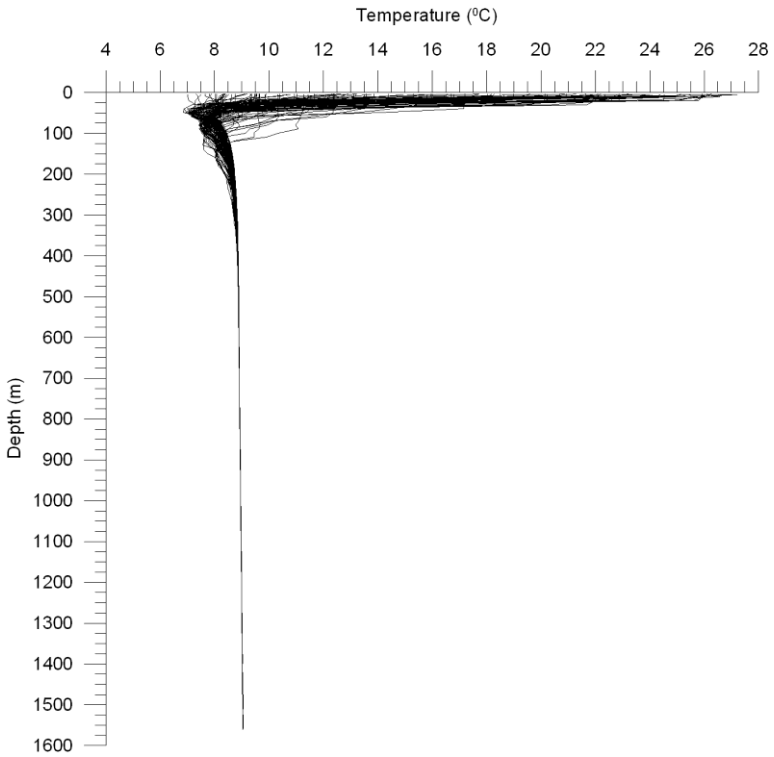

Figure 3. 28 Composite Temperature profile for float 2619

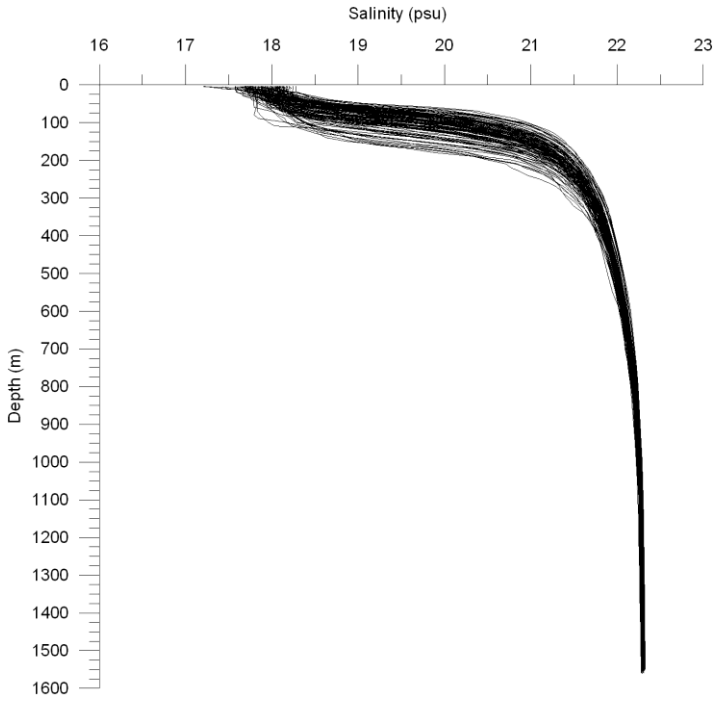

Figure 3. 29 Composite Salinity profile for float 2619

3.3 Surface Properties

In this section, the surface properties of the Black Sea extracted from the data set is described. Temperature data at the surface reveals a seasonal cycle, which can be clearly seen in Figure 3.44. This cycle starts with low values at ~7 ^{o}C, reaching up to 25 ^{o}C in July-August. This cycle shows an increasing trend, with its upper boundary increasing from 25^{o}C to 27 ^{o}C. At this point it is important to note that the first peak of this cycle (~25 ^{o}C) is measured by floats 0587-0631-0634 in 2003 which is known as one of the coldest years of the last decade. This is further confirmed with the lowest temperature measurements. There is also the fact that the positions of the floats vary, for example in July-August 2004, 0634 was at 42.8^{o} N, 30.1^{o} E which is close to the Western Gyre, whereas 0631 was at 42.1^{o} N, 40.9^{o} E which is in the east, close to Batumi. In this example, 0634 was in a cyclonic region whereas 0634 was in an anti-cyclonic region and it is a known fact from previous studies (Oguz et al., 1993) that the anticyclones have warmer surface temperatures whereas the cyclones contain colder surface temperatures. It can be clearly seen that in July 2004, 0631 has a temperature measurement that is almost 0.5 ^{o}C greater than 0634's temperature measurement (Fig. 3.30). It can be observed that many of the different float temperature measurements coincide, due to close values of the measurements. There are of course low and high values of temperature, which are mainly due to cold seasons or different locations in the Black Sea, respectively. The lowest temperature measurement which is 4.7 ^{o}C was recorded by float 0587 on 03/03/2003 at 42.5^{o} N, 35.5^{o} E (Fig. 3.30).

Salinity data does not show a seasonal cycle (Fig. 3.31), but the salinity varies spatially. As mentioned above, in July 2004, 0631 was in an anticyclone and 0634 was in a cyclone. This difference is also seen in the salinity measurements of these floats. 0634 measures higher salinity values than 0631 suggesting upwelling of subsurface waters in the cyclonic region and down-welling of surface waters in the anticyclone. This situation is also observed with floats 2206 and 2619 (Fig. 3.31). This cyclone and anticyclone effects will be further examined with sea level anomaly maps in the discussion section.

Sigma-theta vs. time at the surface also shows a seasonal cycle with denser surface waters corresponding to spring mainly due to spring stratification whereas the less dense surface waters are observed at the end of the summer (Fig. 3.32).

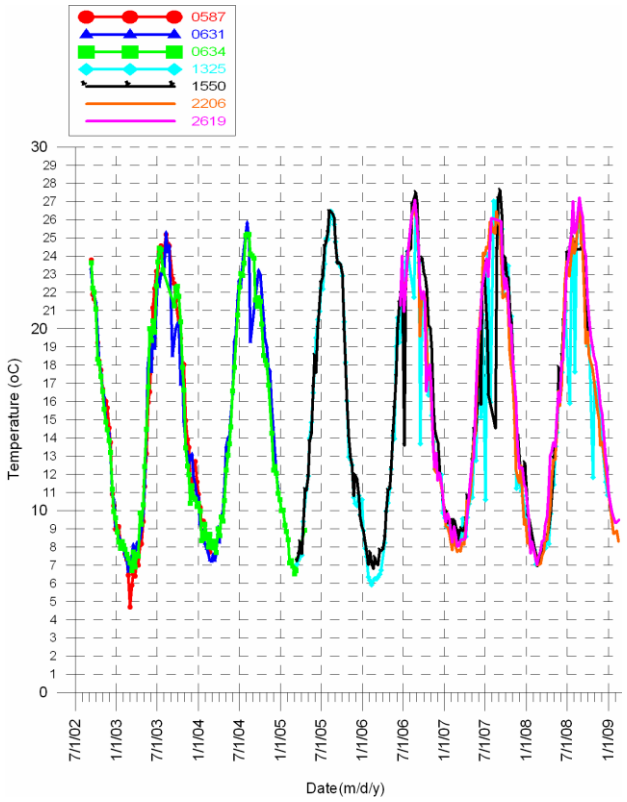

Figure 3.30 Surface temperatures of all floats over time.

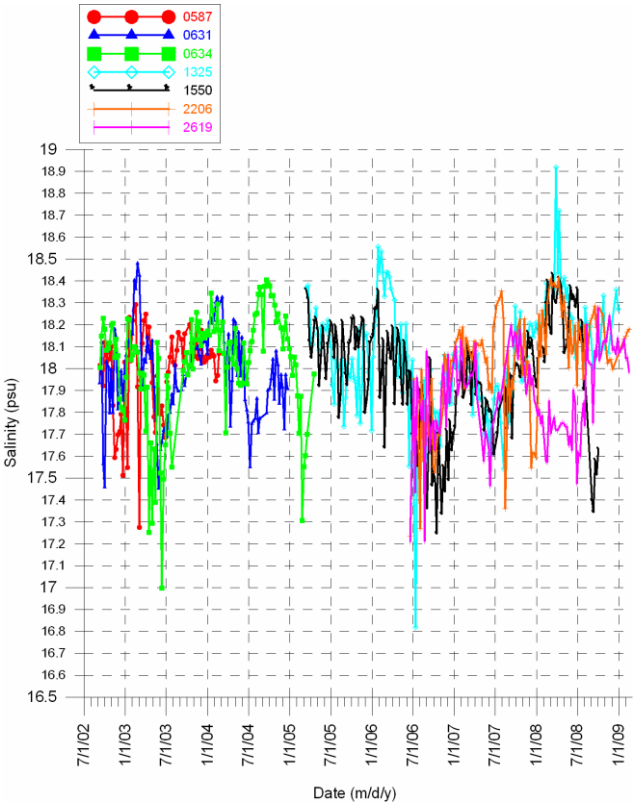

Figure 3. 31 Surface salinity of all floats over time.

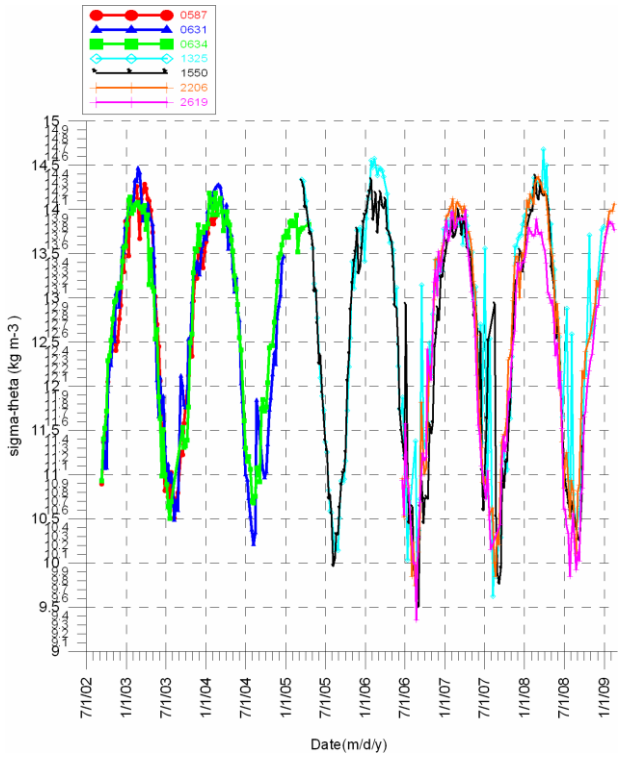

Figure 3.32 Surface density of all floats over time.

3.4 Cold Intermediate Layer (CIL) Properties

The Cold Intermediate Layer is one of the most distinguishing characteristics of the Black Sea, which has been studied frequently. In this section, the CIL properties of the Black Sea, obtained from the Argo floats are given.

The CIL thickness at different depths in the Black Sea varies considerably (Fig. 3.33). The maximum CIL thickness measured was 152.5 meters by float 0634 in February 2005 at 42.08°N, 33.23°E whereas the minimum CIL thickness was measured by the same float in November 2002 on 42.38 °N, 31.58°E. Thicker CIL is observed in March, but there is no seasonal cycle or a specific parameter affecting CIL thickness. Floats 0631 and 0634 have different CIL thicknesses in July 2004 (Fig. 3.33), when the floats were in a cyclone and an anticyclone respectively, as described above (section 3.3). Float 0634 has its CIL lower boundary at ~60 m (Fig. 3.34) at this date with a CIL thickness of ~30 m (Fig. 3.33) whereas float 0631 has its CIL lower boundary at ~140 meters (Fig. 3.34) with a CIL thickness of ~90 m (Fig. 3.33). It is obvious that the CIL is thicker and deeper in anticyclones whereas it is thinner and is at shallower depths because it is suppressed by the upwelling caused by the cyclonic movement. The deepest CIL was found by float 0631 as 159.6 meters in June 2003, at 44.18°N, 37.15°E and by float 0634 as 159.9 meters in February 2005, at 42.08°N,

33.23^{o}E; whereas the shallowest CIL was found by float 2619 on January 2008 at 41.32 ^{o}N, 39.44^{o}E (Fig. 3.34).

Among the average thickness values obtained from the floats, float 2206 has the smallest thickness value which is 29.37 meters. The overall average temperature of the CIL was found as 7.54 ^{o}C (Table 3.8). Similarly, the overall average salinity was calculated as 18.7 psu and the overall average sigma-theta was estimated as 14.55 kg/m^{3} (Table 3.8).

The CIL, and its mean temperature, salinity and density were estimated for each profile individually (Fig 3.35 – 3.37). The CIL waters have temperatures of 7-8 ^{o}C except for extraordinary cases. The lowest temperatures of CIL waters were observed in March (Fig. 3.35). CIL waters generally have a salinity of 18 to 19.5 psu (Fig.3.36). Similarly, sigma-theta of the CIL waters generally varies between 14 to 15 kg/m^{3} (Fig. 3.37).

Table 3. 8 Average Cold Intermediate Layer Properties

Float no.	Mean Depth (m)	Mean Temperature(^{o}C)	Mean Salinity(psu)	Mean Density(kg/m^{3})	Average thickness(m)
0587	61.10	7.46	18.62	14.50	44.66
0631	66.62	7.42	18.62	14.50	54.61
0634	62.24	7.47	18.60	14.48	46.63
1325	73.86	7.57	18.83	14.65	43.56
1550	59.46	7.54	18.75	14.59	47.16
2206	51.24	7.65	18.84	14.65	29.37
2619	70.07	7.67	18.64	14.49	42.09
Overall					**44**

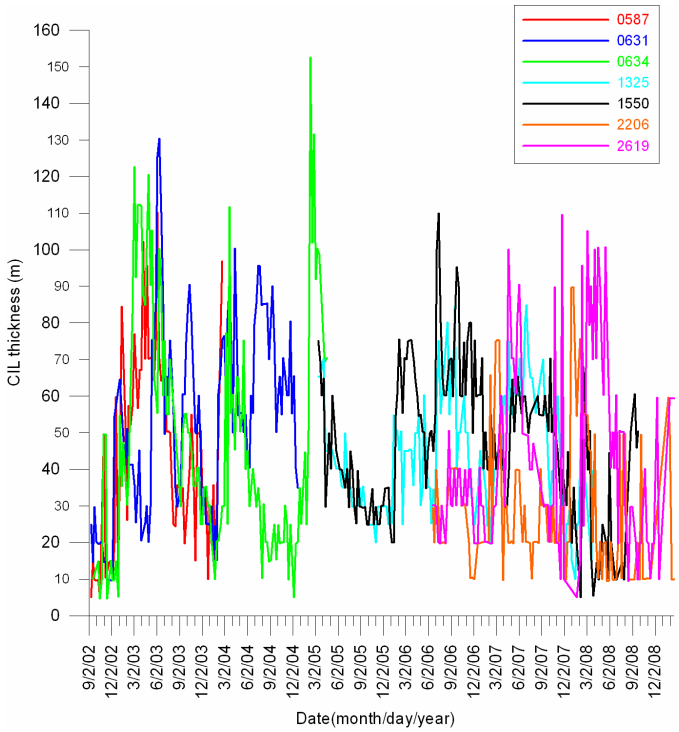

Figure 3. 33 Estimated Cold Intermediate Layer thicknesses over time for all seven floats.

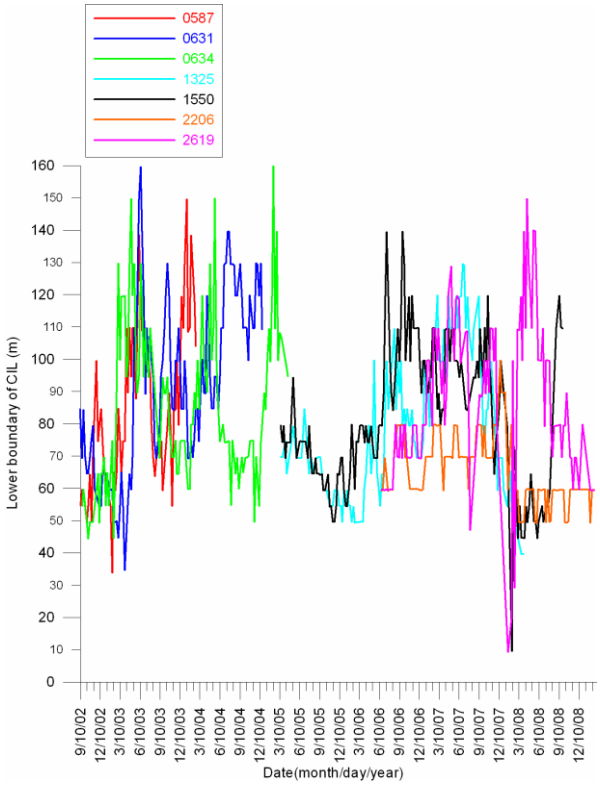

Figure 3. 34 Depth of the lower boundary of the Cold Intermediate Layer over time for all seven floats.

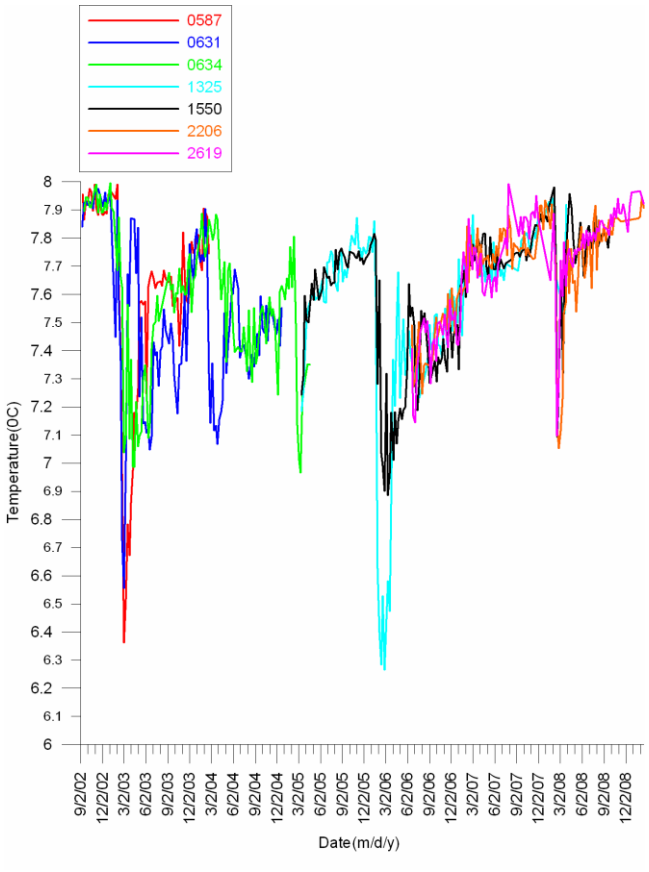

Figure 3. 35 Averaged temperature of the Cold Intermediate Layer over time for all seven floats.

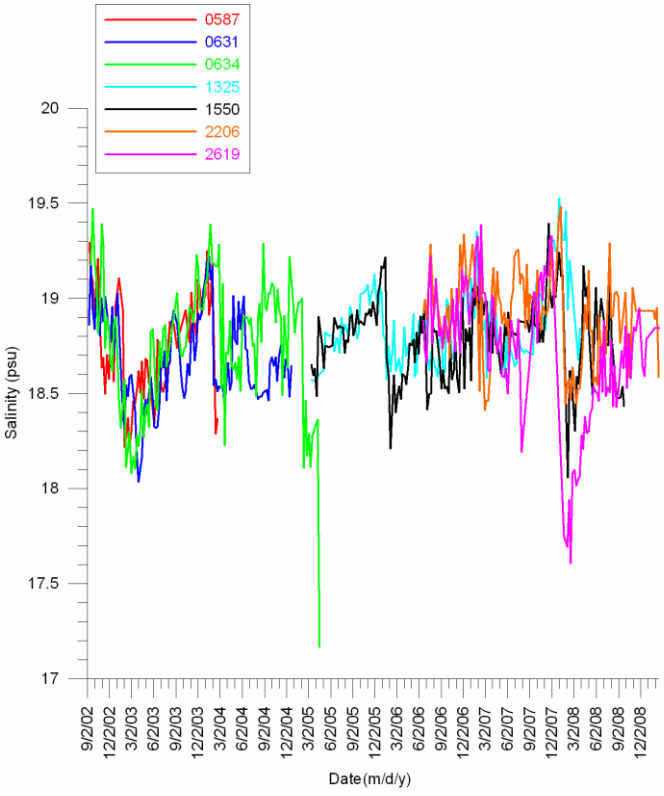

Figure 3. 36 Averaged salinity of the Cold Intermediate Layer over time for all seven floats.

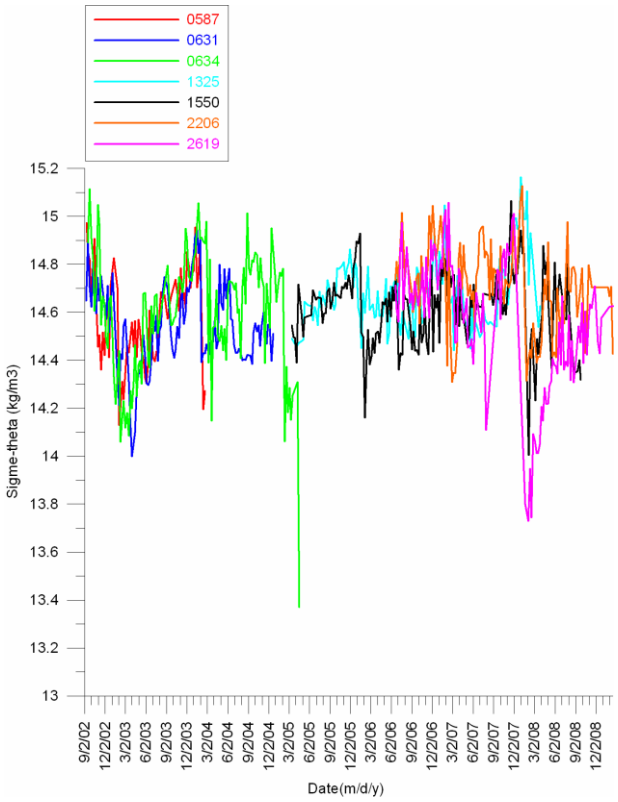

Figure 3. 37 Averaged sigma-theta of the Cold Intermediate Layer over time for all seven floats.

3.5 Mixed Layer Properties

Mixed layer has been studied extensively all around the world oceans because of its importance for sea surface variations, sea surface height changes, air-sea exchange, formation of water masses and also the ventilation of the subsurface waters and particulate matter transfer to these water masses. Therefore mixed layer is an important part of this study, revealing information about the mixed layer from the Argo floats.

In this study, the mixed layer has been studied using a few methods, the details of the methods applied in the study is explained in the material and methods section (chapter 2). These methods were applied to float 0587 first to test the different mixed layer determination criteria. All profiles of 0587 were visually examined and a reference mixed layer depth was obtained (Figure 3.38). Results of the different methods applied were compared with this reference mixed layer depth.

After setting a reference mixed layer depth, a threshold difference of 0.5 was applied for density. This criterion was too large for the mixed layer. This was then reduced to 0.3, giving better results but still not finding the mixed layer depth in some data.

Decreasing this criterion further to 0.2 gave much better results and the best result was obtained with a density threshold difference of 0.15 (Fig. 3.39).

Reducing the density threshold difference values gradually gave better results, but the density threshold difference method overestimated the mixed layer in winter months where there is a deepening of the mixed layer (Fig. 3.39). There was an obvious difference in the values between the reference values and the estimated values, so the threshold difference method was applied for salinity.

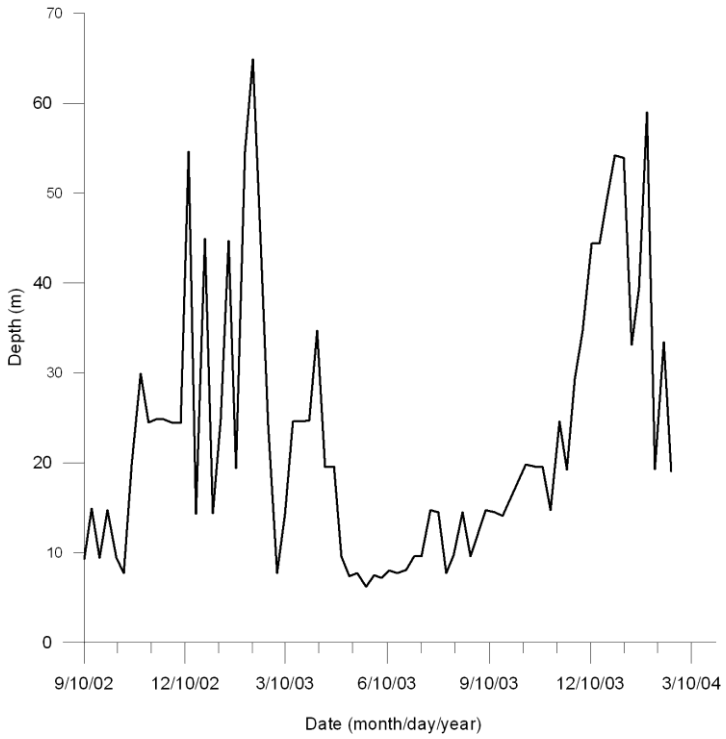

Figure 3. 38 Reference mixed layer depth of float 0587 obtained by visual examination

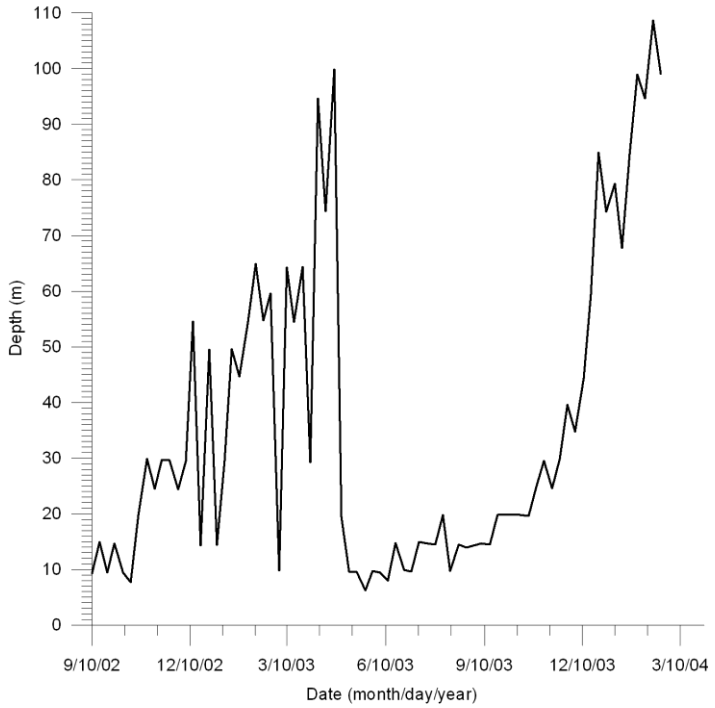

Figure 3. 39 Mixed layer depth of float 0587 calculated with a density difference of 0.15.

In order to obtain results that are closer to the reference mixed layer depth, salinity threshold difference method was applied, starting with a difference of 0.35. The result obtained from this value was a failure, so the value was decreased to 0.3 giving a better result. The deepening of the mixed layer between December and March was still missed with this criterion, so the value was again decreased to 0.25, 0.2 and then 0.15 (Fig. 3.40). Using 0.15 better results were obtained for the winter season but results for the other seasons were not satisfactory (Fig.3.40).

The next step then was to apply a threshold gradient method where a density gradient of 0.01 (Fig. 3.41) was applied giving close results to the reference mixed layer depths except the winter period. The deepening of the mixed layer in this season was overestimated once again. This result, together with the threshold difference method results suggest that the winter mixed layer depends more on salinity. Thus a salinity gradient of 0.01 was used, giving similar results with the density gradient but with the use of this salinity gradient, mixed layer of the summer period and the winter period were both overestimated.

The best result was obtained by separating the data into parts as winter and non-winter data. The same density gradient of 0.01 was applied to non-winter data whereas for the winter data a salinity gradient of 0.005 was applied (Fig. 3.42).

This method was used to calculate the mixed layer depth for all the floats. The mixed layer depths obtained via this method clearly show a seasonal cycle (Fig. 3.42). The mixed layer deepens between December and March reaching up to ~70 meters. The shallowest mixed layer depths are observed in summer as a result of the stratification. The December-March period in 2006 (in other words the mixed layer depth from floats 1325-1550) were shallower (~40 meters) than other seasons. There was extensive cooling at this period at the surface of the Black Sea (Fig.3.30) but the floats were in the center of the cyclonic Western Gyre at this period, thus the cold waters could not penetrate deep into the water column due to the upwelling in the region. The jump in the mixed layer depth observed in Fig.3.42 is caused by the difference in the vertical resolution of the floats deployed in 2002 and 2005.

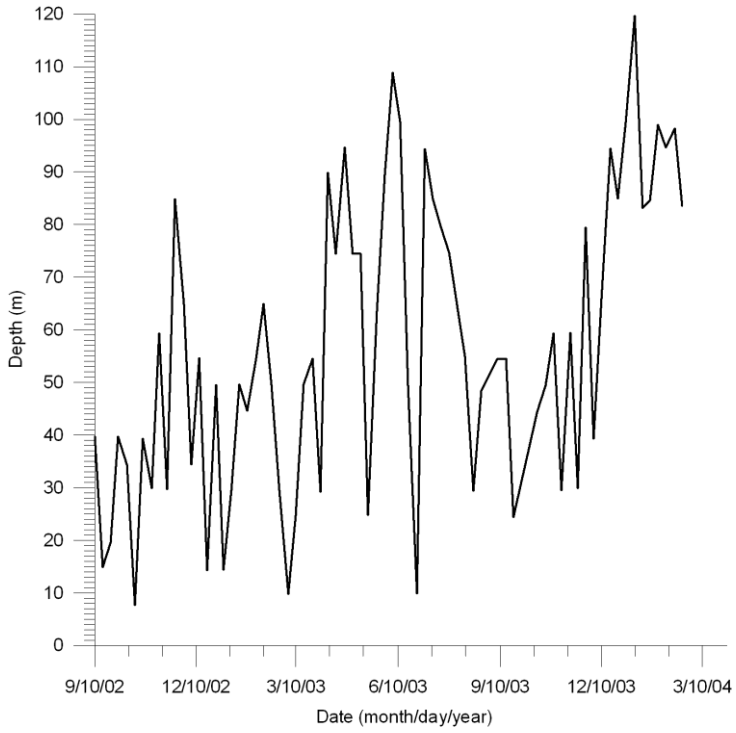

Figure 3. 40 Mixed layer depth of float 0587 calculated with a salinity difference of 0.15

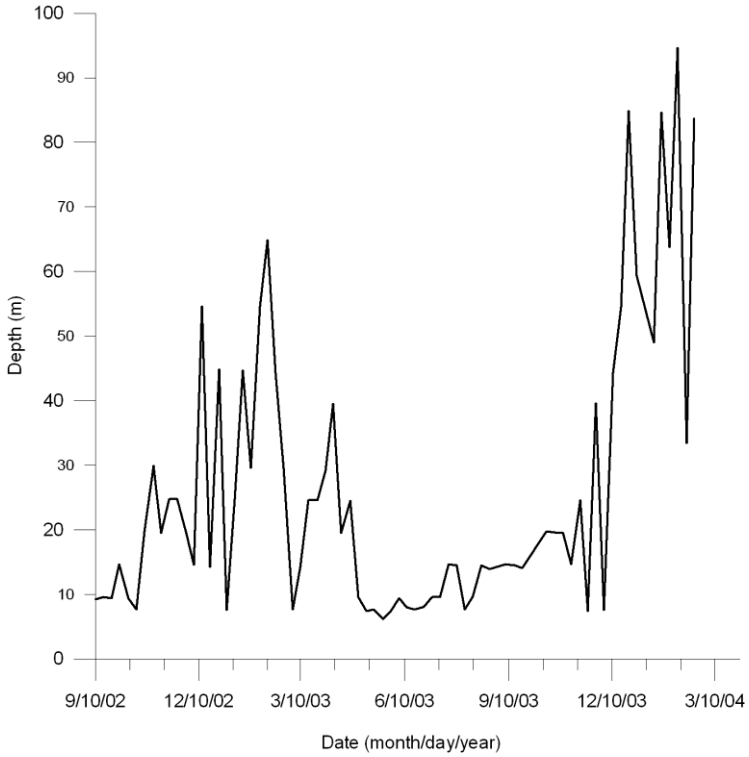

Figure 3. 41 Mixed layer depth of float 0587 calculated using a density gradient of 0.01.

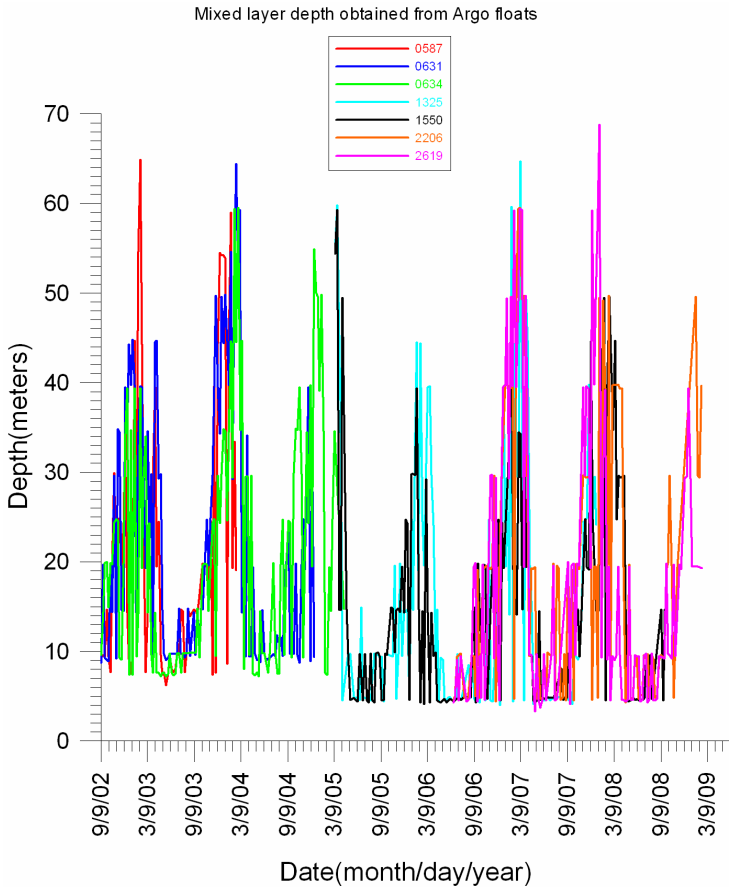

Figure 3.42 Mixed layer depths calculated for all floats using a salinity gradient of 0.005 during winter and a density gradient of 0.01 during the rest of the year.

3.6 Water properties at 100meters and 200meters

One of the most distinguishing characteristics of the Black Sea is its anoxic water found below 200 meters. The vertical transport of water masses has great importance for the ventilation of the subsurface layers. In order to observe possible vertically-migrated water masses, the temperature, salinity and sigma-theta values for the 100 meters and 200 meters depths were extracted from the float data. As in the previous sections, the floats were grouped according to their release dates.

Most of the temperature measurements at 100m depths are below 8 ^{o}C for floats 0587, 0631 and 0634 (Fig. 3.43), corresponding to the Cold Intermediate Layer. Looking at all float data (Fig. 3.43, 3.46 and 3.49), it is clear that the temperature of the waters lying at 100 meters is generally below 8.5 ^{o}C. There are of course exceptions such as one measurement in Figure 3.49 with a temperature value of 10.31 ^{o}C, which was measured at 41.17^{o}N, 38.56^{o}E on 12/29/2007.

In the previous sections it was stated that floats 0631 and 0634 observed water masses with very different characteristics in July 2004 which can also be seen in Figures 3.60-3.62. There is almost 2 psu salinity difference between 0631 and 0634's measurements. It is important to note here that the different properties observed at this day can also be clearly seen in the 200 meter level (Figures 3.52-3.54).

Floats 1325 and 1550 have mainly similar measurements (Fig. 3.46) except during the time from September 2006 to December 2006 and the time from June 2007 to September 2007. These differences can also be clearly seen in salinity (Fig. 3.47) and density (Fig. 3.48) and are also observed in the 200 m layer (Figs. 3.55-3.57), where they are rather small compared to the 100 m layer. Temperature difference is about 0.1-0.2 ^{o}C and salinity difference is about 0.3-0.4 psu.

Floats 2206 and 2619 have different measurements at 100 meters almost throughout their entire lifetime. The difference in temperature measurements varies between 0.3 to 0.8 ^{o}C (Fig. 3.49). It is important to note here that the measurements are so similar at the start of the graph for almost 5 months. After this point, there is clearly a different temperature pattern. One reason for this might be the locations of the floats. Float 2206 was captured by the Western Gyre and spent all its lifetime in this region whereas float 2619 kept moving to the east and was entrapped there. The salinity map also shows similar results (Fig. 3.50), with differences ranging from 0.5 to almost 3 psu.

Similarly, temperature differences can also be observed at 200 m depth (Fig. 3.58) with relatively smaller values such as 0.1 to 0.3 ^{o}C. Salinity measurements at this depth (Fig. 3.59) show greater differences, from 0.4 to almost 1 psu. The density plot (Fig. 3.60) also shows a density difference of 0.2 to 0.5 kg/m^3.

From these plots for 100 meter and 200 m levels, it is clear that there are obvious differences among the measurements done by the floats. In order to understand the reasons of these differences, these plots should be clearly examined. For this reason, sea level anomaly maps corresponding to the dates with different float measurements will be used in order to interpret the ongoing processes on these dates. Sea level anomaly maps will be helpful to understand the cyclonic and anticyclonic regions in the Black Sea and together with the 100m-200m depth vs. time plots, it will be possible to say if a water mass is uplifted or down-welled. This is done in the next chapter, which is the discussion of the results.

In addition to the 100 and 200m water properties, the location of isopycnals corresponding to the temperature minimum (14.5 kg/m^3), the peak concentration of nitrate (15.5 kg/m^3), and the first appearance of sulfide in the water column (16.2 kg/m^3) which are important indicators of water column chemical properties (Oguz et al., 1994; Tugrul et al., 1992) were investigated. The 14.5 kg/m^3 isopycnal is distributed in 20 to 160 meters (Fig. 3.61). The distribution of this isopycnal varies spatially according to the geographical location of the float. The same property is observed in the distribution of the 15.5 kg/m^3 isopycnal, ranging from 60 to 200 meters (Fig. 3.62). Distribution of the 16.2 kg/m^3 isopycnal also changes spatially with a range of 100 to 240 meters (Fig. 3.63). The spatial distributions of these isopycnals are clearly seen from the graphs (Fig. 3.61-3.63). Different floats at the same time measure different isopycnal depths suggesting different water mass characteristics. The difference between float measurements (0631 and 0634) for the depth of the 15.5 kg/m^3 isopycnal is ~60 meters, suggesting once again different water masses. These are investigated in the discussion chapter.

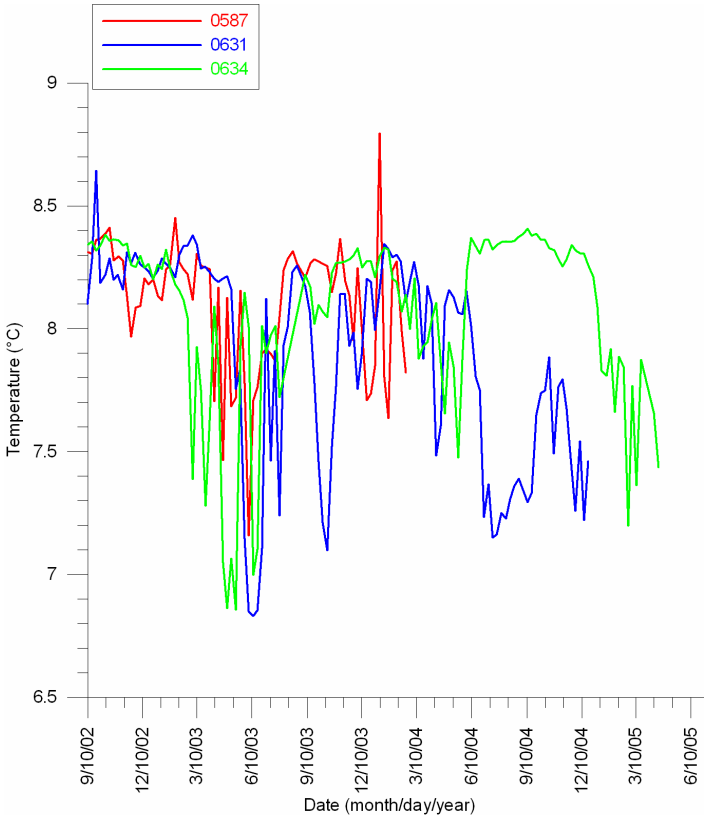

Figure 3. 43 Temperature over time at 100 meters for floats 0587-0631-0634

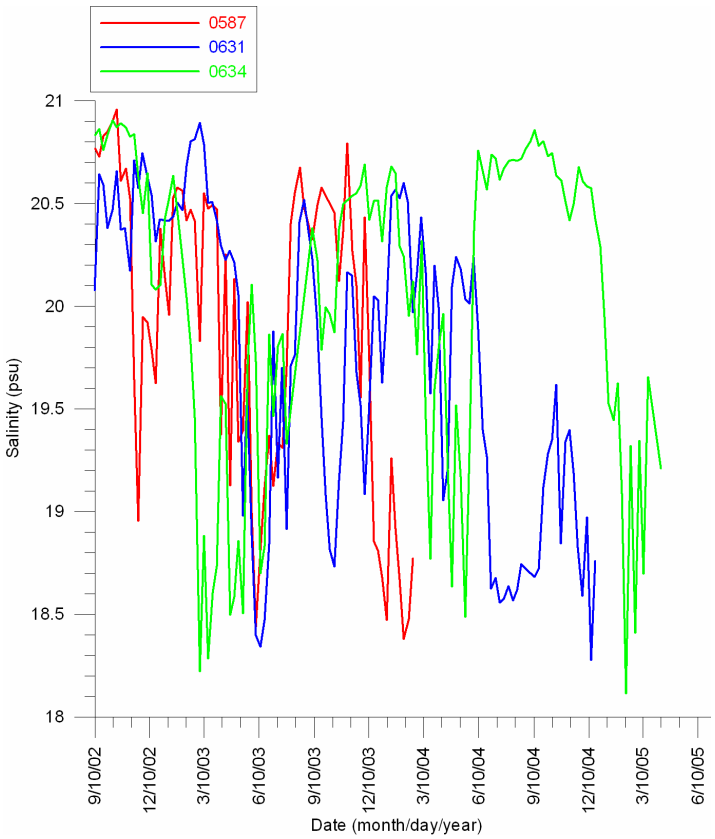

Figure 3. 44 Salinity over time at 100 meters for floats 0587-0631-0634

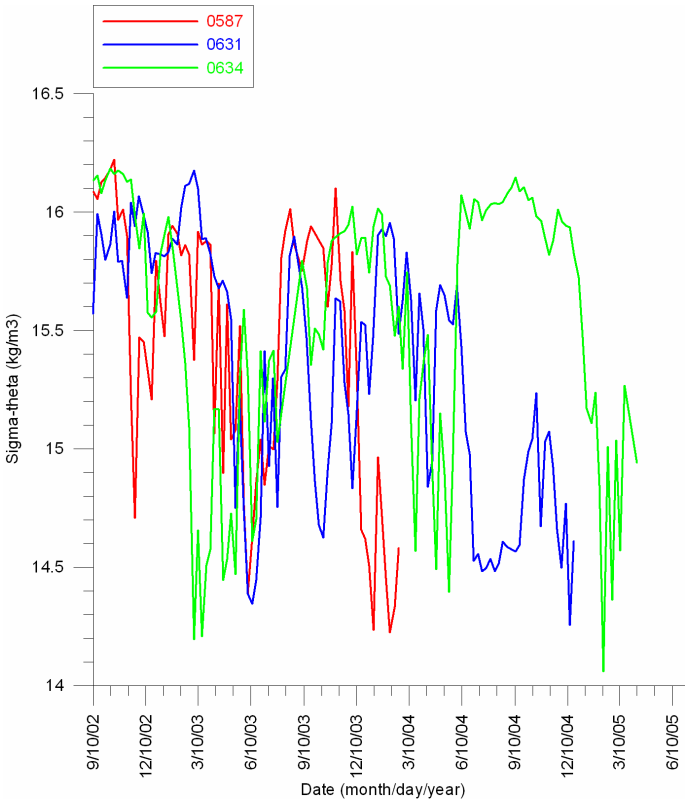

Figure 3. 45 Density over time at 100 meters for floats 0587-0631-0634

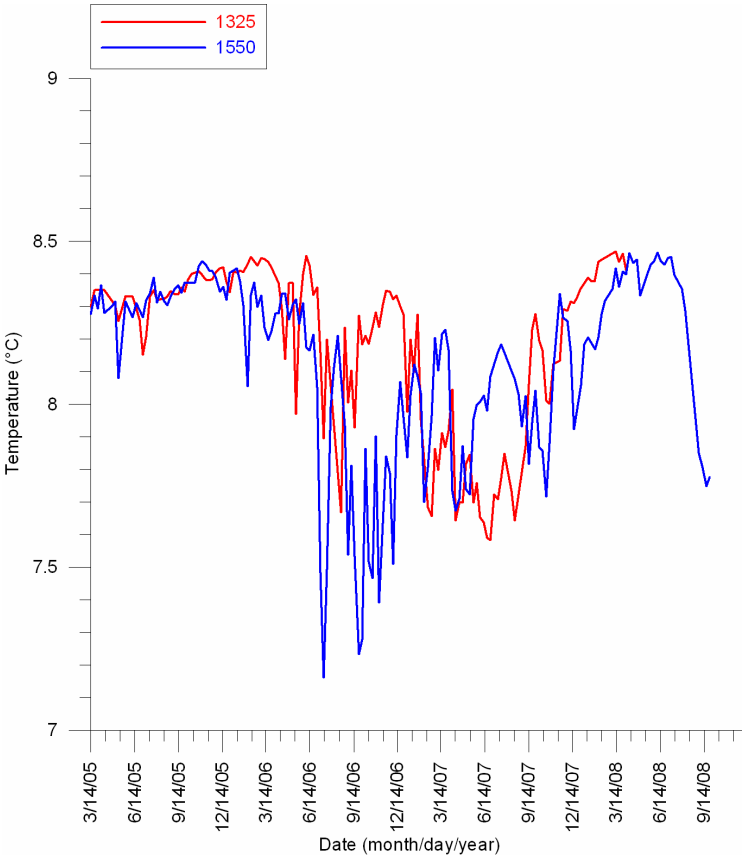

Figure 3. 46 Temperature over time at 100 meters for floats 1325-1550

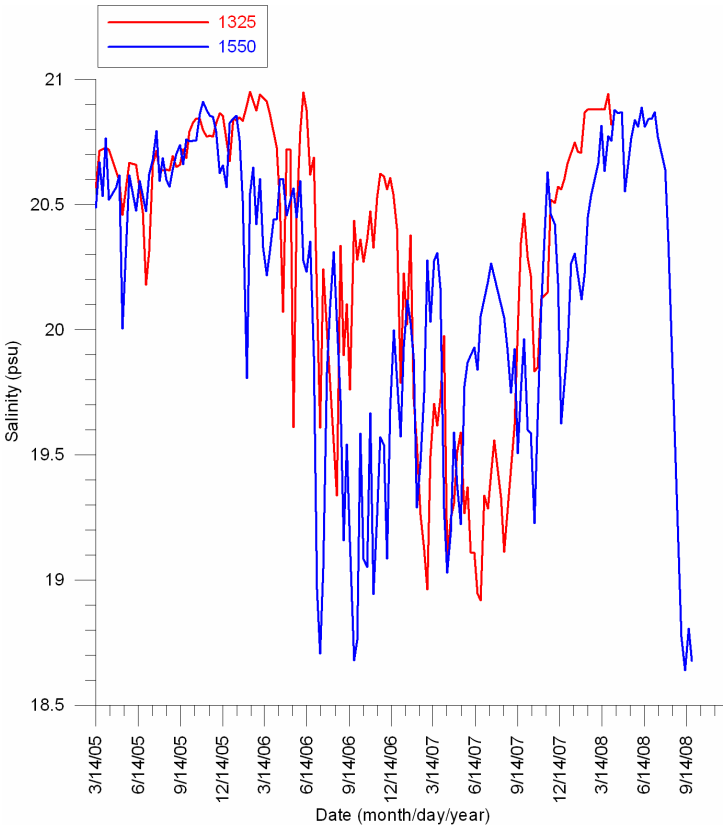

Figure 3. 47 Salinity over time at 100 meters for floats 1325-1550

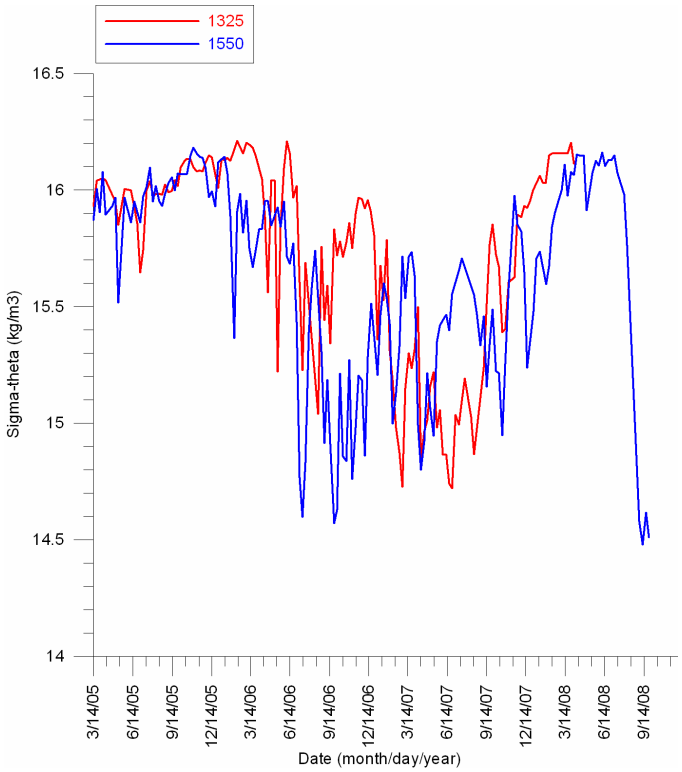

Figure 3. 48 Density over time at 100 meters for floats 1325-1550

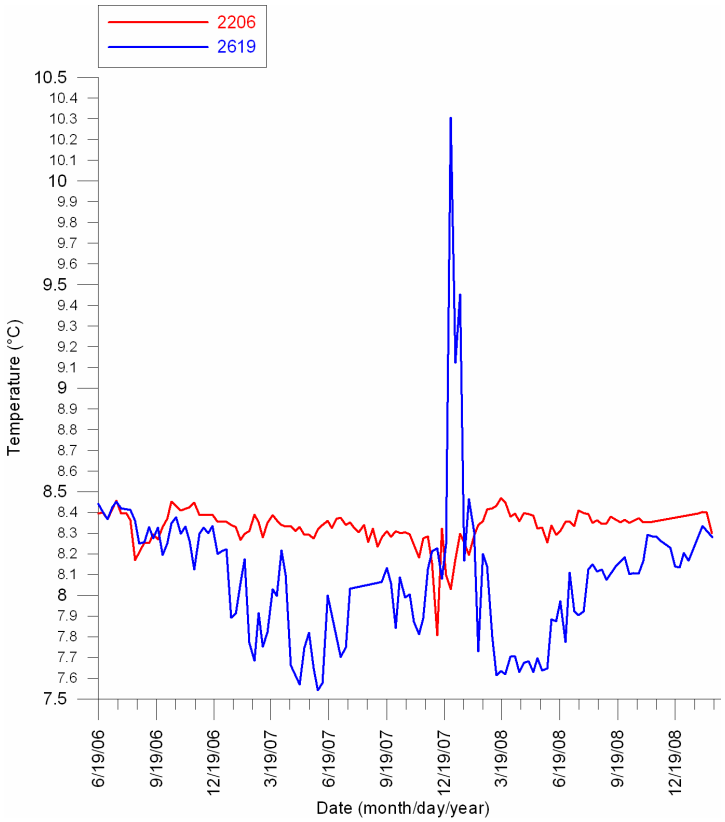

Figure 3. 49 Temperature over time at 100 meters for floats 2206-2619

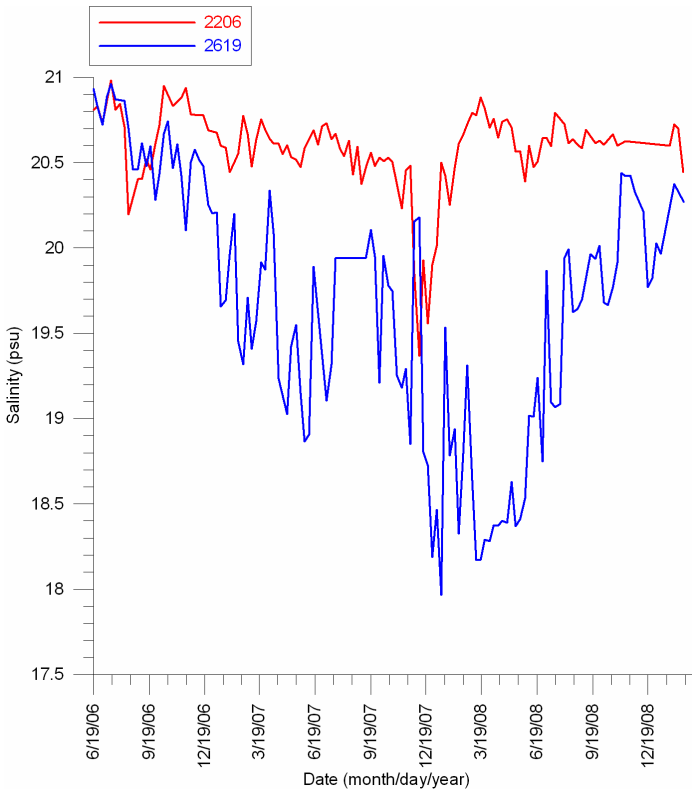

Figure 3. 50 Salinity over time at 100 meters for floats 2206-2619

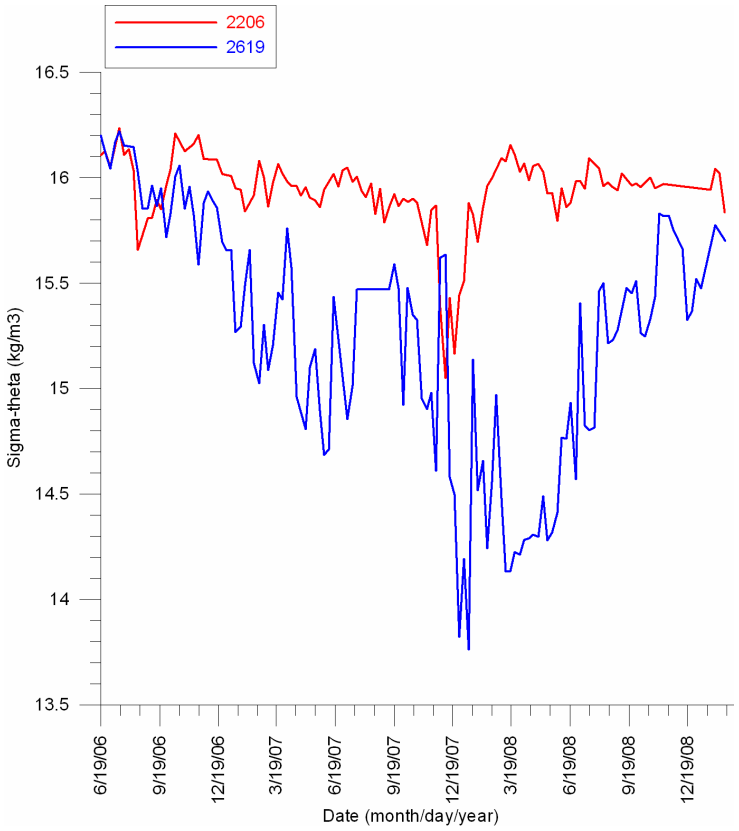

Figure 3. 51 Density over time at 100 meters for floats 2206-2619

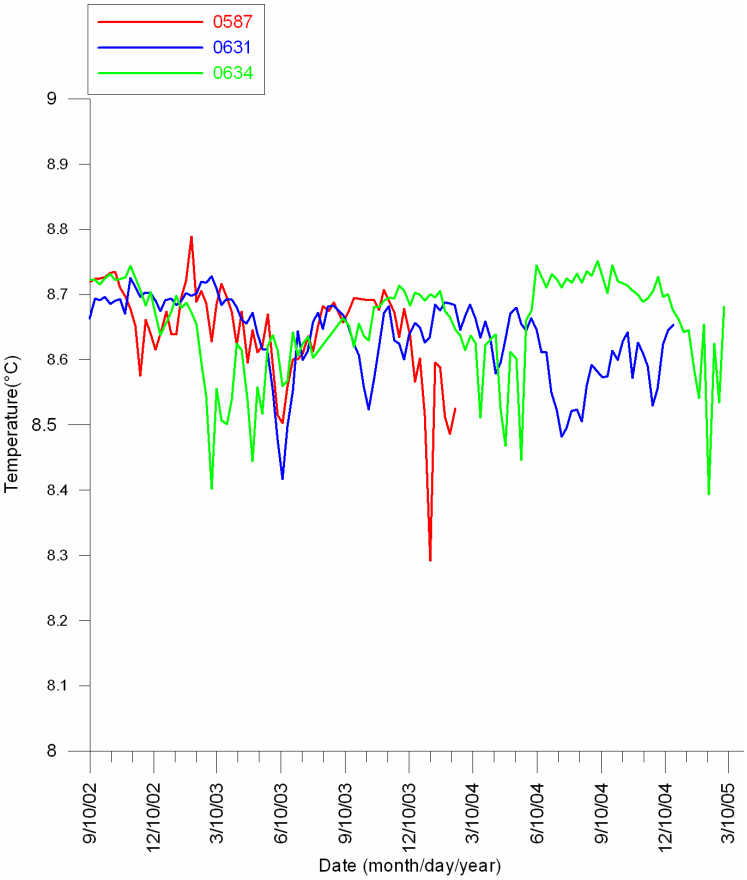

Figure 3. 52 Temperature over time at 200 meters for floats 0587-0631-0634

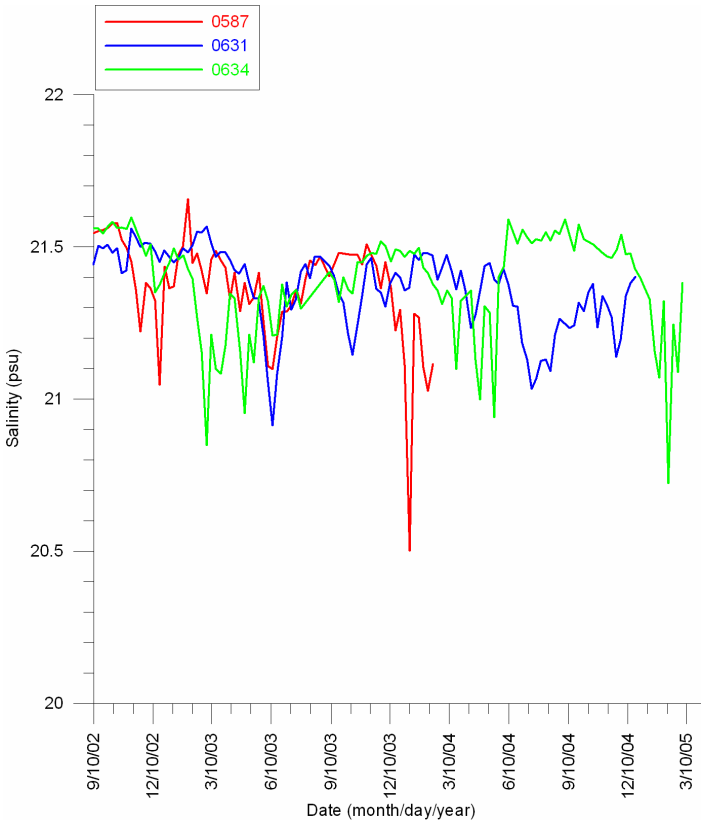

Figure 3. 53 Salinity over time at 200 meters for floats 0587-0631-0634

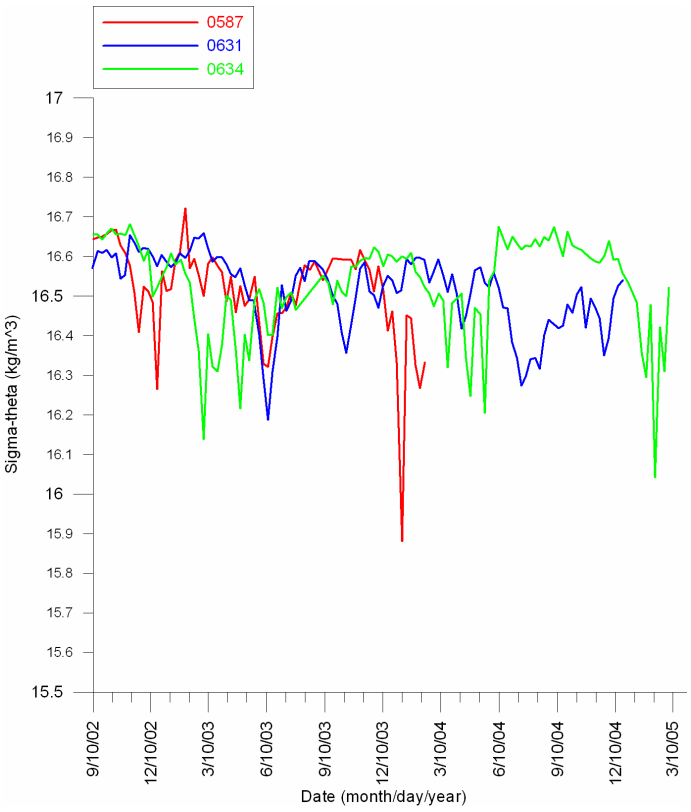

Figure 3. 54 Density over time at 200 meters for floats 0587-0631-0634

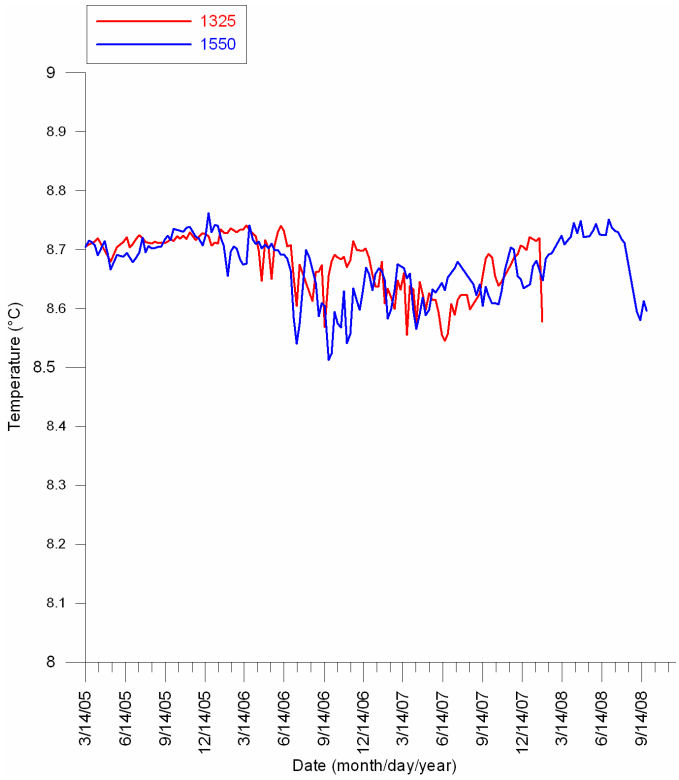

Figure 3.55 Temperature over time at 200 meters for floats 1325-1550

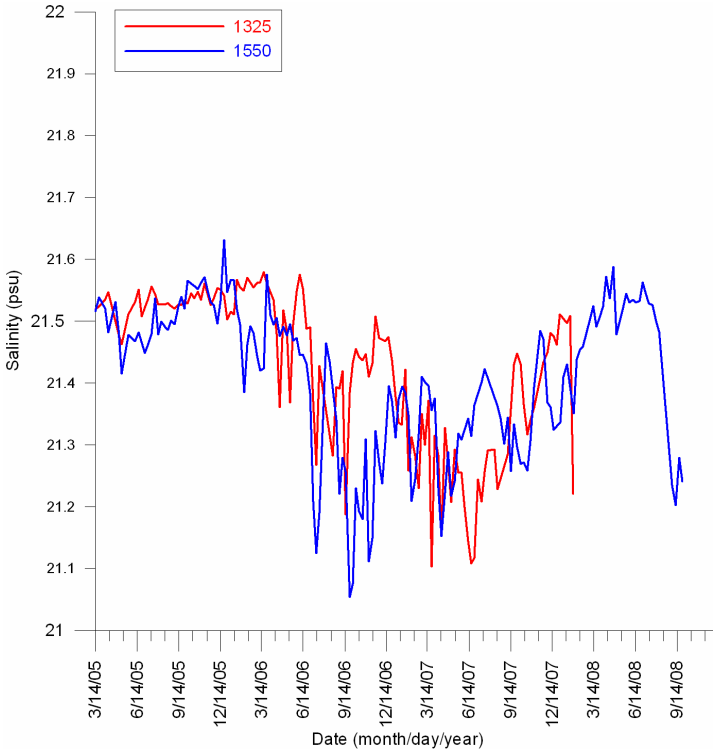

Figure 3. 56 Salinity over time at 200 meters for floats 1325-1550

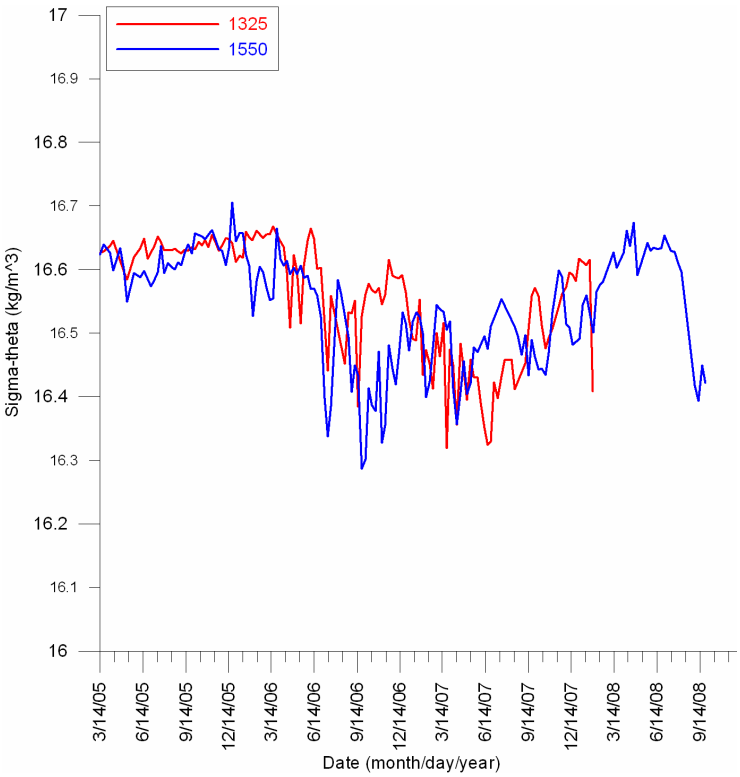

Figure 3. 57 Density over time at 200 meters for floats 1325-1550

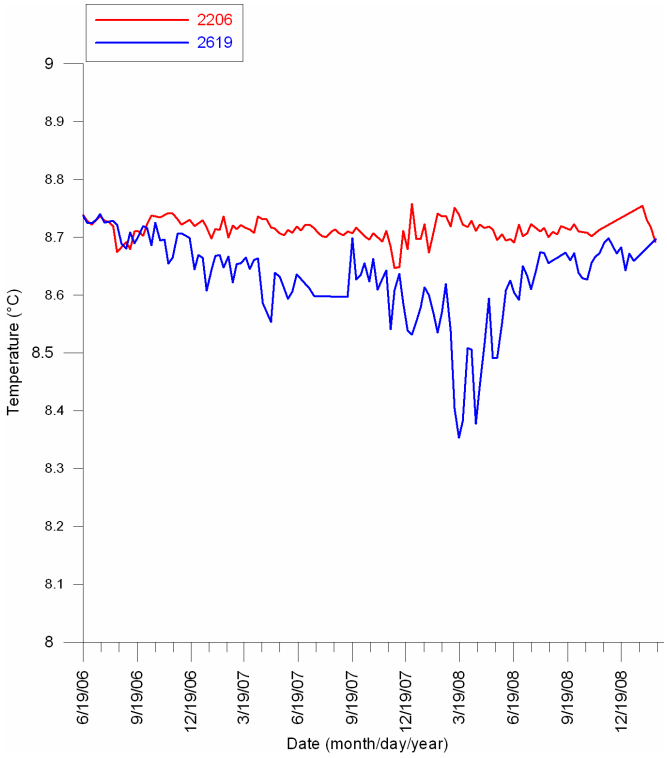

Figure 3. 58 Temperature over time at 200 meters for floats 2206-2619

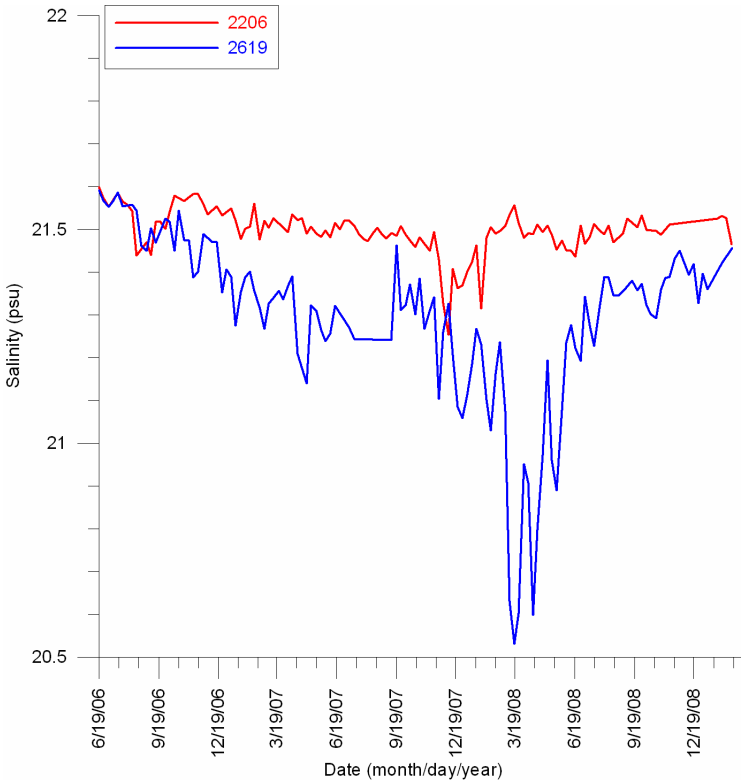

Figure 3. 59 Salinity over time at 200 meters for floats 2206-2619

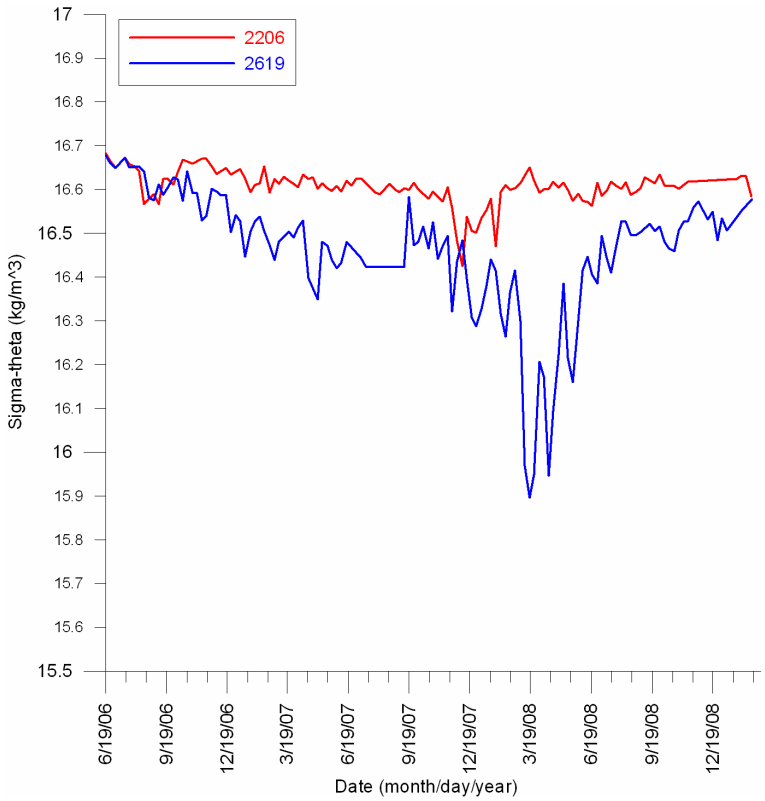

Figure 3. 60 Density over time at 200 meters for floats 2206-2619

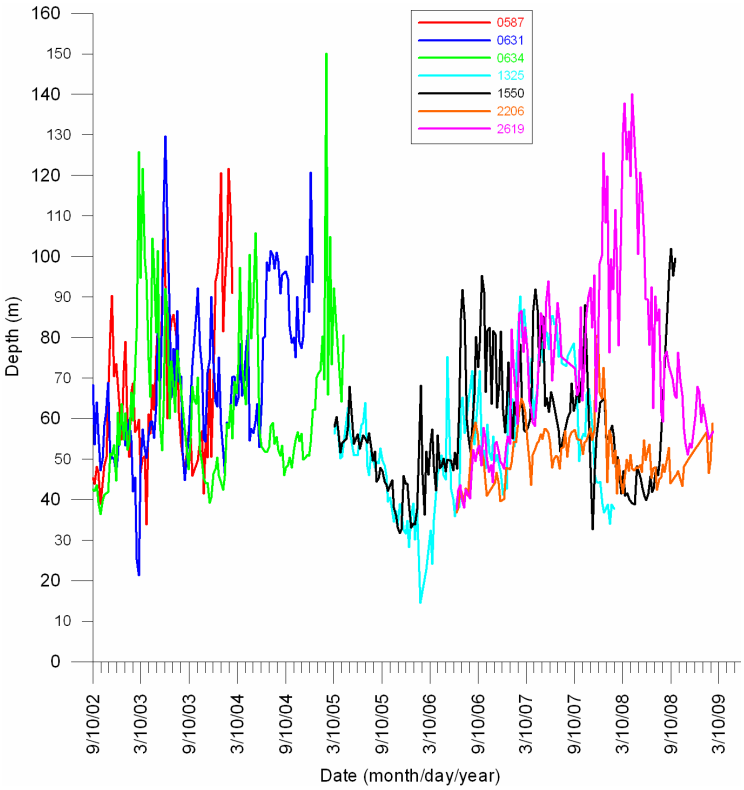

Figure 3. 61 Distribution of σ_θ =14.5 kg/m^3 density surface over time.

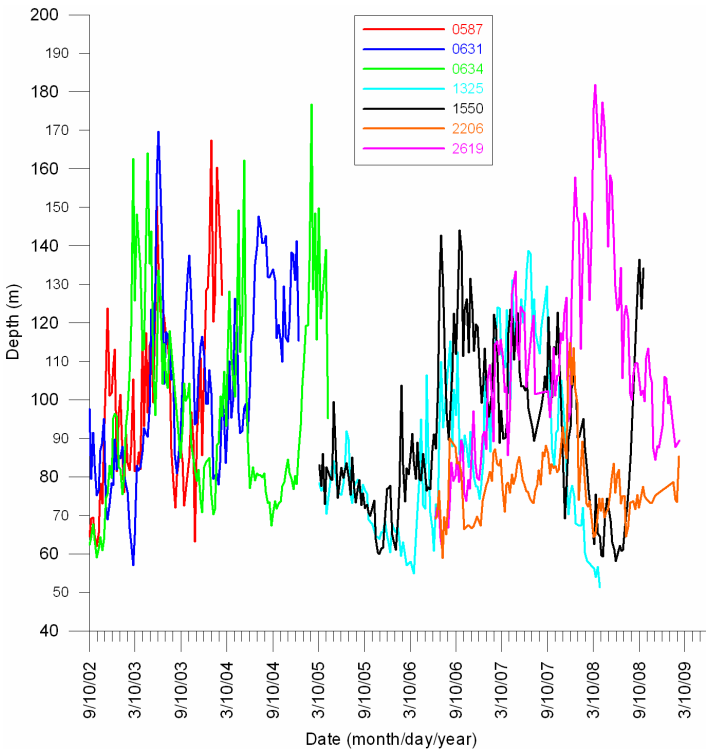

Figure 3. 62 Distribution of σ_θ =15.5 kg/m^3 density surface over time.

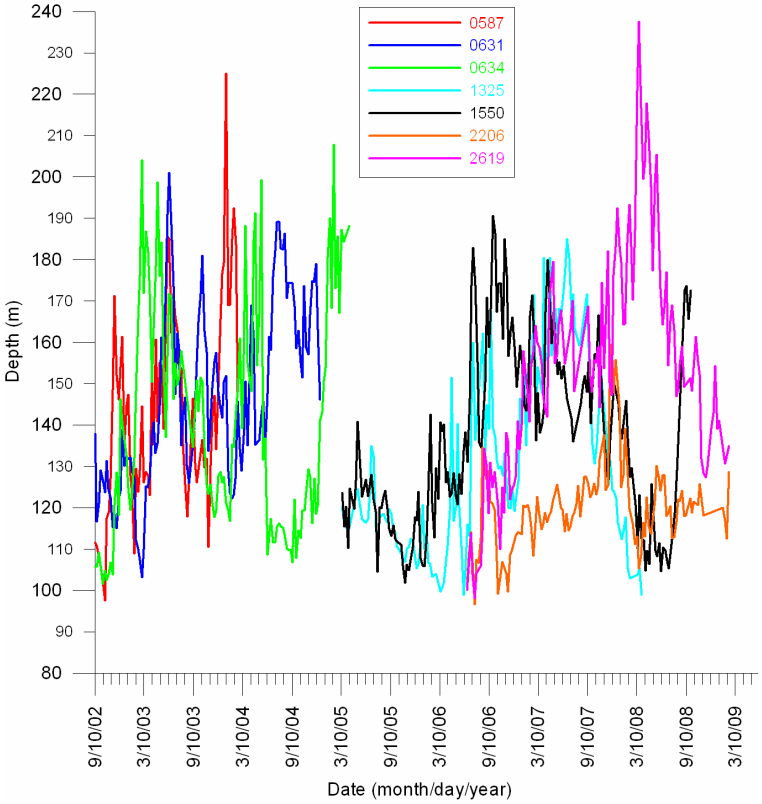

Figure 3. 63 Distribution of σ_θ =16.2 kg/m^3 density surface over time.

CHAPTER 4

DISCUSSION

The data quality of the Argo floats has been debated among Argo data users. In order to minimize errors the Argo float data undergoes various quality checks as described earlier in Chapter 2 (Material and Methods). In previous studies (Ohno et al., 2007, Oka et al., 2006) the Argo float data were either compared to or used together with shipboard CTD data, satellite data, model outputs or large scale climatology (mostly Levitus climatology). In order to compare the Argo float data, shipboard CTD data gathered from the Black Sea via the R/V Bilim were used. Unfortunately, finding CTD data along the trajectories of the Argo floats was a problem at this stage. It was almost impossible to find measurements at the same location and time for the Argo data, therefore data with similar locations and time were used to compare. Comparison of the available CTD data with Argo float data showed strong similarities, except for small differences that can be accounted to the differences in location and time (Figs. 4.1 – 4.4). The surface temperatures of float 1325 and a corresponding CTD station show 1-2 ^{o}C of difference which is possibly due to the time lag of five days between the measurements (Fig. 4.1), since the salinity values are almost the same (Fig. 4.2). Surface temperatures of float 2206 with a corresponding CTD station shows much better agreement (Fig. 4.3), despite differences in time and space, while the salinity profiles show differences between 50 – 100 m (Fig. 4.4). Visually examining these plots, both Argo and CTD measurements show a mixed layer of ~10-20 meters and a CIL thickness of 20-30 meters (Fig. 4.1-4.4).

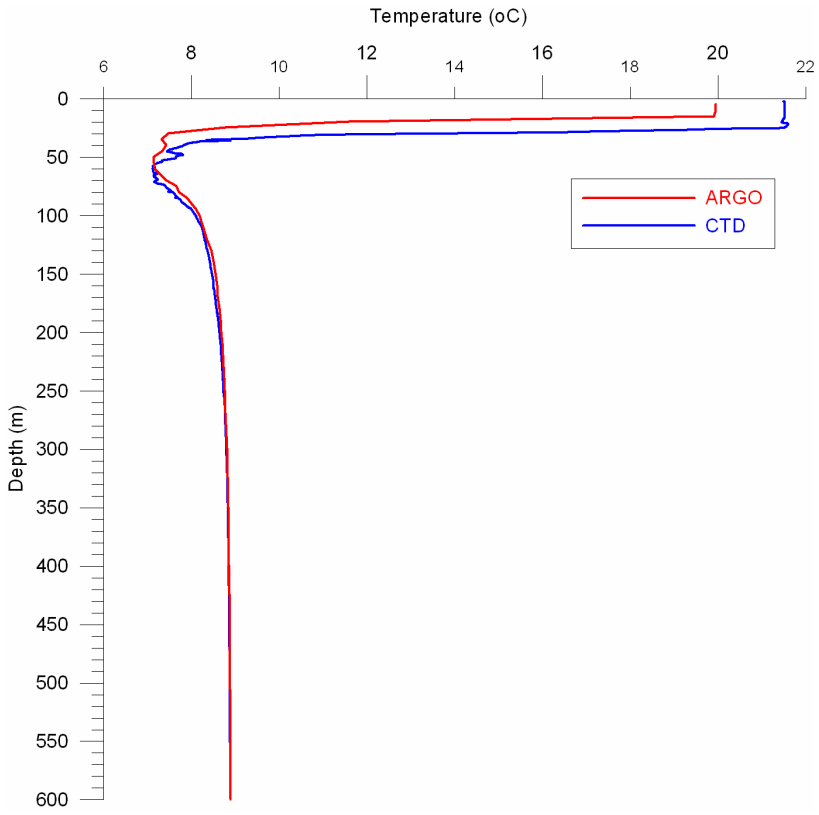

Figure 4. 1 Temperature Profile from float 1325 on 10/15/2006 at 42.39°N, 34.28°E (red line) and temperature profile from shipboard CTD on 10/10/2006 at 42.15°N, 35.14°E (blue line).

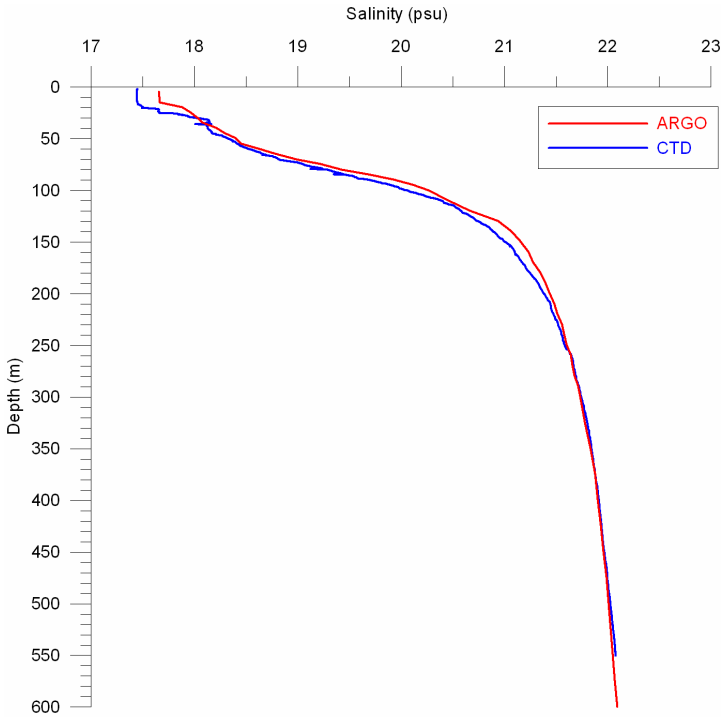

Figure 4. 2 Salinity profile from float 1325 on 10/15/2006 at 42.39°N, 34.28°E (red line) and salinity profile from shipboard CTD on 10/10/2006 at 42.15°N, 35.14°E (blue line).

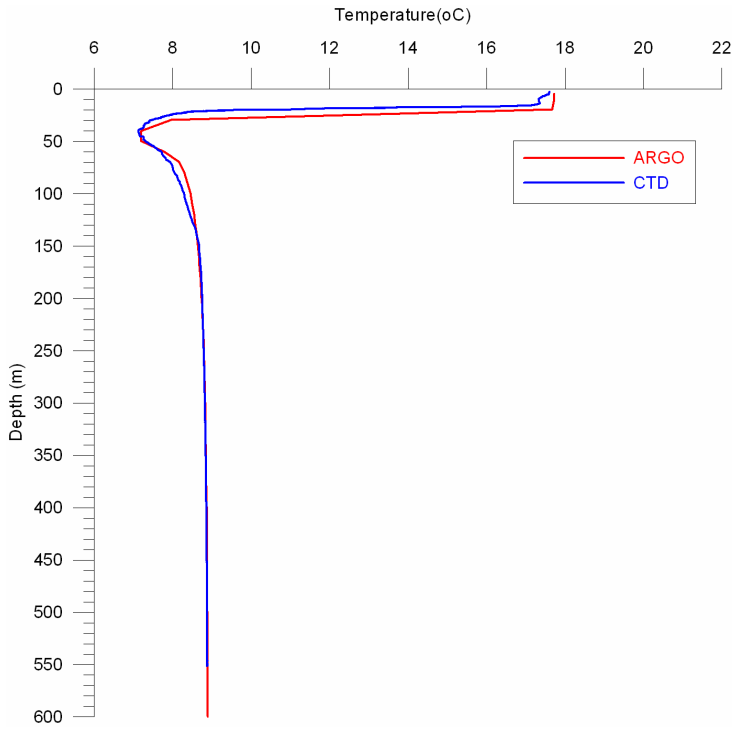

Figure 4. 3 Temperature profile from float 2206 on 10/27/2006 at 42.36°N, 32.06°E (red line) and salinity profile from shipboard CTD on 10/22/2006 at 42.30°N, 32.45°E (blue line).

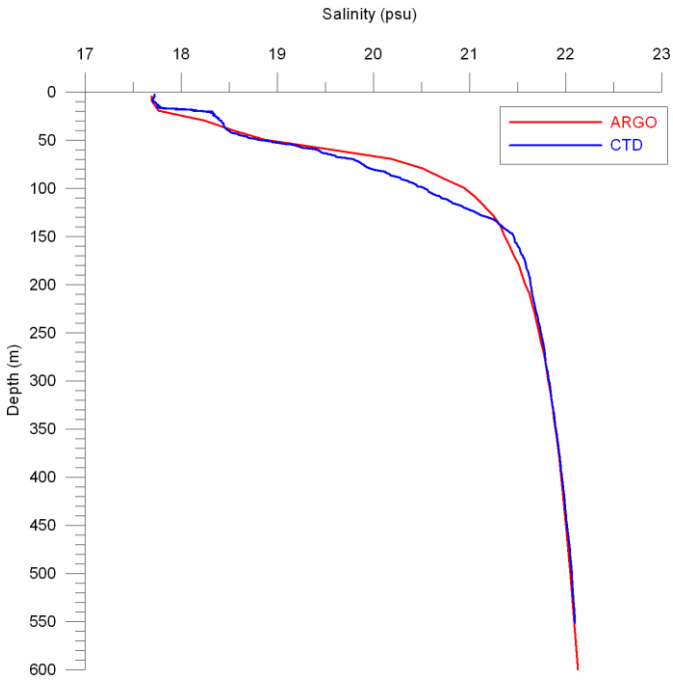

Figure 4. 4 Salinity profile from float 2206 on 10/27/2006 at 42.36°N, 32.06°E (red line) and salinity profile from shipboard CTD on 10/22/2006 at 42. 30°N, 32.45°E (blue line).

The first look on the trajectories of the Argo floats (Fig. 3.1-3.15) made us to assume that there was a strong effect of topography and the mesoscale eddies of the Black Sea on these trajectories. For instance, looking at the trajectory of the float 2206 (Fig. 3.12), it was interpreted that this float was first close to the Western Gyre and then it was entrapped in it. This interpretation is confirmed by sea surface anomaly maps of the Black Sea at the time of entrapment, showing strong cyclonic movement around the area which is a known characteristic of the Western Gyre (Fig. 4.5). In the previous chapter, it was noted that the float 2206 after point "7" (Fig. 3.13) started to move along the southern edge of the Western Gyre, this can also be seen in the sea surface anomaly map (Fig. 4.6).

The trajectories of the floats show that the main characteristics of the circulation at various depths of the Black Sea are the Rim Current, topographic control, Eastern Gyre, Western Gyre and mesoscale eddies which is consistent with the previously known features of the circulation (Oguz et al.,1993, Korotaev et al., 2003). Floats 0587, 2206 and 2619 were all drifting at 1550 m. The trajectories of these floats (Fig. 3.2, 3.12, 3.14) follow the cyclonic features of the Black Sea. As previously explained, 2206 followed the Western Gyre mainly whereas 0587 and 2619 followed the axis of the Rim Current. The circulation at 200m was revealed via float 0634 (Fig. 3.6) which showed the Rim Current at this depth as well as the Eastern Gyre and mesoscale eddies. The circulation at 500m was observed via the trajectory of float 1325 (Fig. 3.8). The trajectory from this float shows a lot of mesoscale features in the Black Sea as well as the main circulation system. The circulation at 750 m was also observed via the trajectory of float 0631 (Fig. 3. 4) which was one of the most interesting trajectories among all the floats. The circulation of this float was affected by the Rim Current, the Eastern Gyre, the Western Gyre and it was also affected by the Batumi Eddy. The circulation at 1000m is also seen via float 1550 which followed the topography for most of its lifetime revealing the strong effect of this current. The only mesoscale feature observed at this depth was the entrapment of this float by an eddy in the eastern part of the Black Sea.

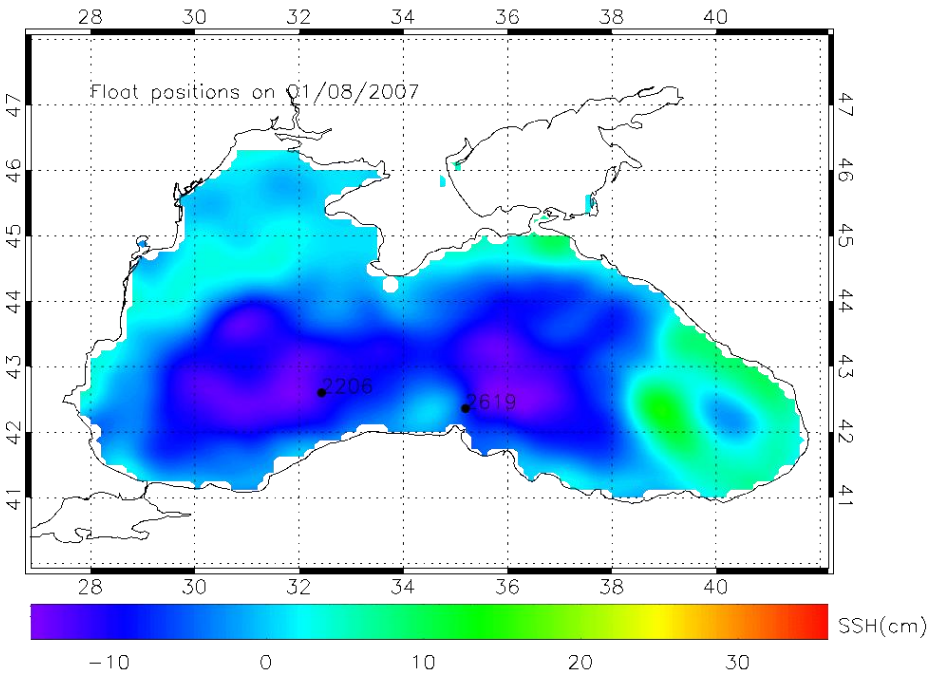

Figure 4. 5 Sea surface anomaly map on 8th of January 2007, with positions of floats 2206 and 2619

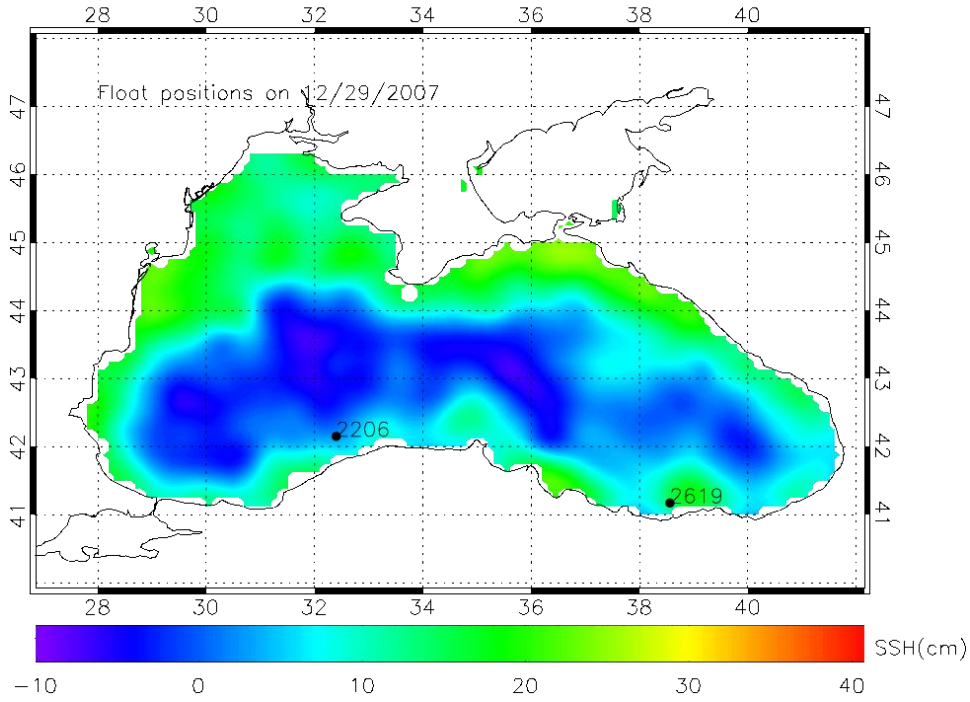

Figure 4. 6 Sea surface anomaly map on 29th of December 2007, with positions of floats 2206 and 2619

The temperature over time plot (Fig. 3.30) reveals an increasing trend in the surface layer of the Black Sea. Looking only at this plot, one may suggest that the Black Sea surface waters have warmed up 2^{o}C from 2003 to 2007, which is a misleading value. It should be considered that year 2003 was a cold year in the Black Sea (Oguz, 2009). It should also be noted that this plot does not include data that are recorded on the same time of the day. One profile might be recorded at noon whereas another one might be recorded at midnight. Another important point is that the data is distributed all over the Black Sea, for example float 2206 spent almost all of its lifetime inside the Western Gyre. Within the center of the western basin, there is a warm spot (T~22^{O}C) (Oguz et al., 1994). This can be clearly seen from the plot, with high values of temperature from this float. It should also be noted that the float locations are of great importance for this reason, since one float might be in a cyclone whereas another float might be in an anticyclone which gives us different temperature measurements. This data must be supported and validated by shipboard data and sea surface temperature data from satellites and the measurement time of each data should be considered before making a comment about the temperature rise in the Black Sea.

Studying one of the most distinguishing features of the Black Sea, the Cold Intermediate Layer was also within the scope of this thesis. Previous studies in the Black Sea found the CIL temperatures to be 6.5-7.5 ^{o}C (Ovchinnikov and Popov, 1987; Ivanov et al., 2001). The minimum CIL temperature was found as ~7.2^{o}C in a previously conducted study (Oguz et al., 1994) whereas in this study the minimum temperature of the CIL was found as ~6.3 ^{o}C. The average temperature of the CIL was found as ~7.5^{o}C which is consistent with the previous studies mentioned above. Another important topic is the thickness of the CIL. The average thickness of the CIL was found to be 44 m from all floats whereas in previous studies (Oguz et al., 1993) the CIL thickness was found as 50 m. It is important to note here that the average CIL thickness from float 2206 was calculated as 29.37 m (Table 3.8). This is because float 2206 spent most of its lifetime in the cyclonic Western Gyre. It is known from previous studies (Oguz et al., 1994) that the CIL is thinner and at shallower depths in the cyclonic regions. The lower boundary of the CIL was found at ~150 m at anticyclones (Batumi & Kaliakra Eddies) in previous studies (Oguz et al., 1994) which is consistent with the findings from Argo floats (Fig.3.34). It was also found in the same study that the lower boundary of the CIL is found ~75 m within the basins interior, which is consistent with the results from Argo floats. Float 2206 was within the basins interior (mainly Western Gyre) and it is obvious that the CIL found by this float varies

between 50 to 80 meters with most of the values ~70m (Fig 3.34). Oguz et al. (1993) concluded that the CIL properties might be used to represent the characteristics of the upper layer circulation. In this study, this has been applied by using CIL thickness (Fig. 3.33) and lower boundary of CIL (Fig.3.34) together with the sea surface anomaly maps in order to identify the possible cyclonic and anticyclonic regions in the Black Sea.

The mixed layer is one of the frequently studied and discussed topics in oceanography. The mixed layer has a great importance since it is the link between the atmosphere and the ocean and it plays a crucial role in climate variability. The thickness of the mixed layer might be referred as the amount of water that is directly interacts with the atmosphere. Better representation of the mixed layer can enhance the predictability of the sea surface temperature anomalies on seasonal and long time scales (Dong et al., 2008). The mixed layer has been studied using Argo data in various studies ((Ohno et al., 2004, 2009; Sreenivas et al., 2008; Bhaskar et al., 2007; Dong et al., 2008) as the primary source of data and also as supplementary data.

The use of Argo data is well suited to studying the mixed layer is because Argo data provide almost weekly profiles for long time series, allowing the distribution of the mixed layer to be observed continuously. This is the first time that the Argo floats have ever been deployed in the Black Sea. These Argo floats provided seven year data set from 2002-2009 which is a time period with only a few scientific cruises in the Black Sea, therefore this data set has great importance for both the mixed layer and also other physical features of the Black Sea. Oguz (2009) showed that the mixed layer is less than 20m in the summer months due to stratification. Results from the Argo data confirmed this with calculated mixed layer depths of less than 20m in summer months (Fig. 3.42). It is found from Argo float data that the mixed layer is ~ 50-60m between December and March. This is the season with the deepest mixed layer observations. There is an obvious seasonal cycle (Fig. 3.42) with deep mixed layers during the December-March period which is the coldest period of the year as it can be seen from surface temperatures (Fig. 3.30) and from CIL temperatures (Fig. 3.35).

The Argo program was launched with close connections with the Jason-1 altimeter (Roemmich et al., 2004). Within this concept the sea surface anomaly data from AVISO was used as a supplementary source to the Argo data set in the Black Sea. The sea surface anomaly maps together with the surface, CIL and 100-200 m depth plots allowed different water masses to be identified and labeled. The observation of different water masses by

floats 0631 and 0634 at 100m depths on the same dates was clearly seen in the previous results section (Fig. 3.43-3.45). These differences are observed by these floats starting from mid-April 2004. At this time float 0631 is in a water mass that is warmer, more saline and denser than 0634's (Fig. 3.43-3.45). This is when float 0634 is on the edge of the Western Gyre and float 0631 is close to the Batumi eddy which is not too strong at the time (Fig. 4.7). Float 0631's measurements did not change much which implies there is no big difference in the characteristics of the water mass it is in. Later float 0634's temperature, salinity and density measurements dropped significantly. This suggests that float 0634 was in an anti-cyclonic region and was in a water mass (cold, less saline, less dense) that is down-welled from the upper layers of the Black Sea to 100m depth, which is actually a portion of the CIL since the temperature measurements of float 0634 are smaller than 8^{o}C at the time.

The measurements by the floats 0631 and 0634 changed completely (Fig. 3.43-3.45) after June 2004 when float 0634 moved into the Western Gyre and 0631 started to intrude the Batumi Eddy. 0631 started to measure low temperature, low salinity and low density waters whereas 0634 was the opposite. The larges differences in the measurements were observed in July 2004 (Fig. 3.43-3.45). In July, the Batumi Eddy was intense which suggests that the reason of the difference in the measurements of floats 0631 and 0634 is the effect of the intensified Batumi Eddy (Fig. 4.8). The possible explanation of the different measurements in July is that float 0631 found a water mass that is down-welled from the upper layers with the anti-cyclonic movement. As in the previous case, this water mass is also the CIL which is down-welled to 100m depth from upper layers. This can also be seen from the high CIL thickness (Fig. 3.33) and deep CIL lower boundary (Fig. 3.34) starting from July. The main reason of this is the anticyclonic and down-welling motion forced the CIL and helped its intrusion to deeper waters.

Different observations were also conducted by floats 1325 and 1550. In September 2006, float 1550 observed colder, less saline and less dense water mass whereas the measurements of 1325 did not change much (Fig. 3.46-3.48). In September float 1325 was at the coast whereas 1550 was at the edge of the anticyclonic Batumi Eddy (Fig. 4.9). This is why float 1550 started measuring low temperature, low salinity and low density waters which were down-welled by the anticyclonic movement in the area. This is supported by the sea surface anomaly map (Fig. 4.9) in which the intensification of the Batumi Eddy can be clearly seen.

The different measurements of the floats 1325 and 1550 then changed as the float 1325 was in an anti-cyclonic region and 1550 was in a cyclonic region (Fig. 4.10) starting from June 2007. This time, 1550 was observing warm, saline and dense (Fig. 3.46-3.48) water at 100m depth. This suggests that 1550 was observing a water mass that is up-welled from deeper parts of the Black Sea, whereas 1325 was observing water mass that is down-welled from the upper parts of the Black Sea which is within the CIL because the temperature of it is below 8^{o}C (Fig. 3.46).

Floats 2206 and 2619 measured different values on the same dates almost as soon as they were deployed. Float 2206 observed warmer, more saline and denser water mass than 2619 almost through all its lifetime (Fig. 3.49-3.51). This is because float 2206 was entrapped by the Western Gyre soon after it was deployed whereas 2619 kept moving eastward following the Rim Current (Fig. 4.11). The observed water masses by float 2206 are up welled deep layer waters. The cyclonic (negative contours) can be clearly seen from sea surface anomaly maps (Fig. 4.11).

It can be stated that the Western Gyre is generally warmer. This can be clearly seen from Fig. 3.49 from the temperature difference between the floats 2206 and 2619 ranging from 0.5^{o}C to almost 1^{o}C throughout the lifetime of the floats. Except for a few measurements, 2206 always had higher temperature, salinity and density measurements than 2619. Float 2619 had high temperature, salinity and density values on 12/29/2007 which is a peak point and can be clearly seen (Fig. 3. 49). On this date, 2619 was in a coastal anticyclonic region whereas 2206 was on the edge of the Western Gyre (Fig. 4.16). After this date, the salinity values of the float 2619 dropped (Fig. 3.50), reaching a minimum value of ~18.2 psu on March 2008. This date corresponds to the domination of the cyclonic movement all over the basin except the Batumi region (Fig. 4.12).

Previous studies in the Black Sea (Tugrul et al., 1992; Oguz et al., 1994) show that the isopycnals corresponding to the temperature minimum, the peak concentration of nitrate and the first appearance of sulfide in the water column, are 14.5 kg/m^3, 15.5 kg/m^3 and 16.2 kg/m^3, respectively Though not the same, the distribution of the 14.5 kg/m^3 isopycnal in the water column (Fig. 3.61) is similar to the distribution of the lower boundary of the CIL (Fig. 3.34) between 15 and 150m depth. The distribution of the depth of this isopycnal depends on the location of the floats. The differences between floats 0631 and 0634 on 07/07/2004 (Fig. 4.8) due to geographical locations are also observed in the distribution of the isopycnal (Fig.3.61).

A layer lying below the CIL with a mean salinity, potential temperature, and density anomaly increasing to 20.8 psu, 8.5°C, 16.2kg/m^3 respectively is known as the Sub-oxic Layer (SOL). This layer has a specific oxygen-nitrate and sulfide-phosphate correlations at its upper (σ_θ ~15.5 kg/m^3) and lower (σ_θ ~16. 2kg/m^3) boundaries respectively. The 15.5 kg/m3 isopycnal represents the peak concentration of nitrate (Tugrul et al., 1992). This isopycnal reaches up to 180 m in the water column, depending on the location (Fig.3.62). Knowing that this isopycnal represents the nitrate maximum in the water column, it can be said that the nitrate maximum of the water masses encountered by the floats lies between 100 to 140m (Fig. 3.62). As mentioned earlier 16.2 kg/m3 isopycnal represents the first appearance of sulfide in the water column. The first appearance of sulfide is at 100-120m in cyclonic (upwelling) regions and up to 200-240m in anticyclonic regions due to downwelling (Fig. 3.63). The effect of the cyclones and anticyclones on the distribution of the isopycnals is clearly observed in all three isopycnals (Fig. 3.61- Fig. 3.63). Note that float 2206 is at a cyclonic region on 03/03/2008 (Fig. 4.12) and the density surfaces (14.5 kg/m^3, 15.5 kg/m^{3,} 16.2 kg/m^3) are all at shallower depths than float 2619 (Fig. 3.61-3.63).

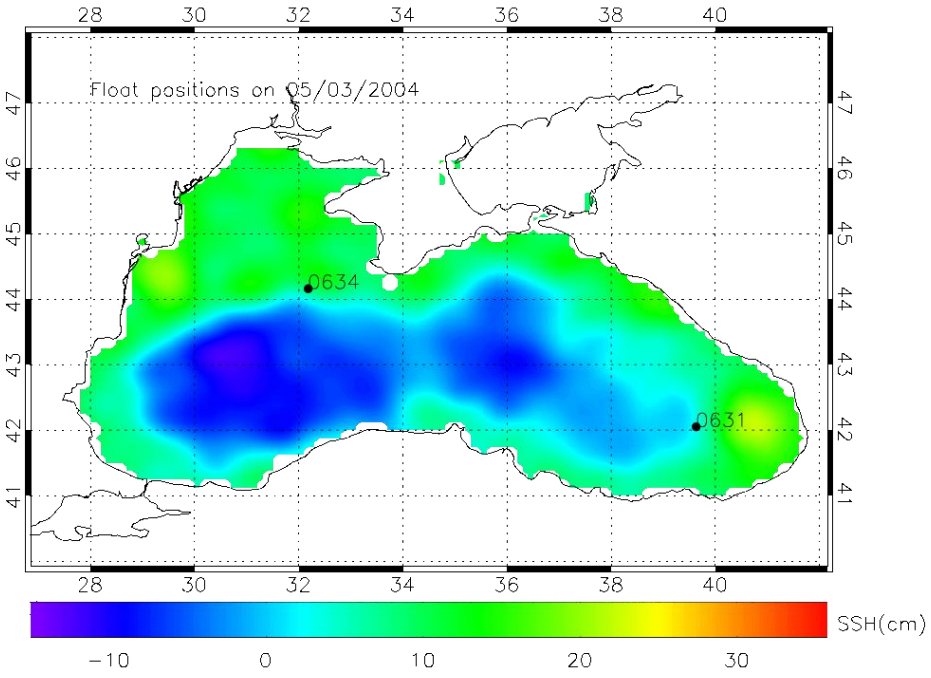

Figure 4. 7 Sea surface anomaly map on 3rd of May 2004, with positions of floats 0631 and 0634

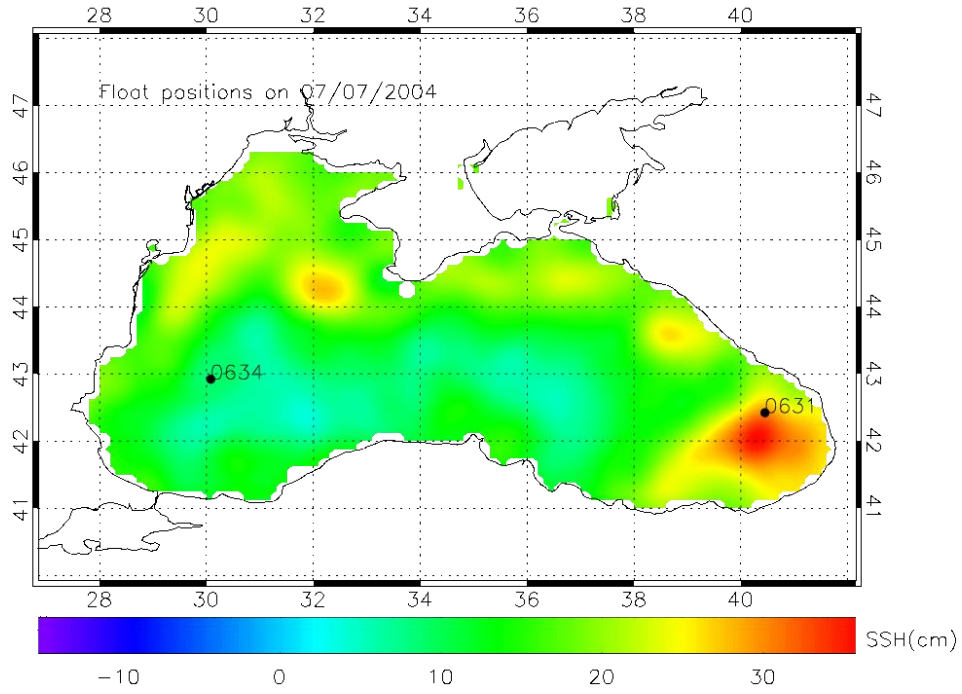

Figure 4. 8 Sea surface anomaly map on 7th of July 2004, with positions of floats 0631 and 0634

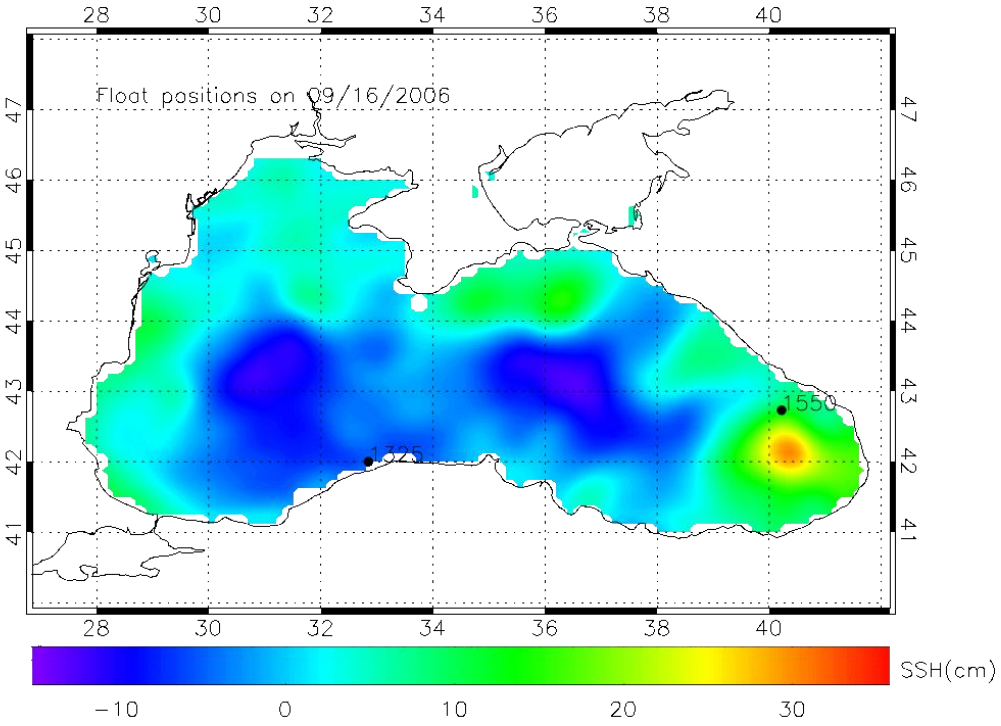

Figure 4. 9 Sea surface anomaly map on 16th of September 2006 with positions of 1325 and 1550

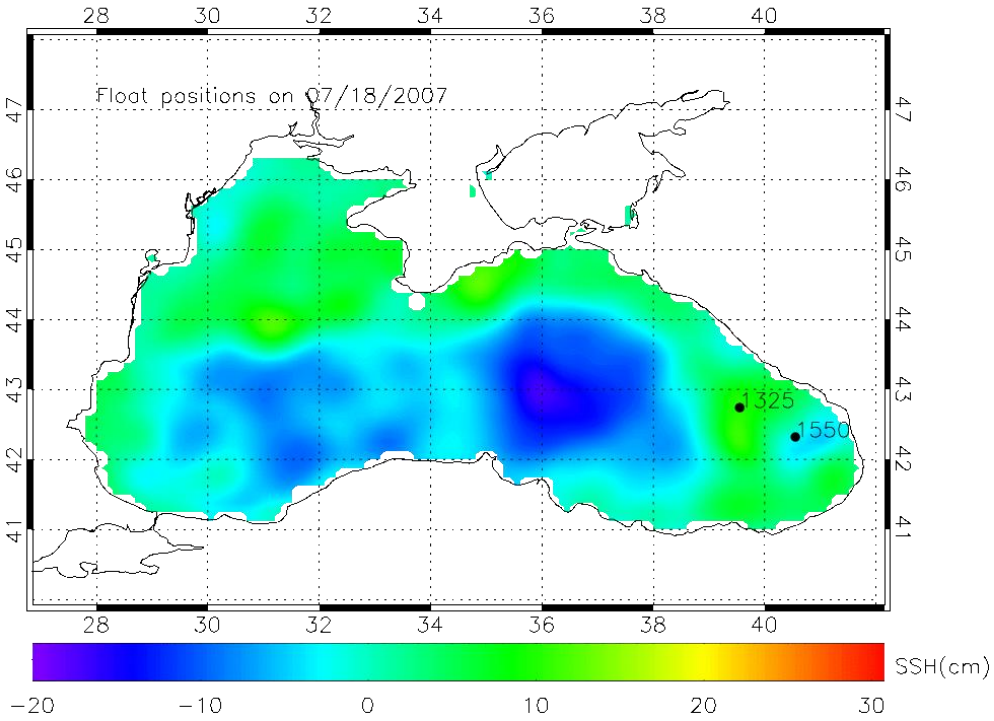

Figure 4. 10 Sea surface anomaly map on 18th of July 2007 with positions of 1325 and 1550. Please note that the scale of the color bar is different than the previous maps.

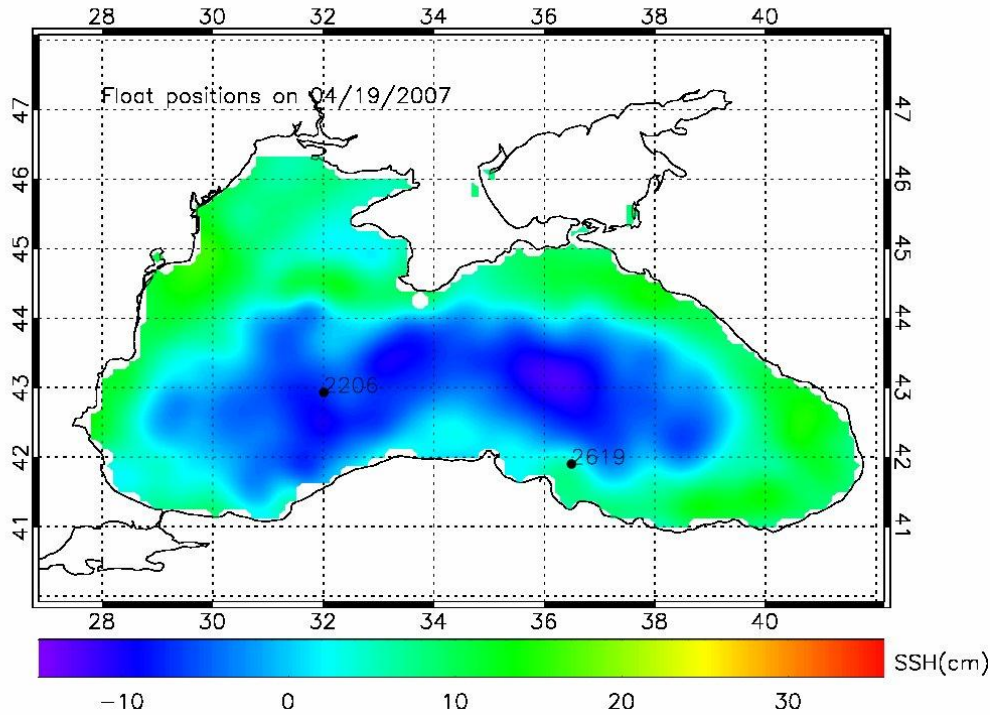

Figure 4. 11 Sea surface anomaly map on 19th on April 2007 with positions of 2206 and 2619

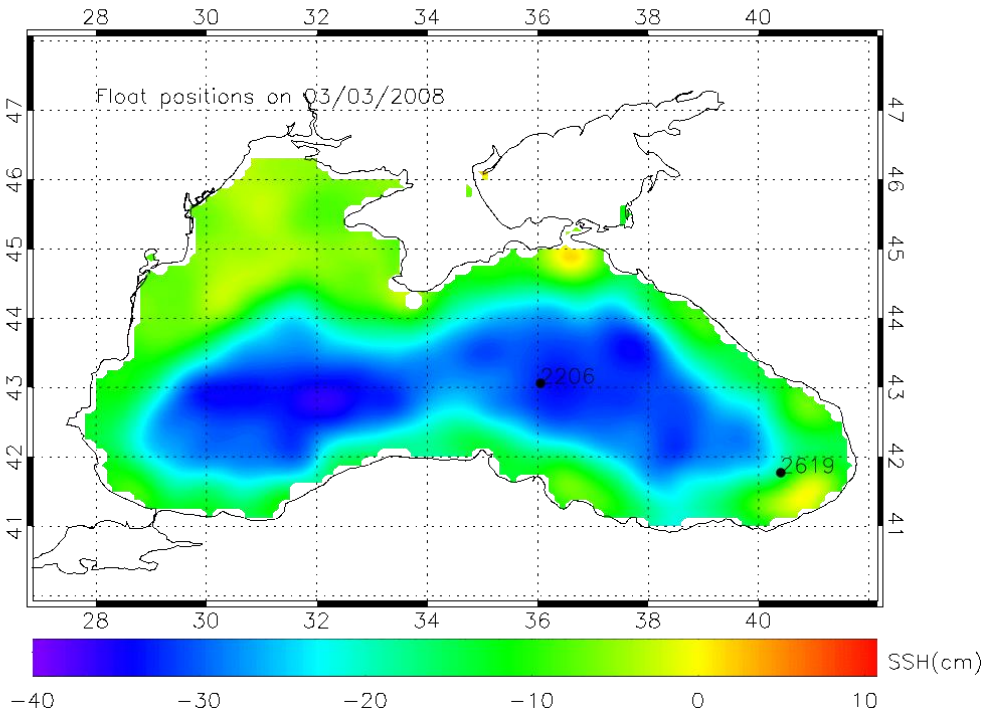

Figure 4. 12 Sea surface anomaly map on 3rd of March 2008 with float positions 2206 and 2619. Please note that the scale of the color bar is different than the previous maps.

CHAPTER 5

CONCLUSION

This thesis provides an analysis of the Argo profiling float data in the Black Sea. This is actually the first time that there is such a high quality, long-term time series data (seven years) available for the Black Sea. This data set is precious for the Black Sea since it was also collected in a period when only a few scientific cruises took place in the area. Using this data set it was possible to obtain information on the circulation characteristics and the thermohaline structure of the Black Sea.

The analysis of the Argo trajectories revealed the main circulation of the Black Sea as well as its mesoscale features. An important finding was that these features existed not only in the surface waters but also in the deeper layers of the water column. The seven-year data set clearly showed the seasonal temperature cycle in the surface layer of the Black Sea. The salinity of the surface waters varied spatially whereas the density varies both temporally and spatially. The analysis of the CIL was another important part of the study and determined the temperature of the CIL, the lower boundaries and the average thicknesses of the CIL. The overall average CIL thickness was found to be 44 meters. The lower boundary and thickness of the CIL depended on the season, but the dominant factor in the distribution of the CIL was the location. It is clearly seen from this study that the lower boundary and the thickness of the CIL depend on the locations of the floats. The cyclonic regions showed shallow lower boundaries and thicknesses whereas the anticyclonic regions showed deeper CIL lower boundaries and thicknesses. The lower boundaries reached the maximum values in the centers of strong anticyclones (e.g. Batumi Eddy).

One of the most important objectives of this study was the determination of the mixed layer of the Black Sea. The mixed layer was obtained, by setting a salinity threshold gradient for winter and setting a density threshold gradient for the rest of the year. The mixed layer depths obtained via this method clearly showed a seasonal cycle with the deepest mixed layers in the winter and the shallowest mixed layer in summer.

The water properties at 100m and 200m were observed to find possible intrusions into the anoxic zone from upper layers and also to observe migrated water masses. At these depths floats measured different properties at the same time suggesting different physical characteristics at different locations, thus revealing cyclonic and anticyclonic

regions with the help of the sea surface anomaly maps. It can also be said that with the deployment of the Argo floats, eastern and western parts of the Black Sea were monitored simultaneously.

Argo floats enable us to continuously monitor the oceans in real time for the first time. These floats provide the main source of data from deep oceans. Argo floats will also be used to monitor climate change in a very near future, as soon as the data is at a superior level for climate analysis. The use of Argo data by climate models should be evaluated carefully and data should be verified through comparisons (Gould, 2002b). The drifting of the Argo floats are also used to track the circulation characteristics of the water column they reside in. Since the data is available in real time, the contribution of Argo program to operational oceanography is of extreme importance. As of today (August 9 2010) there are over 3100 floats active all over the world ocean. With the increasing numbers of Argo floats, the forecasting will be available on smaller scales such as weeks or days. Unfortunately, all of the floats used in this study have been presumed dead as of 2009 and there are only 1-2 Argo floats being deployed by the bordering countries other than Turkey in 2009.

The Black Sea has great importance for the surrounding countries, especially for the fisheries in the region. Continuous monitoring of the Black Sea has extreme importance to detect climate signals, pollution, eutrophication and many other aspects. Argo floats and similar autonomous profilers (gliders, other floats etc.) are a great way to sustain continuous monitoring of the Black Sea. With the upcoming developments in the autonomous floats such as improved irradiance, oxygen, nitrate and chlorophyll sensors Argo floats will be indispensable and unique for the monitoring of the Black Sea. If the Black Sea monitoring is supported by Argo floats equipped with biogeochemical sensors, a lot of information about the anoxic parts of the Black Sea might be revealed, enabling us to better understand the Black Sea, its ecosystem, climate and dynamics. This kind of data sets supported by satellite measurements, model results and shipboard collected data will enable us to solve the unknowns of the Black Sea.

REFERENCES

Bhaskar, T. V. S. U., D. Swain, and M. Ravichandran, 2007: Mixed layer variability in Northern Arabian Sea as detected by an Argo float. *Ocean Science Journal*, **42,** 241-246.

Gould, J. ,2002b: Data Management Handbook, Technical report, http://www.usgodae.org/argodm/manuals/argo_data_management_handbook_v1.2.pdf

Gould, J., and the Argo Science Team, 2004: Argo Profiling Floats Bring New Era of In Situ Ocean Observations. *EoS, Transactions of the American Geophysical Union*, **85,(19),** 179,190-191

Ivanov L I., Backhaus J., Özsoy E. and Wehde H. ,2001: Convection in the Black Sea During Cold Winters, J. Mar. Sys., **31**, 65-76.

Kara, A.B., Helber, R.W., Boyer, T.P., Elsner, J.B., 2009: Mixed layer depth in the Aegean, Marmara, Black and Azov Seas: Part I: General features. *Journal of Marine Systems.***,78**, 169-180

Korotaev, G., T. Oguz, and S. Riser, 2006: Intermediate and deep currents of the Black Sea obtained from autonomous profiling floats. *Deep Sea Research Part II: Topical Studies in Oceanography*, **53**, 1901-1910.

Korotaev, G.K., Oguz, T., Nikiforov, A., Koblinsky, C.J., 2003: Seasonal, interannual and mesoscale variability of the Black Sea upper layer circulation derived from altimeter data. Journal *of Geophysical Research* **108** (C4), 3122.

Murray, J. W., Top, Z. and Ozsoy, E. (1991): Hydrographic properties and ventilation of the Black Sea. *Deep-Sea Res.*, **38**, Suppl.2A, 663-690.

Oguz T., 2009: Chapter 1. General oceanographic properties: physicochemical and climatic features. In : State of the Environment of the Black Sea (2001-2006/7). Edited by T.Oguz. Publications of the Commission on the Protection of the Black Sea Against Pollution (BSC), Istanbul, Turkey, 421 pp.

Oguz, T., Besiktepe, S., 1999: Observations on the Rim Current structure, CIW formation and transport in the western Black Sea. *Deep-Sea Research I* **46**, 1733–1753.
Oguz, T., P. La Violette, U. Unluata (1992):"Upper layer circulation of the southern Black Sea: Its variability as inferred from hydrographic and satellite observations". *J. Geophys. Research,* **97(C8)**, 12569-12584.

Oguz, T., Latun, V.S., Latif, M.A., Vladimirov, V.V., Sur, H.I., Makarov, A.A., Ozsoy, E., Kotovshchikov, B.B., Eremeev, V.V.,Unluata, U., 1993: Circulation in the surface and intermediatelayers of the Black Sea. *Deep-Sea Research* I **40**, 1597–1612.

Oguz, T., D.G. Aubrey, V.S. Latun, E. Demirov, L. Koveshnikov, H. I. Sur, V. Diacanu, S. Besiktepe, M. Duman, R. Limeburner, V. Eremeev ,1994: Mesoscale circulation and thermohaline structure of the Black sea observed during HydroBlack'91. *Deep Sea Research I*, **41**, 603-628.

Ohno, Y., Kobayashi, T., Iwasaka, N., Suga, T., 2004: The mixed layer depth in the North Pacific as detected by the Argo floats. *Geophysical Research Letters*, **31**, L11306, doi:10.1029/2004GL019576

Ohno, Y., N. Iwasaka, F. Kobashi, and Y. Sato, 2009: Mixed layer depth climatology of the North Pacific based on Argo observations. *Journal of Oceanography*, **65,** 1-16.

Oka, E., L. D. Talley, and T. Suga, 2007: Temporal variability of winter mixed layer in the mid- to high-latitude North Pacific. *Journal of Oceanography*, **63,** 293-307.

Ovchinnikov, I. M., and Yu. I. Popov, 1987: Evolution of the cold intermediate layer in the Black Sea, *Oceanology*, Engl. Transl., **27(5)**, 555-560

Ozsoy, E., Unluata, U., 1997: Oceanography of the Black Sea: a review of some recent results. Earth-Sci Rev. **42**, 231-272

Ozsoy, E., D. Rank and İ. Salihoğlu, 2002: Pycnocline and Deep Vertical Mixing in the Black Sea: Stable Isotope and Transient Tracer Measurements. *Est., Coastal and Shelf Sci.*, **54**, 621-629.

Roemmich, D., S. Riser, R. Davis, and Y. Desaubies, 2004: Autonomous profiling floats: Workhorse for broad-scale ocean observations. *Marine Technology Society Journal*, **38,** 21-29.

Sreenivas, P., K. Patnaik, and K. Prasad, 2008: Monthly variability of mixed layer over Arabian Sea using ARGO data. *Marine Geodesy*, **31,** 17-38.

Sur, H. I., E. Ozsoy, Y. P. Ilyin, and U. Unluata,1996: Coastal/deep ocean interactions in the Black Sea and their ecological/environmental impacts, *J. Mar. Syst*., 7, 293– 320

Tolmazin, D., 1985: Changing Coastal oceanography of the Black Sea. I: Northwestern Shelf, *Progress in Oceanography,* **15**, 217-276.

Tugrul, S., O. Basturk, C. Saydam, and A. Yilmaz, 1992: The use of water density values as a label of chemical depth in the Black Seas. *Nature*, **359**, 137-139.